Master Thesis

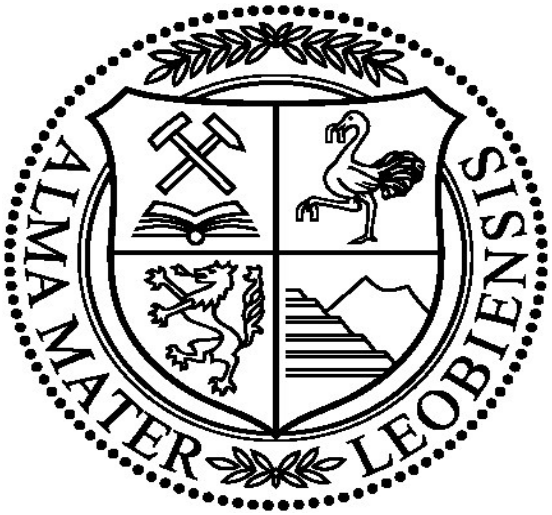

Well Flow Modelling in a Gas Condensate Reservoir

Written by:
Mohammadhossein Khosraviboushehri, BSc
1035401

Advisors:
Univ.-Prof. Dipl.-Ing.Dr.mont. Herber Hofstätter
Dr. Reza Azin

Leoben, 17.06.2014

EIDESSTATTLICHE ERKLÄRUNG

Ich erkläre an Eides statt, dass ich die vorliegende Diplomarbeit selbständig und ohne fremde Hilfe verfasst, andere als die angegebenen Quellen und Hilfsmittel nicht benutzt und die den benutzten Quellen wörtlich und inhaltlich entnommenen Stellen als solche erkenntlich gemacht habe.

AFFIDAVIT

I hereby declare that the content of this work is my own composition and has not been submitted previously for any higher degree. All extracts have been distinguished using quoted references and all information sources have been acknowledged.

Mohammad-Hossein Khosravi-Boushehri

DEDICATION

This master thesis is dedicated with all my heart to my understanding mother to my beloved wife, and to my lovely sister.

Mohammad-Hossein Khosravi-Boushehri

ACKNOWLEDGEMENTS

There are several people I would like to express my gratitude towards in making of this thesis.

My deep gratitude goes to my supervisor Professor Herbert Hofstätter, professor in production engineering and Head of The Department of Petroleum and Geothermal Energy Recovery for his help, support, and encouragement during this master thesis work.

I would like to express my hearty appreciation to my supervisor Dr. Reza Azin for providing real simulation data and giving the opportunity to have discussion with NIOC engineers. His invaluable supervision, support, and encouragement made this study possible.

I am thankful to the academics, research staff, secretaries, librarian, and those who helped during the course of this study at Persian Gulf University and Mining University of Leoben.

I am grateful for love, support, and understanding from my dear wife F. Arshad and my loving parents M. Hemmatnia and H. KhosraviBoushehri.

Finally, Special thanks are extended to many of my friends and all of those who supported me in any respect during the completion of my thesis.

Leoben, June 2014

M.H. Khosravi Boushehri

Kurzfassung

Gaskondensatlagerstaetten haben im Vergleich zu anderen Gaslagerstaetten unterschiedliche Fliesseigenschaften. Das Gaskondensat ist gasfoermig bei den vorherrschenden Bedingungen in der Lagerstaette. Jedoch nach Produktionsbeginn, sobald der Druck unter dem Taupunkt faellt, formen die schwereren Kohlenwasserstoffanteile Gaskondensate nahe des Bohrloches und limitieren somit die Fliessmoeglichekeiten des Gases, was zu reduzierter Produktion fuehrt. Deswegen ist es wichtig das Fliessverhalten und Fliessbedingungen zu kennen, um den Druckgradienten, den Druck am Bohrlochboden berechnen zu koennen, Produktionsdaten zu analysieren, und Vorhersagen ueber die Produktionsrate machen zu koennen. In anderen Worten, die Vorhersage und Berechnung des Druckgradienten in Gaskondensatlagerstaetten ist aufgrund des komplexen verhaltens der Bohrungen sehr wichtig um ein kosteneffizientes Design der Bohrlochskomplettierung und Optimierung der Produktion zu erzielen.

Die in dieser Studie untersuchte Lagerstaette ist eine Gaskondensatlagerstaette vor der persischen Kueste. Da keine Durchflussemengenmessgeraete in den Bohrungen installiert sind, gibt es keine Fliessratendaten der einzelnen Bohrungen. Nur die Fliessmengen an zwei Platformen, die 20 Bohrungen verbinden sind vorhanden. Da es notwendig ist die einzelnen Fliessraten zu kennen um Aussagen ueber zukuenftige die Produktion machen zu koennen, wurde Pipsim zur Simulation der Ventile und zum Berechnen der individuellen Fliessraten verwendet. Das Vorhandensein von variablen Ventilen anstatt von fixen Ventilen ist eine grosse Herausforderung bei der Berechnung der Produktionsdaten. Daher wurden 77 Datenpunkte der des Separators gesammelt um die Ventile zu simulieren und Zusammenhaenge zwischen der Oeffnung des variablen Ventils und des festeingestellten Ventils zu erstellen. Abschliessend wurde die berechnete Gesamtgasmenge mit der gemessenen Menge verglichen und es wurde ein Fehler von nur 3.4% erzielt.

Im naechsten Schritt wurden die Bohrungen simuliert um das bestmoegliche Model fuer den Druckgradienten zu bestimmen. Dafuer wurde mit den gesammelten Daten ein passendes Model gewaehlt und mit Hilfe der Ventilberechnungen die Bohrungen simuliert und der Druck am Bohrlochsboden bestimmt. Weuiters sind Temperaturprofile sowie Liquid-hold-up Profile Ergebnisse der Simulation. Schlussendlich wurde noch eine Sensitivitaetsanalyse der Parameter durchgefuehrt.

Mohammad-Hossein Khosravi-Boushehri

Abstract

Gas condensate reservoirs have a different flow behavior from other gas reservoirs. The gas-condensate reservoir is initially gas at the reservoir condition. However, with the beginning of production, pressure decreases below dew point once heavy hydrocarbons in gas phase start to form condensates near the wellbore and consequently may limit gas flow path in the wellbore which causes gas production decrease. Thus it is important to know well flow behavior and flow patterns for calculating pressure gradient, bottom-hole pressure, predicting production rate and analysing production data. In the other words, predicting and calculating pressure gradient in gas condensate reservoirs due to complex nature of flow will be important for cost effective design of well completions and production optimization.

The field being studied in this project, located in Persian Gulf coastline, is a gas condensate reservoir. Since no flow meter is installed on the wells, the individual flow rate of each well is not available. But total flow rate of two platforms which is cumulative production of twenty wells' flow rate is known instead. And, since it is necessary to determine each well's production rate in order to analyse production data and predict the future of production, Pipesim simulator was used to simulate choke valve and calculate the gas and condensate flow rate of each well. Having opening percentage instead of bean size in adjustable chokes is a challenging issue in calculating production rate. Therefore, 77 data points of test separators were collected to simulate the choke and to obtain an applicable relation between the choke opening percentage and the bean size. At the end, the total calculated enriched gas flow rate was compared to the total measured enriched gas flow rate and consequently the mean percentage error of 3.4 was obtained.

In the next step, the wells were simulated to determine the best pressure gradient model using Pipesim software. Therefore, with measured data of wells (PSP) being used, a proper model was chosen, then with the aid of chosen model and output data from choke calculations, the wells were simulated and the bottom hole pressure was determined. Moreover, pressure-temperature profiles as well as liquid hold up profile are more outputs of this simulation. Ultimately, a sensitivity analysis was performed for the parameters undergoing uncertainty.

List of Tables

List of Figures

Nomenclatures

μ	viscosity
A	Cross sectional area
λ	no-slip fraction
ρ	Density
V	Volume
θ	Pipe inclination angle
dZ ,dX	Vertical and Horizontal distance
dL	Pipe length
NFR	dimensionless Froude number
N	Dimensionless number
MW	Molecular Weight
a	Constant Gilbert Equation
b	Constant Gilbert Equation
C	Specific heat capacity
ε/d	relative roughness
S	slip ratio
v	Velocity
p	pressure
q	volumetric flow rate
d	pipe inside diameter
Cd	Discharge Factor
Cp	Specific heat capacity at constant pressure
Cv	Specific heat capacity at constant Volume
f	Moody friction factor
C′	Constant of AL Attar equation
H	Hold up
k	Specific heat ratio
Q	Flow Rate
Y	Upstream downstream Pressure ratio
σ	Interfacial Tension
λ	No slip hold up
τ	Shear Stress
ND	Dimensionless number for diameter
NV	Dimensionless number for velocity
QL	Liquid flow rate
QG	Gas flow rate
Ac	Choke cross section area
d1	Diagonal of the choke's upstream pipe
d2	Choke's diagonal
P1	Choke's upstream pressure
P2	Choke's downstream pressure
Y	Compressibility
ft	Exact value
at	Approximation value

Abbreviations

API	American Petroleum Institute
BHP	Bottom Hole Pressure
CPR	Choke Performance Relationship
Dn	Downstream
G	Gas
GE	Gas Equivalent
IPR	Inflow Performance Relationship
IPM	Integrated Production Modeling
ID	Iran Development
MD	Measured Depth
PLT	Production Logging Tools
PI	Productivity index
PSP	Pseudo Spontaneous Potential
SCF	Standard Cubic Feet
STB	Stock Tank Barrel
SSSV	Subsurface Safety Valve
TVD	True Vertical Depth
TPR	Tubing Performance Relationship
Up	Upstream
VLP	Vertical Lift Performance
VLP	Vertical lift performance
WCT	Water cut
WPR	Wellhead Performance Relationship
WHP	Wellhead Pressure

Table of content

Page

1 Introduction

Crude oil is composed of a variety of hydrocarbons which are seen in forms of gas, liquid or solid or in tri-phasic form (gas, liquid, and solid) based on pressure, temperature or physical properties of reservoir rocks. Thus hydrocarbon reservoirs can be classified into five types based on composition of hydrocarbons in reservoir fluid, reservoir initial pressure-temperature, and fluid pressure-temperature at surface: Black Oil, Volatile Oil, Gas Condensate, Wet Gas and Dry Gas. If reservoir temperature is lower than critical point, it is an oil type categorized into two types of Black Oil and Volatile Oil. And if reservoir temperature is lower than hydrocarburic fluid critical point, it is termed as natural gas type. Based on phasic diagrams and reservoir condition, natural gas reservoirs are classified into three groups of Gas Condensate, Wet Gas and Dry Gas reservoirs [1] [2].

Based on the definition, Gas Condensate reservoir lies between volatile oil reservoir and wet gas reservoir. In other words reservoir temperature ranges from critical point and Cricondentherm. Among properties of retrograde condensate reservoirs is liquid gas ratio ranging from 10 to 300 STB/MMscf. This ratio is stable at the beginning of production while reservoir pressure is above dew point pressure and then it rises. Heavy components concentration (C7+) is generally below 12.5 % in these reservoirs and the fluid behaves as liquid if the concentration rises up. Condensations color is milky white or dark and they are of a relatively high specific weight. And their API is usually above 50 as well [1] [2] [3] [4].

Condensate gas reservoirs have a different flow behavior with other gas reservoirs. In early stages of production period these reservoirs behave as single-phase. But with the beginning of producing from well, pressure decreases below dew point once heavy hydrocarbons in gas phase start to form condensates in reservoir as a pile of precious intermediate components. This retrograde behavior of hyrocarburic fluids is a reason behind naming these reservoirs. On the other hand bottom-hole pressure drop below dew point causes condensate formation and consequently limits gas flow path. This phenomenon is called condensate blockage or condensate bank that depends on factors including fluid phasic properties, reservoir conductivity, and pressure and temperature in reservoir and well bore. Forming condensate bank close to well bore is considered as the greatest cause of decrease in well productivity and gas recovery in these reservoirs compared to other reservoirs. It is important to comprehend these concepts in filed development and ignoring them will lead to production damage. With flow regime being defined in condensate gas reservoir, some phenomena are of a high importance and ignoring these phenomena and errors in numerical values in related parameters would lead to high levels of errors in prediction of reservoir production [1] [2] [3] [5].

In condensate gas systems when gas flow rate is high enough, annular-mist flow persists and produced liquid will flow to well head accompanied by gas. But when gas velocity is so low in pipe that is not capable of raising liquid up well flow regime transforms from annular-mist to slug or churn. In this case, well liquid holdup would be a problem [6]. With pipe diameter increasing fluid velocity decreases, consequently the amount of liquid holdup rises

up. Thus it is important to have details of pipe lines to gain desirable results of pressure drop and liquid flow rate [1] [2] [3].

1.1 Statement of Problem

The filed being studied in this project is located in Persian Gulf coastline and is one of the biggest world gas fields with an in-place gas capacity of 40 trillion cubic meters. This is a multi-well, multi-layer gas-condensate reservoir. The major producing formations are Kangan of Triassic age and Dalan of Permian age. Kangan is alteration of Limestone, Dolomite and Anhydrite, whereas Dalan is alteration of Limestone and Dolomite. The filed wells are of deviated and cased-hole types and completed in monobore.

In these reservoirs, condensates usually adhere to walls of the wellbore and narrow gas path to the surface which leads to decrease in gas effective permeability and well production drops consequently. Thus it is important to know well flow behavior and flow regime for calculating pressure gradient, bottom-hole pressure, predicting production rate and analysing production data. Since there is no flow meter installed on the wells, the individual flow rate of each well is not available. But total flow rate of each platform which is cumulative production of several wells' flow rate is known instead. Therefore, it is necessary to determine each well's production rate in order to analyse production data and predict the future of production. Having information of opening percentage instead of bean size in adjustable chokes is a challenging issue in calculating production rate.

1.2 Literature Review

Calculation of pressure drop in oil and gas wells will be important for cost effective design of well completions and production optimization [7]. Many multiphase flow correlations have been proposed. Still, none of them have been proven to give good results for all conditions that may occur when producing hydrocarbons [8].

Empirical correlations have been the very first methods for detecting flow pattern in pipelines developed based on experimental data. Several empirical correlations have been proposed for multiphase flow calculation. None of which have been proven to be functional in all conditions of oil and gas production [8]. There have been many developed mechanistic methods, which are approved by limited experimental data, to forecast flow behavior, and they can be applied for different processing conditions considering flow kinetics and important variables. This study is to calculate pressure gradient and predict flow regimes, vertical flows, and inclined flows. In the following principles of measuring flow data and calculations for flows in chokes are investigated.

1.2.1 Single-phase and two-phase flow pressure gradient

Mass conservation, momentum equation, and energy balance are bases of all calculations of flow in pipelines. Pressure and temperature difference along flow path are measured using these principles. Mass conservation rule for a persistent controlling volume of pipe is as 1-1.

$$\frac{\partial \rho}{\partial t} + \frac{\partial}{\partial L}(\rho V) = 0 \qquad (1-1)$$

ρV is constant in a steady-state flow regime and mass accumulation won't be satisfied. Thus equation 1-2 will transform to the following:

$$\frac{\partial}{\partial L}(\rho V) = 0 \qquad (1-2)$$

In a certain part of the pipe output momentum minus input momentum plus momentum accumulation rate equals fluid forces burden. θ is pipe inclination angle to the horizon dL pipe length element and dZ and dX are vertical and horizontal distance elements respectively. Linear momentum correlation in a certain volume of the pipe come by the beneath equation [9].

$$\frac{\partial(\rho V)}{\partial t} + \frac{\partial}{\partial L}(\rho V^2) = -\frac{\partial p}{\partial L} - \frac{\tau \pi d}{A} + g\ \rho \sin\theta \qquad (1-3)$$

Combining equations 1-2 and 1-3 and with permanent flow assumed the equation below develops usually called as Mechanical Energy Balance [9].

$$\frac{dp}{dL} = -\frac{\tau \pi d}{A} - g\ \rho \sin\theta - \frac{dV}{dL}(\rho V) \qquad (1-4)$$

Equation 1-4 indicates that total pressure gradient consists of three parts in steady state. Thus:

$$\frac{dp}{dL} = \left(\frac{dp}{dL}\right)_f + \left(\frac{dp}{dL}\right)_e + \left(\frac{dp}{dL}\right)_{acc} \qquad (1-5)$$

The first sentence in equation 1-4 is due to friction or shear stress on the walls. The second sentence is because of elevation difference which is called elevation pressure drop. The last sentence is due to difference in velocity and is often called acceleration pressure drop which is usually ignored. It could only be remarkable in situations in which compressible phase exists in a relatively low pressure [9].

Principles of uniphase flow are ground for multiphase flow calculations [9]. Flow at surface is usually two-phase due to production flow pressure drop even if the reservoir is single-phase or under saturated [10]. Single-phase flow pressure gradient equation is applied with some expressions including two-phase friction coefficient, mixture density for multiphase flow.

$$\frac{dp}{dL} = \frac{f\rho_f v_f^2}{2d} + \rho_f\, g\ sin\theta + \rho_f\, v_f \frac{dv_f}{dL} \qquad (1-6)$$

Several empirical correlations exist for calculating pressure gradient each of which calculates three parts of pressure gradient in a different way.

Pressure gradient calculation is divided into four categories:

1- Using pressure gradient profiles.

2- Using empirical correlations in pressure drop calculations.

3- Using mechanistic models in pressure drop calculations.

4- Permanent recording by pressure measuring devices in well bottom.

Using pressure gradient is about obsolescence due to inaccuracy and installing pressure measuring devices is not measured to be economic to use due to high expenses. Thus empirical correlations and mechanistic models are going to be discussed in next sections due to higher importance in pressure drop calculation. But it is initially necessary to determine the flow regime to calculate two-phase flow pressure gradient and holdup as well [11].

1.2.2 Two-phase Flow Regimes in Vertical and Inclined Pipelines

The basic difference between single-phase and two-phase flows is existence of flow regime or flow pattern in two-phase flow. The phrase “flow regime” refers to geometrical form of gas and liquid phases when gas and liquid phases develop in the pipe a variety of flow forms appear. Flow forms differ on the boundary distance though flow qualities change in this distance [12]. Flow regimes depend on following parameters in two-phase flows:

1. Operational parameters like gas and liquid flow rate.

2. Geometrical variables including inclination angle and pipe diameter.

3. Flow physical properties including density, viscosity and surface tension.

There are four types of flow regimes including annular, churn, slug, and bubble for two-phase flow in vertical pipelines [12]. For multiphase inclined pipelines in downward flow the dominant flow regime is always a wave stratified one. This flow regime develops in an extended area amongst horizontal flow inclination and -80 angles and a vast area of gas and liquid flow rate. For multiphase inclined pipelines alternative in upward flow, annular and bubble flows are observed in high gas and liquid flow rate [12] .

When in-well gas flow rate in gas condensate systems is high enough a annular-mist flow persists and gas entrains produced liquid to the well head. But when gas rate is so low that is not capable of lifting liquid with it, the flow regime changes from annular-mist flow to slug or transient one [6].

1.2.3 Empirical Correlations in Pressure drop Calculation

Empirical correlations calculate pressure drop based on experimental data and dimensional analysis. In order to calculate bottom-hole pressure the equation beneath is used having well head data.

$$BHP = WHP + \Delta P_{friction} + \Delta P_{gravity} + \Delta P_{acceleration} \quad (1\text{-}7)$$

Several empirical correlations have been proposed to calculate multiphase fluids pressure drop in pipelines.

The main difference between the correlations is how liquid holdup, mixture density, and friction factors are estimated. It is important to notice that application of empirical correlations is limited to the range of data used when it was developed [13] [14].

1.2.4 Empirical Correlations to calculate liquid holdup value and pressure drop in vertical pipelines

In vertical flow, 80-95 % of pressure drop is due to difference in elevation. Pressure drop caused by fluid acceleration is usually ignored even though the volume flow rate is really high.

Vertical pipelines empirical correlations are classified into three groups:

1. Two-phase flow empirical correlations with no slip and no flow regime consideration.

2. Two-phase flow empirical correlations considering slip and ignoring flow regimes.

3. Two-phase flow empirical correlations considering slip and flow regimes.

Table 1-2 shows different method for calculating pressure drop according to this classification.

Table 1-1: categorized method of calculation pressure drop in vertical pipelines [15].

Method	Comment
Poettmann-carpenter	no flow regime and no slip consideration
Baxendell-thomas	
Fancher-Brown	
Hagedorn-Brown	slip is considered ; no flow regime consideration
Gray	
Duns–Ros	slip and flow regime is considered
Orkiszewski	
Beggs & Brill	
Mukherjee & Brill	
Chierici-ciucci-sclocehi	
Aziz-Govier-Fogarasi	

1.2.5 Empirical Correlations to calculate liquid hold up and pressure drop in inclined pipelines

Several correlations exist for calculating two-phase flow pressure drop in horizontal and vertical pipelines few studies have been developed in the field of inclined flow however. In this chapter, different methods to predict liquid hold up and pressure drop are elaborated.

- **Flanigan correlation:** Flanigan suggested applying Panhandle equation with a correction coefficient gas flow frictional pressure drop and a correlation for liquid holdup in some upward parts of pipe flow as well. Inclination angle is insignificant in this method and it is ignored to retrieve pressure in upper parts of the pipe [16].

- **Beggs & Brill correlation:** It was developed using 584 experimental data in small tubing size. Studied parameters include gas flow rate 1-300 Mscf/D, liquid flow rate 0-300 Gl/m, system average pressure 35-95 psia, nominal pipe diameter 1”-1.5”, inclination angle -90 - +90 . Beggs & Brill suggested a specific correlation to calculate liquid holdup in each flow regime. In this method liquid holdup is first obtained in horizontal situation and it is corrected applying tube actual angle. Based on Palmer’s, Beggs & Brill correlation over-predicts liquid holdup value insignificantly in upward parts and significantly in downward parts. Thus in order to reach a zero error liquid holdup value in upward and downward parts should be multiplied in 0.924 and 0.685 respectively [17]. Payne has also claimed that friction coefficient predicted by Beggs

& Brill under-predicts frictional pressure drop and applying a rough tube would lead to better results than normalized friction coefficient in smooth tube. Applying Palmer and Payne modification Beggs & Brill correlation's prediction resembles Flanigan's [17].

- **Mukherjee and Brill Correlation:** In this method Palmer and Payne suggested modifications are applied in Beggs & Brill correlation [9].

- **Ghozov et al. Correlation:** Only two flow regimes of stratified flow and slug flow are being studied in this method. Liquid holdup in upward parts of the pipe is independent from pipe angle in stratified flow and depends onN_{FR}, but in upward parts of the pipe liquid holdup value is a function of angle. Liquid holdup value is also a function of angle in slug flow regimes [11].

1.2.6 Mechanistic and Physical Models to calculate Liquid Holdup and Pressure Drop in Wellbore

Mechanistic models have been formulated for well bore and pipelines since 1970. Vertical upward flow pattern prediction model was first proposed by Taitel et al. and it was then developed by Barnea et al. [18]. These models calculate pressure drop based on phenomenological approach and considering physical phenomena and basic fundamentals as mass and energy conservation rule [14].

1.2.7 Vertical Flow Comprehensive Models

Comprehensive mechanistic models for vertical flows have been proposed by Ansari et al. [16], Hassan and Kabir et al. [19], Ozon et al. [20], and Chokshi et al. [21].

- **Ansari et al. model 1994**

In Ansari et al. model bubble, annular and slug flow regimes have been modeled. Transient flow regime has not been modeled yet due to complexities and is usually considered as a slug flow regime. In Ansari et al. model the initial bubble flow regime model is used to calculate the void fraction. Since the incompressible liquid phase is dominant in bubble flow regime, no significant change is observed in fluid density and fluid velocity is almost stable. Therefore acceleration pressure drop is ignored beside two other pressure drops [16]. In a dispersed bubble flow there is no slippage between two phases due to even distribution of gas bubbles in liquid phase therefore dispersed bubble flow is assumed to be quasi-single-phase and no-slippage homogeneous model is used. In slug flow Silvester model is used to

calculate liquid holdup in slug and pressure drop equation. In Silvester model pressure drop is ignored in huge bubble region –film region- liquid film is assumed to be fixed. However, acceleration pressure drop is concerned which it would lead to overestimation, especially about cases in which huge bubble region is not so huge. In this case Ansari et al. have developed a slug flow model. In Taitel and Barnea models pressure drop is ignored in huge bubble region –film region- as well as acceleration pressure drop in cases in which liquid film is assumed to be fixed and balanced. So if Ansari et al. had applied Taitel and Barnea model they wouldn't need to develop slug flow model. Alves et al. model has been used in Ansari et al. model for annular flow and Wallis correlation is applied to calculate liquid tiny drops entrainment fraction from film to gas core (f_E) and two correlation of Whalley & Hewitt and Wallis to calculate friction coefficient of dimensionless shared surface (I) [12].

$$f_E = 1 - exp[-.125(\phi - 15)] \qquad (1-8)$$

$$\phi = 10^4 \frac{\mu_g V_{SG}}{\sigma}\left(\frac{\rho_g}{\rho_L}\right)^{.5} \qquad (1-9)$$

$$\begin{cases} I = 1 + 300\dfrac{\delta_L}{d} & If \quad f_E > .9 \quad \text{Wallis} \\ I = 1 + 24(\dfrac{\rho_L}{\rho_g})^{\frac{1}{3}}\dfrac{\delta_L}{d} & If \quad f_E > .9 \;\; Whalley \quad Hewitt \end{cases} \qquad (1-10)$$

Ansari et al. have thrived to evaluate 8 methods to predict pressure drop using 1712 well test data from flow projects literature of Tulsa University. The methods include Hagedorn and brown, Duns and Ros, Aziz et al, Orkiszewski, Mukherjee and Brill, Ansari et al. proposed model, and Mukherjee and Brill, and Hassan & Kabir mechanistic model. This comparison is conducted for entire data of vertical and deviated wellbores. Moreover, this comparison is performed on wellbores with 100% slug/annular flow regime, 75% bubble flow regime. Ansari et al. model has demonstrated a supremacy over all other methods. The model has also led to better results in annular flow regime comparing to other and relative function coefficient is zero. Relative function coefficient is a combination of all errors. Comparing to Ansari et al. Hassan and Kabir model leads to better results in case of wellbore in which bubble flow regime exists. This is because Hassan & Kabir have applied revised bubble flow model rather original bubble flow model used by Ansari et al. Ansari et al. have also concluded that flow parameters in mechanistic model (such as bubble lifting rate and film thickness) depend on tube angle and model functionality would improve considering angle effect [16].

- **Chokshi et al. model 1996**

Chokshi et al. (1996) have developed a mechanistic model for vertical flows. Chokshi et al. considered five different flow regimes such as bubble, slug, and annular flow. Drift-flux model concept is used for flow regime transition from bubble to slug [21].

- **Kaya et al. model (1999)**

Kaya et al. (1996) have developed a mechanistic model for vertical and deviated wells. This model consists of five different flow regimes as bubble, dispersed bubble, slug, churn, and annular flows. They have presented a new hydrodynamic model for bubble flow and used hydrodynamic homogenous model and revised slug flow model of Chokshi et al. for dispersed bubble and slug flow respectively. Kaya et al. have never modeled transient flow regime due to its complexities and instability. Hence Tengesdal et al. have suggested modified hydrostatic model of slug flow for churn flow. Tengesdal churn flow model has been revised for pipe inclination in Kaya et al. model. Ansari et al. vertical annular flow model in which film thickness is assumed to be stable is also used in Kaya et al. model [22].

Yahaya and Gahtani (2010) have administered a comparison on several different empirical correlations and mechanistic models using 414 field data in Middle East with tube sizes ranged from 2.375" to 7", oil flow rate of 280-23200 B/D, and maximum ratio of gas/oil 927.7 SCF/STB which is shown in Table 1-2 [14].

Table 1-2: Mechanistic model and empirical model compared by Yahaya and Gahtani [14]

Mechanistic Model	**Empirical Correlation**
Ansari et al.	Hagedorn and Brown
Aziz et al.	Duns And Ros
Chokshi Et al.	Orkiszewski
	Beggs and Brill

It is been concluded that Ansari et al. showed better results comparing other correlations and Beggs & Brill correlation stood the second place.

1.2.8 Unified mechanistic models

In recent years so many attempts have been made to develop unified mechanistic model applicable to any angle inclined pipe from horizontal flow (θ=0) to upward vertical flow (θ=90). Therefore there is no need to apply different models for pipelines with different angles. Flow pattern prediction unified model was proposed by Barnea et al. validated for all angles [18]. Felizola and Shoham (1995) have proposed a slug flow unified model for horizontal to vertical upward flow [23]. Petalas and Aziz have presented a unified mechanistic model for horizontal to vertical upward and downward flows [24]. Gomez et al. have proposed a unified correlation to predict liquid holdup in slug flow. Gomez et al.

homogenous model consists of a unified flow pattern prediction model and specific unified models for stratified, slug, bubble, annular, and dispersed bubble flow regimes [25].

Zhang et al. have lately proposed a comprehensive unified model based on slug flow dynamic for all angles [26]. Khassanov et al. (2007) have also presented a new mechanistic model for two-phase flow in vertical and inclined axes based on drift -flux model [27].

Xiao et al. [28], Ansari et al. [16], and Zhang et al. [26], mechanistic models is able to predict pressure gradient accurately even though they are challenging and sophisticated with math computations since momentum and mass integrated equations are separately applied for both phases in two-phase flow pressure gradient calculations. Two-phase flow reformulation in drift -flux model decreases these challenges to a significant level [27]. Drift –flux theory developed based on two-fluid considered as a mixture with average characteristics of two fluids.

Noteworthy that Khassanov et al. have evaluated four mechanistic models as Hassan and Kabir, Zhang et al., Ansari et al., and their own suggested model using University of Tulsa databank. Relative performance factors for different models are brought in table 1-3.

Table 1-3: Relative performance factors [27].

Case Number	Case Description	Number of Wells	Ansari et al.	Zhang et al.	Khassanov et al. (Proposed Model)	Hassan & Kabir
1	All	2028	773/0	028/0	865/2	6
2	$\theta < 70$	401	84/1	28/1	1	651/5
3	$\theta < 60$	292	806/2	346/1	668/0	092/5
4	d < 8cm	663	348/1	521/0	231/1	616/5

Studying Table 1-3 it can be claimed that Zhang et al. model has shown a better total function comparing to other models, but Khassanov et al. model would lead to better results in cases in which $\theta>70$. It is also observed that Khassanov et al. model have shown significantly better results than Hassan and Kabir model since void fraction has improved slug flow.

1.2.9 Two-Phase Flow Modelling in Condensate Gas Pipelines

Condensate gas wells two-phase flows haven't got as much attention as oil wells. Govier, Aziz, and Fogarasi pioneered comparing field data with empirical correlations prediction (Duns and Ros annular-mist and churn flow model, Hagmark and Wallis) a new method based on flow mechanism. In this method liquid film distributed as a current film on the wall and scattered in gas core are combined. Consequently momentum equations are separately

applied for gas/liquid mixture in gas core and the whole pipe contain. Results obtained from correlations and field data comparison, have indicated that the new suggested method shows less errors and more accuracy [29]. Gray has used a quasi-homogenous model to calculate acceleration, frictional, and static pressure drop. He claimed there is no possibility even for condensate gas wells for liquid drops to move with a velocity similar to gas. That's why there is just one value for liquid holdup. Therefore in order to calculate holdup, gas in-place fractional volume correlation is presented as equation 1-11 where, ND and NV are dimensionless number for diameter and velocity [24].

$$f_g = \left\{1 - e^{-2.314}\left[N_v\left(1 + \frac{205}{N_D}\right)\right]^B\right\}\left(\frac{v_{sg}}{v_m}\right) \qquad (1-11)$$

$$B = 0.0814\left[1 - 0.0554\, ln\left(1 + \frac{730 v_{sL}/v_{sg}}{1 + v_{sL}/v_{sg}}\right)\right] \qquad (1-12)$$

Peffer et al. have used a homogenous mixture to measure pressure drop. They have modified Cullender-Smith correlation developed to measure pressure drop in dry gas wellbore subsequently compared it with average temperature and compressibility coefficient method and developed two-phase model of Govier, Aziz and Fogarasi. Since suggested temperature difference and compressibility coefficient method is a function of elevation difference is supposed to be more accurate compared to average temperature and compressibility coefficient method. Cullender-Smith method modifications are as follows:

1. Gas production rate modification due to existence of liquid in flow.

2. Frictional pressure drop modification using actual pipe roughness [30].

Finally Hassan and Kabir calculated bottom-hole pressure from Ansari et al., Gray et al., Peffer et al., Aziz et al. correlations and no-slippage homogenous model using measured flow rate and well head pressure from condensate gas wellbore (used data by Govier, Aziz and Fogarasi, Peffer et al. and West African field). These data were afterward compared with measured values outlined in the following [31].

1. In condensate gas wells a mist flow is a no-slippage flow in the whole well bore. As a result homogenous model has a strong functionality in a vast range of conditions since it utilizes gas/liquid phase average properties to calculate pressure drop. Homogeneity condition improves by time as condensate system gets lighter. Therefore using a homogenous model in a combined model including reservoir, well bore and tubing system is satisfactory and simple.

2. Ansari mechanistic model and Gray empirical correlation have a tendency toward homogenous model under mist flow condition. Since liquid film thickness is not much on wall and these correlations have high accuracy.

3. Aziz et al. model have shown a fairly good agreement with homogenous model but not as well as compared to Ansari et al. and Gray et al. In Aziz et al. model Duns and Ros correlation is applied for mist flow. Duns and Ros assumed that liquid tiny drops have no impacts on pressure gradient. In other words they have concerned gas single-phase flow. In Aziz et al. model friction coefficient value was also applied as it was in Ansari et al. with no 300 +1 index. In other words Aziz et al. model underestimates pressure drop in gas condensates wells compared to Ansari et al. model.

1.2.10 Flow through choke

The wellhead choke is the only device used to regulate the production rate of a reservoir and thus can control formation draw down [32].

The reason that is not possible to use other types of valves such as master or control valves rather than the choke is related to the operating mechanism of chokes. Unlike Chokes, these valves would allow production fluid containing solid particle to cross the sealing surface of the valve when they try to reduce the fluid flow rate. This could lead to a failure in surface or subsurface equipment in sand containing reservoirs.

A choke is basically designed with small opening which can prevent erosion problems and a leaking master valve which may killing the well to replace the valve [33].

The main idea of using a choke is to make reservoirs to produce at the optimum rate while maintaining a sufficient back pressure for a reservoir to prevent formation damages such as gas or water coning and sand entry [34].

Due to high sensitivity of oil and gas production to choke size, production engineers should select the optimum choke size by accurate modelling of choke performance which plays an increasingly important role in the reservoir management. In other words, finding the optimum choke size can maximize economic recovery of oil and gas from a reservoir [34].

Choke flows can be classified into two main categories: critical flow and sub-critical flow. Critical flow occurs when fluid’s velocity will reach sonic speed and the flow rate is independent of downstream pressure. In this case, any fluctuation in downstream of the choke will not influence on upstream conditions.

On the contrary, in sub-critical case, flow rate depends on both upstream and downstream pressures [35]. The dependency of flow rate to pressure ratio (downstream/upstream) is represented in the following figure.

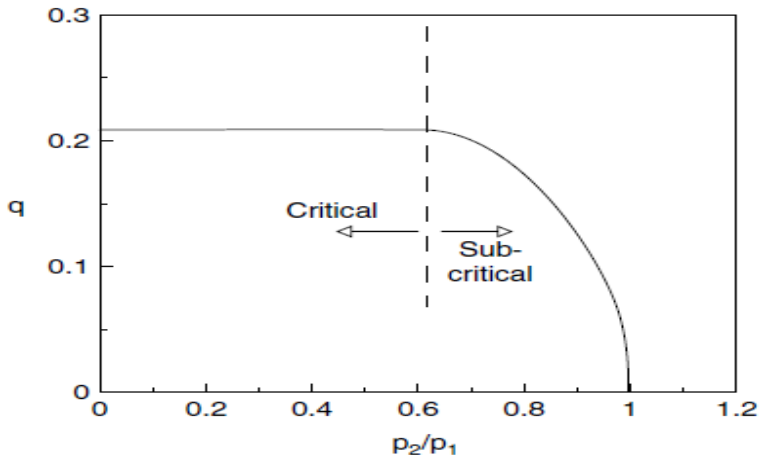

Figure 1-1: Flow rate versus downstream/upstream pressure [36]

Theoretical and empirical methods are available in the literature to predict the choke flow performance. Tangeren et al. [37] did the first theoretical study on two-phase flow through restrictions. He assumed polytropic expansion of gas that is dispersed uniformly in the mixture having liquid as the continuous phase in critical conditions. Fortunati [12] developed the first correlations for both critical and sub-critical flow and the boundary between these regimes.

Ashford [38] presented a model for two-phase critical choke flow based on the work of Ros [39]. Gould [40] plotted the Ashford boundary, showing the dependency of boundaries to the polytropic exponent. Ashford and Pierce [41] derived an equation to predict the critical pressure ratio.

Pilehvari [42] also studied choke performance under sub-critical conditions. Sachdeva et al. [43] presented a model to predict mass flow rate through chokes for both regimes. The Perkins' models [44] presented an approach to estimate the critical pressure ratio and the mass flow rate in a way nearly same to Sachdeva et al. [43]. Perkins [44] included the three phase effects for the polytropic expansion exponent, n, and also found the mixture average velocity at the throat.

Guo et al. [44] [33] evaluated the accuracy of the Sachdeva's model using field data from oil and gas condensate wells in Southwest Louisiana. Comparisons of the results indicated that Sachdeva's model generally under-estimates gas and condensate flow rates. Guo et al. [33] minimized models error using different values of choke discharge coefficient (CD).

Calculation of the sound velocity or the separating boundary of the critical and sub-critical flow is necessary for evaluating the behavior of compressible fluid in chokes [38].

Tangeren was the first who studied the restrictor’s two-phase gas-liquid flow and showed that when gas bubbles are added to uncompressible fluid flowing above the critical velocity, pressure variation in choke’s downstream won’t have any effect on the flow [37]. The first

empirical relation for critical flow was developed by Gilbert. He introduced new factors relating upstream pressure to gas/condensate ratio, nominal choke size and the gas/liquid production ratio. Later, other researches such as Baxendell (1957), Pilehvari (1980), Achong (1961) and Ros (1960) modified his method and introduced some new factors which could fit the method to a variety of fluids and flowing conditions [45] [42] [39].

Other studies suggested some new methods for prediction of critical and sub-critical flow that describe the behavior of multi-phase fluids flowing through a choke. These studies include the following methods:

Ashford and Pierce (1975) developed the total mass flow rate equation based on below assumptions:

1) Choke flow is Isentropic.

2) Fluid is uncompressible.

3) There is no sudden evaporation in the choke.

4) The mixture is homogeneous.

They assumed that the derivative of the flow rate respect to the pressure ratio in the critical flow boundary is zero, and then introduced the critical pressure ratio as a function of gas to liquid ratio (R1). It should be mentioned that gas to liquid ratio is an input parameter while it is unknown when flow rate is not specified. Therefore a try and error method is needed for utilizing this equation. Following relations are used to define the critical pressure ratio (yc):[42]

$$y_c = \frac{\frac{2R_1}{(1+R_1 y_c^{\frac{-1}{k}})}\left[\left(\frac{R_1}{b}\right)\left(1-y_c^b\right)-y_c+1\right]y_c^e-1}{R_1} \qquad (1-13)$$

$$b = \frac{k-1}{k} \qquad (1-14)$$

$$e = \frac{k+1}{k} \qquad (1-15)$$

Sachdeva et al. combined theoretical studies with laboratory experiments and restate the critical pressure ratio equation [43]:

$$y_c = \frac{N^{\frac{k}{k-1}}}{D} \qquad (1-16)$$

$$N = \frac{k}{k-1} + \frac{\left(1-x_{g1}\right)\rho_{g1}(1-y_c)}{x_{g1}\rho_L} \qquad (1-17)$$

$$D = \frac{k}{k-1} + \frac{n}{2} + \frac{n(1-x_{g1})\rho_{g2}}{x_{g1}\rho_L} + \frac{n}{2}\left[\frac{(1-x_{g1})\rho_{g2}}{x_{g1}\rho_L}\right] \quad (1\text{-}18)$$

$$n = 1 + \frac{x_{g1}(C_{pg} - C_{vg})}{x_{g1} + (1 - x_{g1})C_L} \quad (1-19)$$

Where,

n is polytropic exponent for gas,

K is specific heat ratio,

Xg1 is in-situ mass fraction of liquid,

Cpg is gas heat capacity at constant pressure,

Cvg is gas heat capacity at constant volume, and

CL is the heat capacity of liquid.

Fortunati presented an experimental method for both critical and subcritical cases. He used the homogeneous compound assumption and specified the critical and sub-critical boundary with the aid of experimental data [12].

Perkin used the mass continuity equations and developed a relation for total mass flow rate, assuming isentropic multiphase homogeneous mixture. He also utilized the same assumption as Ashford and Pierce and suggested an equation for critical pressure ratio. Again a try and error method is need in using this equation as in Sachdeva and Ashford equations.

Several different relations have been developed for gas and liquid flow rate calculations so far. Some of these equations resulted from experimental measurements and some other derived based on physical theories [9].

1.2.11 Equations for flow rate calculation in critical condition

A classic method for choke modeling is based on Gilbert equation [46]. This equation derived by experimental flow data analysis of 10 different fields in California. Simplicity and ability to define new factors responding to flow conditions are among reasons for increasing popularity of this equation. Reports show the successful usage of this equation for flow rate calculation in Iranian condensate gas reservoirs. Here is the general form of gilbert equation:

$$p_1 = \frac{bq_{L_{sc}}R_p^c}{d_{ch}^a} \quad (1-20)$$

Where, ql stands for flow rate, p1 Upstream pressure before the choke, Rp gas to liquid (condensate + water) ratio of produced fluid, dch choke size in 1/64 inch and a,b and c are adjustment factors of the equation.

Deriving the equation, Gilbert assumed that the flow rate of the mixture exceeds the sound velocity. When the speed of sound is reached, downstream pressure has no effect on the rate of upstream pressure, and to reach the speed of sound, the upstream pressure has to be at least twice the downstream pressure.

Later researchers modified Gilbert method and introduced some new factors that qualified the equation in responding to different fluids and flow conditions. Table 1-4 presents some values for adjustment parameters, a, b and c, suggested by different researchers.

Table 1-4: Gilbert equation Parameters

Investigator	a	b *10^{-3}	c
Ros	2	4.25	0.5
Gilbert	1.89	3.86	0.546
Baxendell	1.93	3.12	0.546
Achong	1.88	1.54	0.65

Poettmann and Beck [47] extended Rose equation and changed its unit to a field unit and proposed equation 1-21.

$$q_{L_{sc}} = \frac{86400 C_d A}{5.61\,\rho_{LS} + .0765 \gamma_g R_p} \times \sqrt{\frac{9273.6 p_t}{V_L(1 + .5 m_L)}} \times \frac{.4513\sqrt{R + .766}}{R + .5663} \qquad (1-21)$$

When there is no water production and the flow is in two-phase critical condition, this equation shows favorable results.

Osman and Dokla modified and extended Gilbert equation to cover critical flow conditions by analysis of nonlinear regression of 87 pieces of data gathered from 8 different wells in a condensate gas field in the Middle East [48].

Guo et al. evaluated Sachdeva model by using 512 pieces of data from south western oil and gas condensate fields of Louisiana (containing 273 pieces of data from gas well and 239 pieces from oil one). Results showed that Sachdeva model failed in 48 cases of gas condensate data with liquid density ranging from 44.7 to 55.1 and choke differential pressure less than 1100 psia. Moreover, in other 225gas condensate pieces of data, Sachdeva model

estimated the gas and condensate flow rates about 40 and 60 percent less than the measured value [33].

To improve the performance of Sachdeva model, Guo et al. used various discharge factors and investigated the accuracy of the model. Comparing calculated and measured gas and liquid flow rate for gas condensate wells with different discharge factors, showed a considerable error reduction by increasing discharge factor. Based on these findings, Guo et al proposed 1.08 and 1.53 for discharge factor in estimating gas and liquid flow rates by Sachdeva model [33].

Al-Attar used production data from 3 wells of a gas condensate field in the Middle East and classified them into 8 different groups according to choke sizes (24, 32, 40, 48, 64, 96, 112, and 128). He then obtained the (P upstream--P downstream/ Qg) graph at GLR in log-log scale and derived C´ and b constants in equation 1-22 which are related to the choke size [49].

$$\mathrm{Q_g} = \frac{\Delta \mathrm{P}\ GLR^{\mathrm{b}}}{\mathrm{C}'} \qquad (1-22)$$

Nasriani et al. used 61 pieces of data gathered from Kish gas condensate reservoir and applied nonlinear regression analysis to modify and improve Gilbert relation for sub-critical flow conditions. They also developed Al-Attar theory to cover Kish gas condensate field and for high choke flow rate and big size in sub-critical flow conditions and compared errors of two methods. Results show that:

1. Al-Attar theory applied for and therefore restricted to a specific size of choke while experimental relation could be used for any choke sizes.

2. Al-Attar theory shows a high accuracy when using some specific choke sizes. It offers also a more accurate prediction of the choke flow behavior comparing to experimental relation derived by using all available data in this case [49].

Several different relations have been developed for gas and liquid flow rate estimation so far. Some of these equations resulted from experimental measurements and some other derived based on physical theories [9]. In general, Chokes are modeled based on analytical or experimental methods.

1.2.12 Analytical Model of choke

Analytical Model of choke developed based on physical phenomena. The amount of pressure drop of two phase flow in critical and sub-critical cases can be found using below relations [28].

$$\Delta P_{TP} = \Delta P_L \lambda_L + \Delta P_G \lambda_G \qquad (1-23)$$

In this equation we have:

λ_G: Slip less part of gas phase in the choke flow

λ_L: Slip less part of liquid phase in the choke flow

Pressure drop of gas and liquid phases in equation 1-23 can be obtained from these relations:

$$\Delta P_L = \frac{\rho_L}{2 g_c 144} \left(\frac{Q_L}{C_L A_C}\right)^2 \qquad (1-24)$$

$$\Delta P_G = \frac{\rho_G}{2 g_c 144} \left(\frac{Q_G}{Y C_G A_c}\right)^2 \qquad (1-25)$$

Where,

ρ: Density (lbm/ft3)

QL: Liquid flow rate (ft3/Sec)

QG: Gas flow rate (ft3/Sec)

Ac: Choke cross section area (ft2)

In above equations, C stands for flow factor that is found from below relation. In this relation Cd is discharge factor that assumed to be 0.6 as a default value in Pipesim software [28].

$$C = \frac{C_d}{\left(1 - \left(\frac{d_2}{d_1}\right)^4\right)^{1/2}} \qquad (1-26)$$

Cd: Discharge factor

d1: Diagonal of the choke's upstream pipe

d2: Choke's diagonal

In pressure drop equation, Y is compressibility factor which can be found by:

$$Y = 1 - \left[.41 + .35 \left(\frac{d_2}{d_1}\right)^2\right] \left(\frac{1}{K}\right) \left(\frac{P_2 - P_1}{P_1}\right) \qquad (1-27)$$

P1: Choke's upstream pressure

P2: Choke's downstream pressure

K: Specific heat ratio (C_P⁄C_V)

Therefore pressure drop of two-phase flow in the choke for sub-critical and critical conditions can be obtained from equation 1-28.

$$\Delta P_{TP} = \Delta P_L \left[1 + \lambda_G \left[\left(\frac{C_{dL}}{Y C_{dG}}\right)^2 - 1\right]\right] \qquad (1-28)$$

The ratio of critical pressure to sub-critical and critical flow condition is described in below relations [28]:

$$\left(\frac{P_{\text{outlet}}}{\mathrm{P_{up}}}\right)_{\mathrm{c}} = \left(\frac{2}{\mathrm{K}+1}\right)^{\frac{\mathrm{K}}{\mathrm{K}-1}} \qquad (1-29)$$

Critical flow:

$$\frac{P_{\mathrm{dn}}}{\mathrm{P_{up}}} \leq \left(\frac{P_{\text{outlet}}}{\mathrm{P_{up}}}\right)_{\mathrm{c}} \qquad (1-30)$$

Sub-critical flow:

$$\frac{P_{\mathrm{dn}}}{\mathrm{P_{up}}} > \left(\frac{P_{\text{outlet}}}{\mathrm{P_{up}}}\right)_{\mathrm{c}} \qquad (1-31)$$

It should be mentioned that analytical model considers both physical phenomena and flow variables and it is possible to develop the model to cover various operational conditions. This is more general than the other experimental models which are derived based on measured data analysis, restricted to some specific operational conditions.

1.3 Objectives

Considering the importance of this gas field in national and international economy and the fact that knowing reservoir fluid flow behavior is crucial to reach maximum excessive value, this master thesis is to gain following objectives utilizing from 20 wells of field data set (including geological, drilling, reservoir, well logging, well testing and daily well production data):

- Extracting, gathering, and evaluating the production data and presenting good recommendation to achieve better production condition.
- Determining gas and condensate production rate according to measured values by surface devices.
- Calculating total enriched gas flow rate of ID1 and ID2 in different dates
- Proposing appropriate pressure drop correlations for studied condensate gas reservoir.
- Well flow regime detection and measuring liquid holdup;
- Creating a comprehensive model to determine gas and condensate flow rate or bottom hole pressure.

1.4 Outline

A definition and introduction of gas condensate reservoir is presented in the first chapter. Subsequently it goes through introducing studied field and problem description. A brief history of works on empirical correlations and mechanistic models for pressure drop occurring in two-phase flows and condensate gas flows as well as flow correlations through chokes is brought in Literature Review. The final section of this chapter summarizes the objectives of this work.

In chapter 2, production rates of individual wells are determined from cumulative daily flow rates using a detailed choke modeling.

Chapter 3 comparing different correlations for calculating pressure drop with measured values, will present proper correlation for well simulation in the concerned field. Obtained simulation results including bottom-hole pressure measurements and well flow regime and liquid hold-up are elaborated in this chapter.

Chapter 4 summarizes the work and the most important results on this study and presents recommendations to keep this work going on.

2 Choke modelling

2.1 Introduction

The production flow of individual well from ID1 and ID2 platforms enters the choke valve on the well head that leads to some pressure drop and then after going through the surface equipment, goes to the refinery to be processed. Information about internal flow rate of the refinery is available; however, to model the well flow performance, flow rate of individual well is required separately. Pipesim Software [28] is employed for choke valve simulation. The production contribution of each well in total production is then determined.

Bean size is one of the factors which are required for choke modelling in Pipesim and since the new adjustable choke valves used in these facilities are able to give the exact percentage of openings, the choke upstream and downstream flow lines are simulated using test separator data. In this way, the bean sizes for test separator data are obtained accurately. Afterwards, a relation between bean size and choke opening percentage is derived which is used to calculate the bean size for different opening percentage by which the specific flow rate of each well can be obtained. Finally, the resulted information is used to compare simulated total flow rates and recorded flow rates in the refinery measured data. These flow rates are among necessary data in modelling well flow performance in chapter 3.

2.2 Basic equation

In the beginning of this chapter some fundamental and basic equations by which choke calculation is performed will be described as follows:

2.2.1 The Gas equivalent of produced condensate

Unlike single phase gas reservoirs that produce only gas, gas condensate reservoirs can produce gas and barrels of an oil product called condensate. In this type of reservoirs, cumulative gas production includes total gas produced and stock tank liquid production, which has to be converted into its gas equivalent, (GE). Assuming ideal gas behavior, the gas equivalent of one stock tank barrel at standard condition (14.7 psi, 60°F) is defined as [2]:

$$GE = V = \frac{n\,R\,Tsc}{Psc} = 133000\frac{\gamma c}{\mu wc} \qquad (2-1)$$

Where Yc is the specific gravity of condensate (water=1) and Mwc is the molecular weight of condensate.

Therefore, the total reservoir gas production, hereafter called enriched gas, q (gtot), is given by equation 2.2:

$$q_{gtot,} = q_g + q_c(GE)_c \qquad (2-2)$$

2.2.2 Percent error

All measurements have a degree of uncertainty regardless of precision and accuracy. There are some indexes such as; percent error and Mean percentage error (MPE) which can evaluate the accuracy of calculation or measurement. The Percent Error and the Mean Percentage Error equations can be defined as [50]:

$$percent\ error = \frac{|ft - at|}{ft} * 100 \qquad (2-3)$$

$$(\mathrm{MPE}) = \frac{100\%}{n}\sum_{t=1}^{n}\frac{ft - at}{ft} \qquad (2-4)$$

Where, ft is the exact value and at is the approximation value.

2.3 Required Pipesim data for simulation

- Phase behavior model determination

The phase behavior model of gas condensate reservoirs can be either compositional or black oil model. In compositional model, information about fluid components and their physical properties are required. In black oil model, some information including gas liquid ratio (GLR), condensate API, gas specific gravity and water cut percentage should be available.

- Choke upstream pressure and temperature
- Bean size
- Correlation determination of choke pressure drop
- Choke downstream pressure

2.4 Assumptions used in choke simulation for ID1 and ID2

1) Black oil model is used for choke simulation. In table 2-1 fluid properties of reservoir are presented based on the analysis of PVT samples.

Table 2-1: Fluid properties for ID1 and ID2, Inputs for Pipesim software

Platform	Gas specific gravity	API condensate
ID1	0.689	53.5
ID2	0.672	55.9

2) Knowing the gas condensate flow through chokes, mechanistic model is considered to calculate total pressure drop for both critical and sub-critical correlations.

3) As water cut percentage has a slight influence on choke pressure drop calculation, the water cut value is assumed to be zero in this reservoir. However this issue will be discussed in detail in sensitivity analysis later on.

4) Flow through choke can be considered as either critical or sub-critical. Here the choke simulation is performed assuming the critical flow. Nevertheless to validate the simulation results, type of choke flow is also determined by Pipesim.

5) Although there is not a great deal of differences between GLR in the daily reports, the average values of GLR are considered for platforms ID1 and ID2 in the period of 2005 to 2010 which are presented in table 2-1.

Table 2-2: Mean GLR for ID1 & ID2 from 2005 to 2010

Mean GLR for ID2 (SCF/STB)	**Mean GLR for ID1 (SCF/STB)**	**year**
22000	21000	2005
22000	21000	2006
22000	21000	2007
22000	21000	2008
48000	21000	2009
30000	22000	2010

2.5 Bean size results by choke modelling of test separator data

As mentioned before, it is essential to have the correct value of bean size for simulating a choke by Pipesim simulator [28] in order to calculate the gas and condensate flow rate of individual well. On the other hand, the adjustable chokes used in these platforms provide the accessibility of choke opening percentage. Therefore, 77 data points of test separators were collected to simulate the choke and obtain an applicable relation between the choke opening percentage and the bean size. In Table 2-3, simulation results of bean size for some of data points in ID1-01 well are listed. Furthermore, the total simulation results of each well of two platforms are tabulated in the appendix A.

Table 2-3: Simulated Bean size for some test separator data points for ID1-01

Date	choke opening	well head p.	Wellhead T.	Downstream p.	GLR	Simulated bean size
	%	barg	°C	barg	SCF/STB	inch
02/09/2008	36	212.8	83.1	120	22010	1.67
03/09/2008	22	222.9	83.6	120	20391	1.49
04/09/2008	21	228.1	83.6	120	21079	1.38
06/01/2011	21	214.8	83.2	120.3	21368	1.44
06/01/2011	15	231.3	79.3	120.1	16096	0.86
06/01/2011	20	220.6	82.8	120.2	18152	1.32
06/01/2011	24	209.7	83	120.3	21301	1.55
06/01/2011	25	207.1	83	120.4	26271	1.59

2.6 Choke opening percentage and bean size relation

After obtaining bean sizes, a relation between the bean size and choke opening percentage is suggested based on regression analysis of each well. An applicable relation should meet the following condition:

1) Determination coefficient (R2) should approach to 1 which indicates a good correspondence with the data points.

2) Preferably it is simple and includes few numbers of constants.

3) Has an increasing trend from 0 to 100 percent choke opening.

4) Presents an exceptionally good trend for the high opening range (more than 30 %) and the low opening range (less than 10 %).

Considering above conditions, following relation suggested as regression equation:

$$y = \frac{a}{b + x^{-4}} \qquad (2-5)$$

Figure 2-1 to figure 2-10 illustrate the regression analysis results for the data points of simulated choke for ID1 wells. In appendix B, figures for all other wells of ID2 are also represented. In addition, the constants of relations obtained for each well and the corresponding coefficient of determinations are indicated in table 2-4.

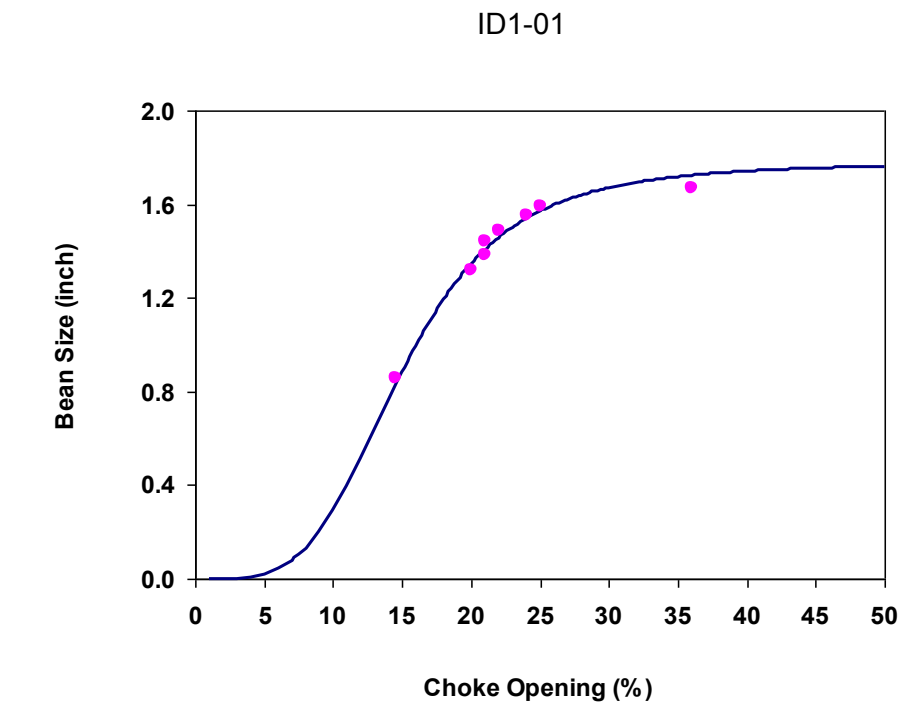

Figure 2-1: Regression analysis results ID1-01 well

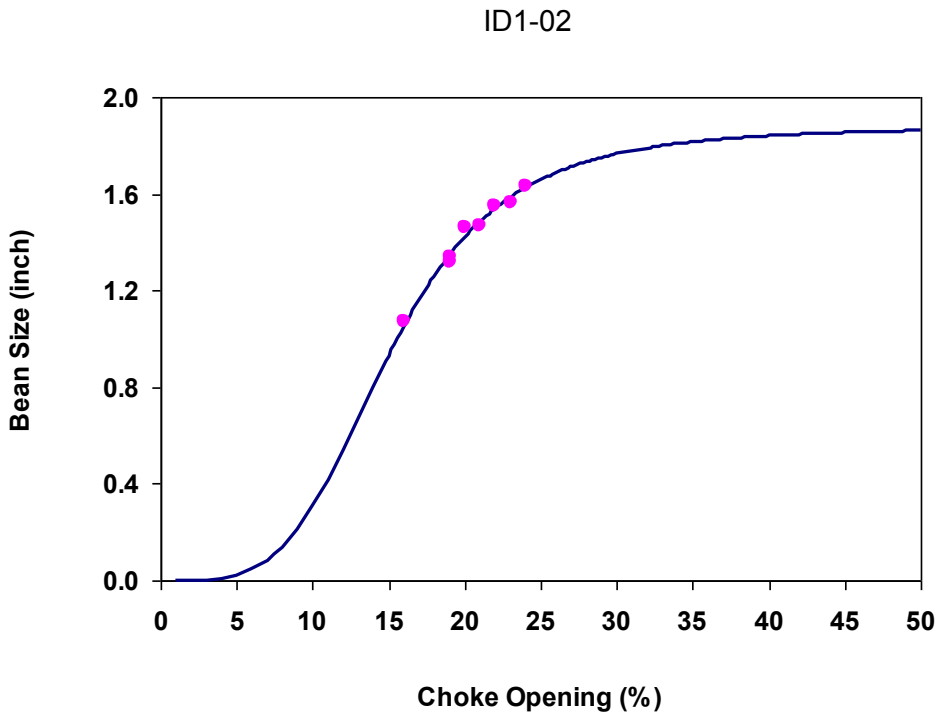

Figure 2-2: Regression analysis results ID1-02 well

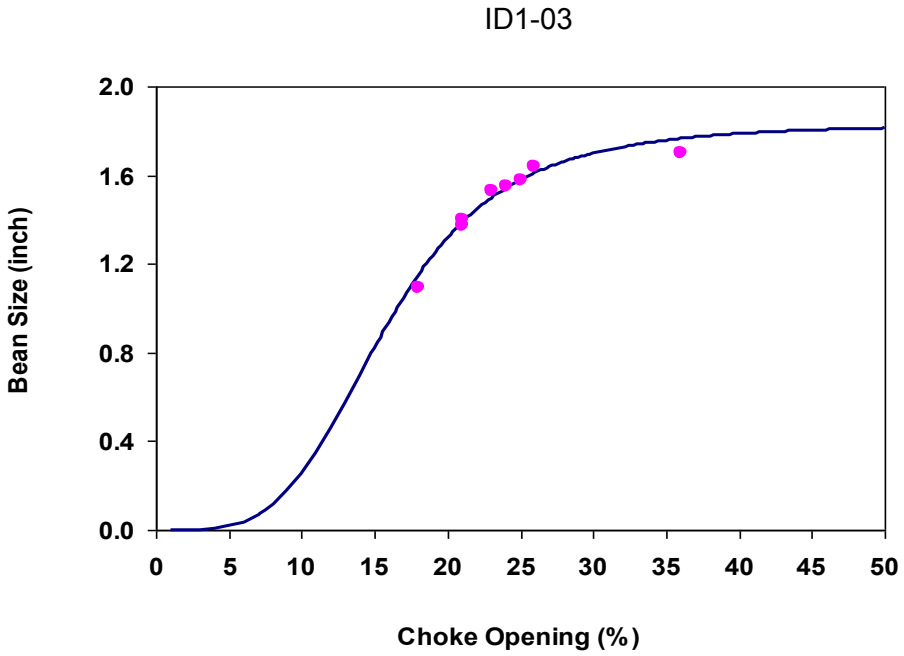

Figure 2-3: Regression analysis results ID1-03 well

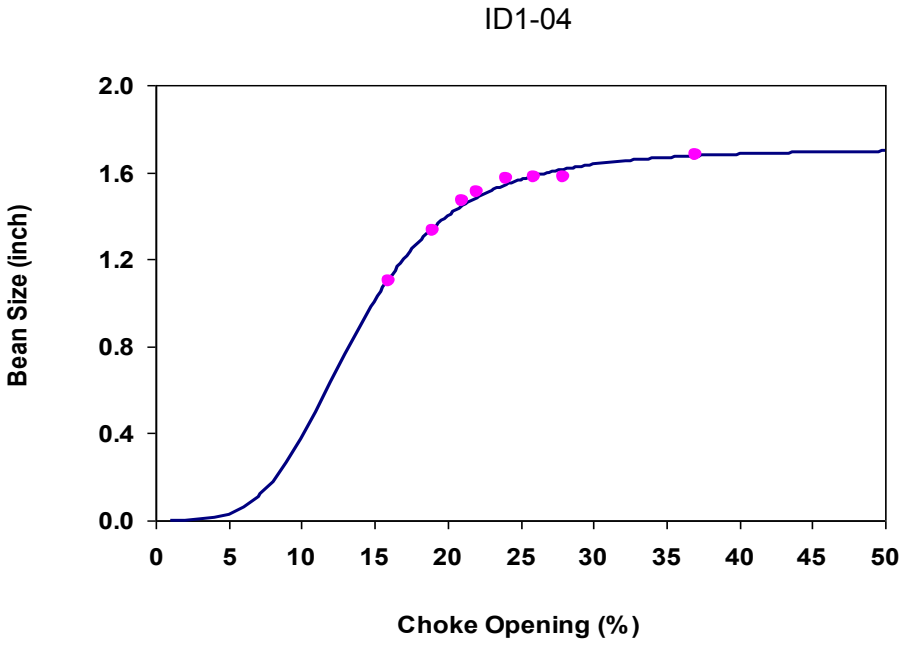

Figure 2-4: Regression analysis results ID1-04 well

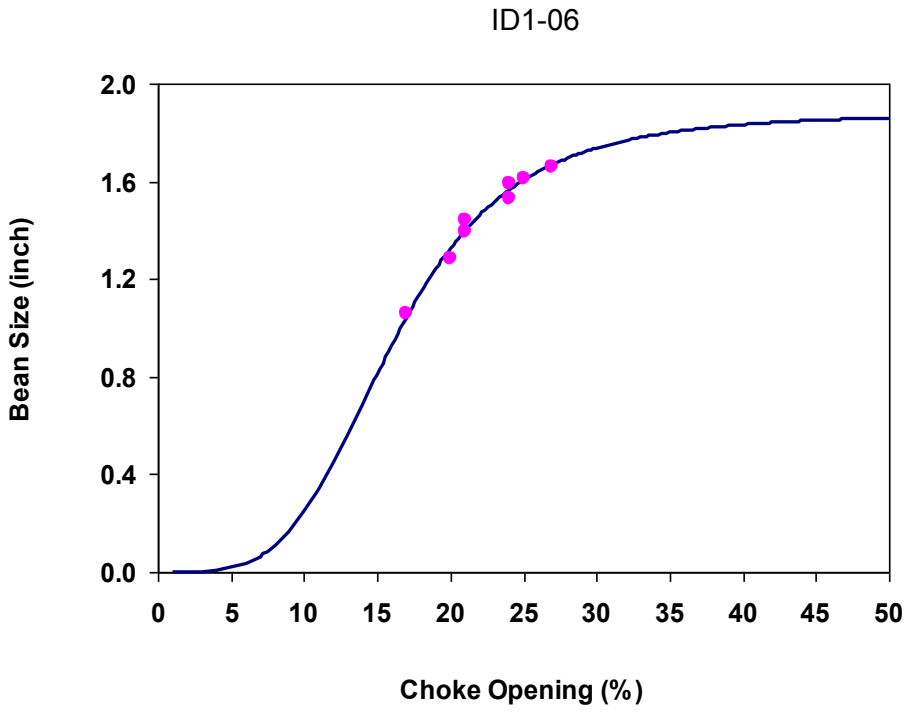

Figure 2-5: Regression analysis results ID1-06 well

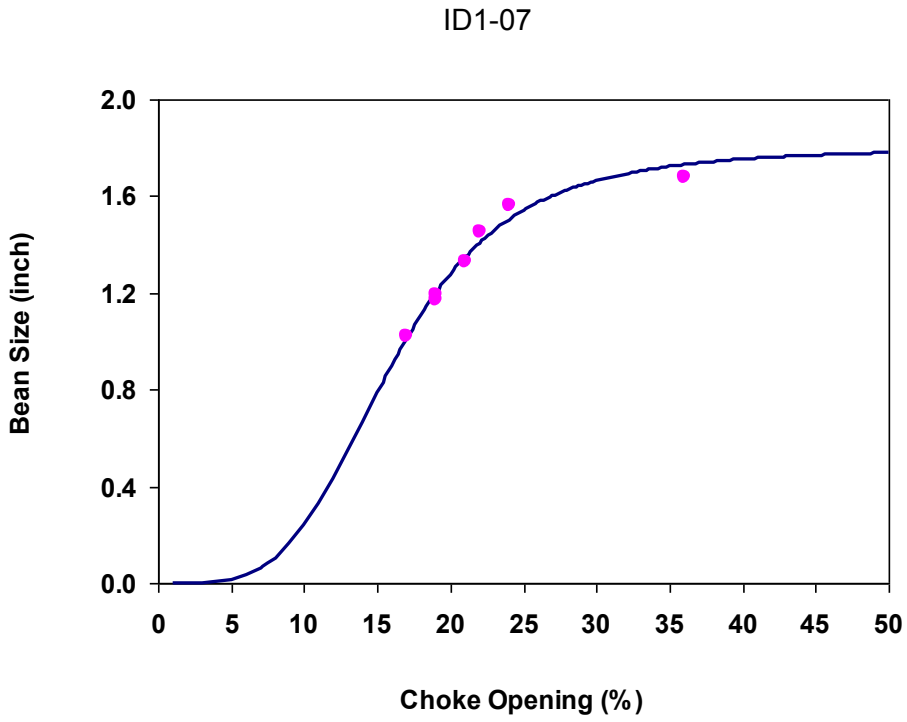

Figure 2-6: Regression analysis results ID1-07 well

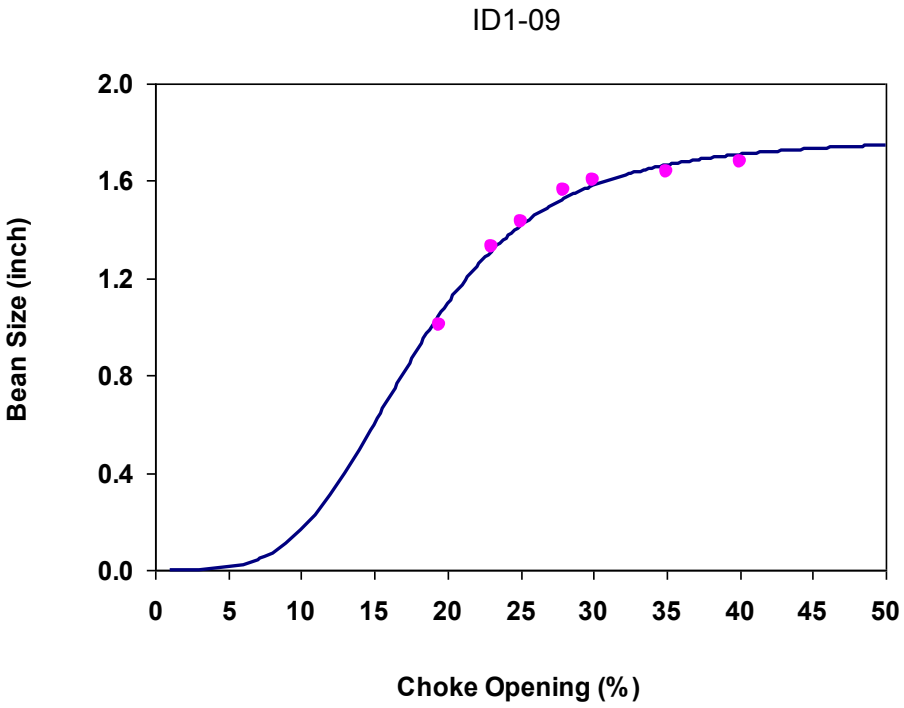

Figure 2-7: Regression analysis results ID1-09 well

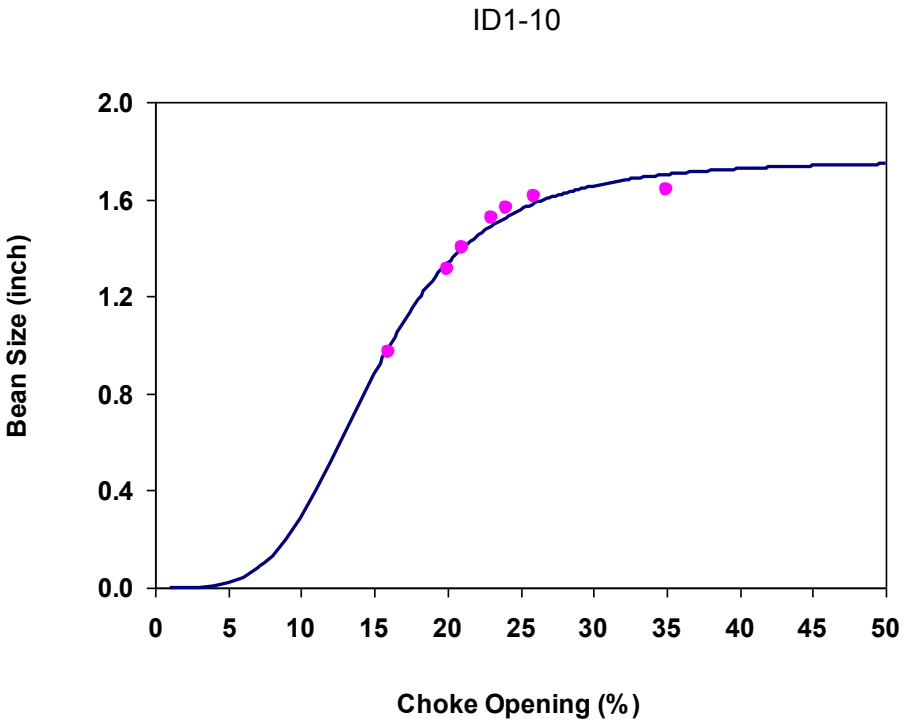

Figure 2-8: Regression analysis results ID1-10 well

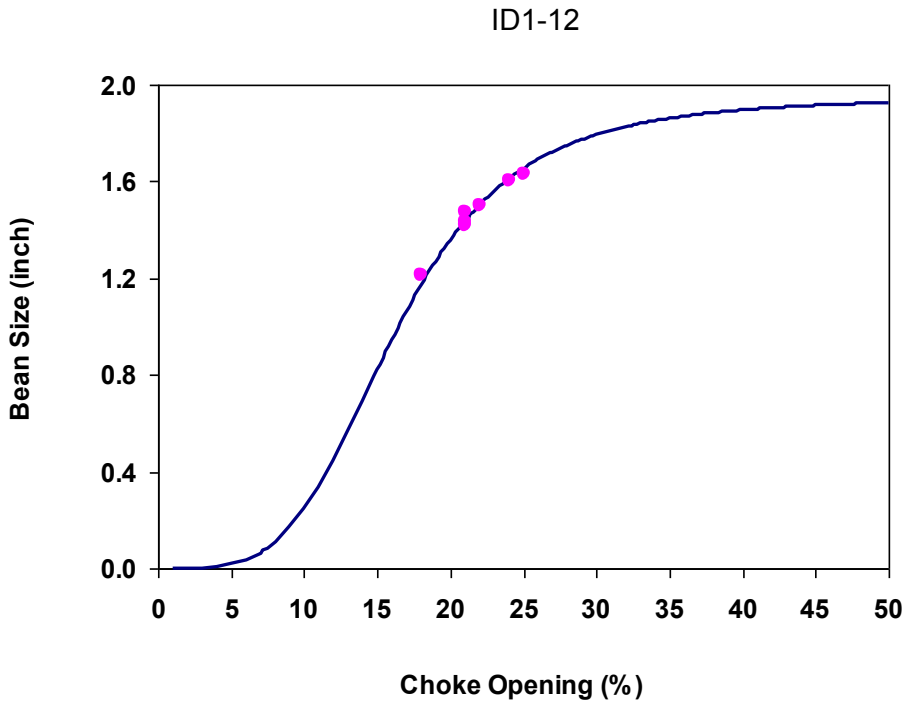

Figure 2-9: Regression analysis results ID1-12 well

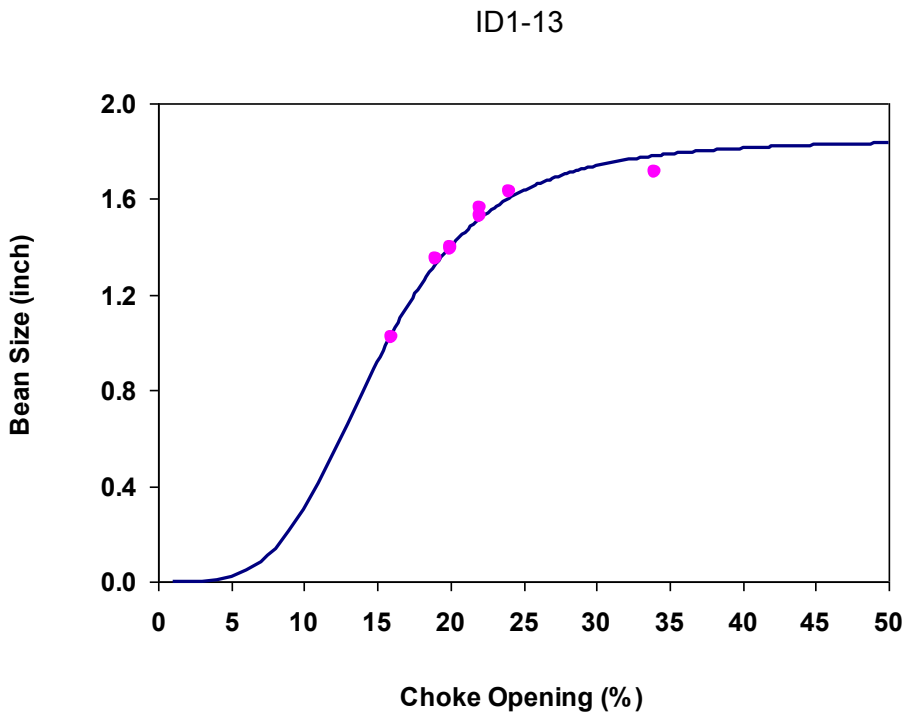

Figure 2-10: Regression analysis results ID1-13 well

Table 2-4: Constants of relations and the corresponding coefficient of determinations for all wells

well	a	b	R^2
ID1-01	1.95E-05	3.46E-05	0.9807
ID1-02	1.94E-05	3.64E-05	0.9837
ID1-03	1.6 E-05	2.93E-05	0.9615
ID1-04	2.84E-05	4.84E-05	0.9848
ID1-06	1.49E-05	2.79E-05	0.9782
ID1-07	1.53E-05	2.75E-05	0.9726
ID1-09	1.01E-05	1.79E-05	0.9842
ID1-10	1.97E-05	3.46E-05	0.9763
ID1-12	1.44E-05	2.8 E-05	0.9686
ID1-13	1.94E-05	3.59E-05	0.9722
ID2-01	3.03E-05	1.61E-05	0.9784
ID2-02	2.56E-05	1.36E-05	0.9923
ID2-03	2.78E-05	1.54E-05	0.9852
ID2-04	2.93E-05	1.51E-05	0.9297
ID2-06	3.05E-05	1.65E-05	0.9761
ID2-07	2.70E-05	1.43E-05	0.9789
ID2-09	2.63E-05	1.40E-05	0.9791
ID2-10	1.90E-05	9.97E-06	0.9873
ID2-12	2.08E-05	1.23E-05	0.9445
ID2-14	1.50E-05	8.64E-06	0.9607

2.7 Water cut sensitivity analysis for bean size calculation

As already mentioned, water cut is one of the Pipesim input data for simulating a choke. Since there are usually some uncertainties in the water production rate of well, the sensitivity analysis is performed to make it clear that how much the water cut would influence on the choke simulation results. For this purpose, one data point of test separator from ID1-01 and another data point from ID2-01 are used, which are demonstrated in the following table.

Table 2-5: Two data points used in simulation for sensitivity analysis

Date	09/02/2008	08.06.2008
Well	ID1-01	ID2-01
choke opening Percent	36	25
Well head Pressure	212.8	210.7
well head temperature	83.1	82.8
downstream pressure	120	122

Through the simulation, while changing the water cut from 0 – 15 % the bean size is calculated. Resulted data are represented in below table.

Table 2-6: The bean size versus water cut for ID1-01 and ID2-01

Water cut percent	**0**	**5**	**10**	**15**
Bean size ID1-01 (inch)	1.674	1.676	1.678	1.68
Bean size ID2-01 (inch)	1.639	1.64	1.642	1.644

As indicated in the table, despite changing water cut by 15 %, the bean size is increased just over around 0.001 inch. As a result, it is assured that this parameter has no considerable effect on the choke simulation and can be neglected in the further simulations.

2.8 API sensitivity analysis for bean size

Since sampling and PVT measurements to define fluid properties have been accomplished only in 1999, there might be some uncertainties in different parameters such as API gravity. In the other words, it should also be noted that such parameters are more likely to be changed during the production time. Therefore, the goal is evaluate the condensate API gravity because it is also utilized in Pipesim for choke simulation. In sensitivity analysis of API gravity, two data points from ID1-01 and ID2-01 (mentioned in table 2-5) were employed. Simulating in Pipesim, the bean size is calculated while changing API gravity in the range of 46 to 54. Obtained results are shown in the table below.

Table 2-7: API Sensitivity analysis for bean size for ID1-01

API	48	50	52	54
Bean size ID1-01 (inch)	1.679	1.677	1.676	1.675

Table 2-8: API Sensitivity analysis for bean size for ID2-01

API	46	50	54	58
Bean size ID2 (inch)	1.645	1.643	1.64	1.638

2.9 Results

2.9.1 Total enriched gas flow rate obtained from choke simulation of the field data set

In the previous section, a relation between the bean size and the choke opening was derived. Applying this relation, choke is simulated based on the field data set and furthermore the enriched gas flow rate of each well is calculated. The steps of this procedure are presented as follows:

1) A specific date (e.g. 3.11.2010) for simulation is picked out.

2) As on that date, upstream pressure and temperature, choke opening percentage and downstream pressure are extracted from the production daily reports.

3) Using equation 2-5, bean size is determined according to choke opening percentage for all 20 wells of ID1 and ID2 platforms.

4) Simulating the choke in Pipesim to obtain gas and condensate flow rates of each well.

5) After the gas and condensate flow rates were determined, flow rates of enriched gas for each well are calculated using equations 2-1 and 2-2.

6) Total enriched gas flow rate of all wells is defined as simulated enriched gas flow rate.

7) Simulated rich gas flow rate is compared with the reported enriched gas flow rate, and the relative error percentage is recorded.

Results for the specific date of 3.11.2010 can be observed in the following tables.

Table 2-9: Production flow rates results for ID1 & ID2 simulated by Pipesim in 3.11.2010

Well number	Up. Press.	Down. Press.	Up. Temp.	bean size	gas flow rate	condensate flow rate	equivalent condensate flow rate	enriched gas flow rate
	barg	barg	˚C	inch	MMSCF/D	STBD	MMSCFD	MMSCFD
ID1-01	214.3	113.7	83.1	1.46	103.21	4691.21	3.74	106.95
ID1-02	212.2	113.7	81.2	1.42	97.15	4415.8	3.52	100.67
ID1-03	210.8	113.7	81.3	1.5	107.72	4896.04	3.9	111.62
ID1-04	209.8	113.7	83.2	1.48	103.95	4724.81	3.77	107.72
ID1-06	211.1	113.7	80.7	1.64	129.12	5868.83	4.68	133.8
ID1-07	209.2	113.7	83.5	1.46	100.82	4582.48	3.65	104.47
ID1-09	210.3	113.7	82.8	1.53	111.44	5065.42	4.04	115.48
ID1-10	212	113.7	82.1	1.39	92.82	4218.85	3.36	96.18
ID1-12	210.3	113.7	81.2	1.43	97.7	4440.72	3.54	101.24
ID1-13	210.6	113.7	83.2	1.46	101.52	4614.38	3.68	105.2
ID2-01	209.5	109.1	83	1.49	109.05	3634.75	2.89	111.93
ID2-02	226	109.1	82	0.89	41.85	1394.85	1.11	42.95
ID2-03	210.3	109.1	82	1.42	99.62	3320.57	2.64	102.26
ID2-04	211.8	109.1	80.7	1.19	70.64	2354.45	1.87	72.5
ID2-06	209.3	109.1	83.3	1.56	119.35	3978.14	3.16	122.51
ID2-07	212.7	109.1	81.4	1.39	96.61	3220.27	2.56	99.17
ID2-09	210.3	109.1	82.9	1.5	110.94	3697.84	2.94	113.87
ID2-10	212.5	109.1	81.4	1.41	99.32	3310.71	2.63	101.95
ID2-12	209	109.1	81.1	1.44	102.06	3401.82	2.7	104.76
ID2-14	209.6	109.1	84.6	1.47	105.8	3526.62	2.8	108.6

Table 2-10: Percent error for ID1 & ID2 in 3/11/2010

Percent error	Total enriched gas flow rate (reported)	Total enriched gas flow rate (simulated)
1.3	2091.68	2063.83

Calculation results for 63 field data set are presented in the table below. It is also possible to perform the same simulation for the production days in which one of two platforms is shut down. Therefore, our derived choke relation is subjected to a practical test when half of the production system is out of service. Studies showed that the suggested model may be used successfully to calculate the gas and condensate flow rate of each platform separately. The symbol “*” in the following table indicates the mentioned dates.

Table 2-11: Final Choke simulated results for ID1 and ID2

Date	Total enriched gas flow rate (reported)	Total enriched gas flow rate (simulate)	percent error	Date	Total enriched gas flow rate (reported)	Total enriched gas flow rate (simulate)	percent error
	(MMSCFD)	(MMSCFD)			(MMSCF)	(MMSCFD)	
03/11/2010	2091.68	2063.83	1.3	01/07/2007	2306.13	2145.9	6.9
28/10/2010	2133.77	2123.83	0.5	19/6/2007	2306.13	2119.83	8.1
20/9/2010	2095.93	2115.13	0.9	05/05/2007	2316.26	2173.92	6.1
15/8/2010	2177.68	2141.17	1.7	19/4/2007	2065.36	2215.09	7.2
10/07/2010	2079.6	2157.34	3.7	04/03/2007	2288.13	2227.42	2.7
20/6/2010	2082.83	2211.56	6.2	27/2/2007	2294.51	2209.44	3.7
24/5/2010	2231.02	2216.08	0.7	09/01/2007	2209	2156.77	2.4
29/4/2010	2122.81	2137.42	0.7	20/12/2006	2277.63	2238.73	1.7
02/03/2010	1854.82	1709.54	7.8	24/11/2006	2289.63	2193.16	4.2
06/01/2010	2316.64	2329.19	0.5	19/10/2006	1908.21	1791.89	6.1
01/12/2009	2294.13	2349.21	2.4	03/09/2006	1979.47	1928.12	2.6
29/11/2009	2293.01	2327.89	1.5	02/08/2006	1725.57	1741.35	0.9
28/10/2009	2306.13	2275.37	1.3	16/7/2006	2037.98	2008.72	1.4
01/09/2009	2348.51	2313.23	1.5	14/6/2006	1775.07	1724.73	2.8
08/07/2009	2320.01	2300.16	0.9	31/5/2006	2055.98	1927.2	6.3
24/6/2009	2321.89	2326.06	0.2	03/04/2006	2150.49	2049.91	4.7
03/04/2009	2312.88	2320.51	0.3	18/3/2006	1908.96	2003.86	5
11/03/2009	2318.51	2298.06	0.9	26/2/2006	2112.24	1985.05	6
17/2/2009	2316.26	2341.44	1.1	14/1/2006	2108.86	1979.14	6.2
06/01/2009	2309.51	2313.83	0.2	05/12/2005	1991.1	1925.31	3.3
08/12/2008	2311.01	2273.26	1.6	14/11/2005	1823.83	1699.35	6.8
04/09/2008	2300.13	2210.74	3.9	30/10/2005	1747.32	1849.09	5.8
19/8/2008	2223.62	2214.85	0.4	1/10/2006*	1154.38	1157.97	0.3
08/07/2008	2266.38	2213.96	2.3	24/4/2007*	1138.63	1046.13	8.1
24/6/2008	2300.13	2212.06	3.8	14/10/200*	1125.13	1076.76	4.3
17/3/2008	2299.76	2130.93	7.3	5/11/2007*	1124.75	1123.74	0.1
02/02/2008	2294.88	2173.02	5.3	26/4/2008*	1132.63	1119.67	1.1
06/01/2008	2309.51	2184.17	5.4	6/10/2008*	1034.37	1114.33	7.7
06/12/2007	2289.63	2204.07	3.7	29/9/2008*	1083.5	1142.41	5.4
06/10/2007	2308.38	2269.1	1.7	4/10/2008*	1066.99	1088.98	2.1
01/09/2007	2288.13	2198.69	3.9	22/4/2009*	1089.5	1045.86	4
27/8/2007	2282.88	2105.86	7.8				
Mean percentage error =3.4							

2.9.2 Critical Flow

As stated earlier, flow through choke can be classified into two main categories: critical and sub-critical. It was assumed in simulation that the flow rate was of critical type and the obtained simulation results confirm this assumption.

On the other hand, the following equation can be used to identify the type of flow through a choke:

$$\frac{P_{dn}}{P_{up}} \leq \left(\frac{2}{k+1}\right)^{\frac{k}{k-1}} \qquad (2-6)$$

Where (Pdn / Pup) is critical pressure ratio at which the flow through the choke becomes critical and k is the fluid specific heat ratio (Cp/Cv).

In table 2-12 the specific heat capacity is presented for ID1-01.

Table 2-12: Heat specific capacity and k for ID1 & ID2

Cv	**Cp**	**k**
J/(g.K)	J/(g.K)	
1.51	1.92	1.28

With the value of k being considered (1.28), the critical flow occurs when the critical pressure ratio is greater than or equal to 0.55 (by equation 2-6). In table 2-13 critical pressure ratios of ID1 -01 in various dates are illustrated.

Table 2-13: Critical pressure ratio for ID1-01

Date	**Upstream Pressure**	**Downstream Pressure**	**critical pressure ratio**
	barg	**barg**	
30/10/2005	233.6	107.9	0.464
24/11/2006	227.6	115.6	0.51
06/12/2007	220.7	116.7	0.531
17/2/2009	233.1	115.9	0.499
19/8/2008	211.5	115.7	0.549
03/11/2010	214.3	113.7	0.533

As it is expected, the critical pressure ratio in the above table is often less than 0.55, which means that the flow is critical.

2.10 GLR sensitivity analysis for production rate

In simulation of choke to determine the gas and condensate flow rates, average value of GLR's was used. Therefore it seems necessary to investigate the effects of GLR on the obtained results. Such sensitivity analysis being performed, data of a typical day (10/7/2010) was extracted. The average value of GLR's had been measured as 22000 (SCF/STB) and 30000 (SCF/STB) for ID1and ID2 respectively, while the range of the GLR used for the sensitivity analysis is listed in the following table:

Table 2-14: GLR used for sensitivity analysis

GLR of ID1 (SCF/STB)	GLR of ID2 (SCF/STB)
17000	25000
22000	30000
27000	35000
32000	40000

Simulated total enriched gas flow rates for different GLR's are demonstrated in the figure 2-11. As can be seen from the figure, the total enriched gas flow rate is not very dependent on GLR. For example1000 SCF/STB increase in GLR, increase a flow rate of 4.4 MMSCFD which is equivalent to about 0.2% of total rich gas flow rate. It is obviously small enough and therefore can be neglected. Consequently, using the average value of GLR's does not lead to a considerable error in the simulation results.

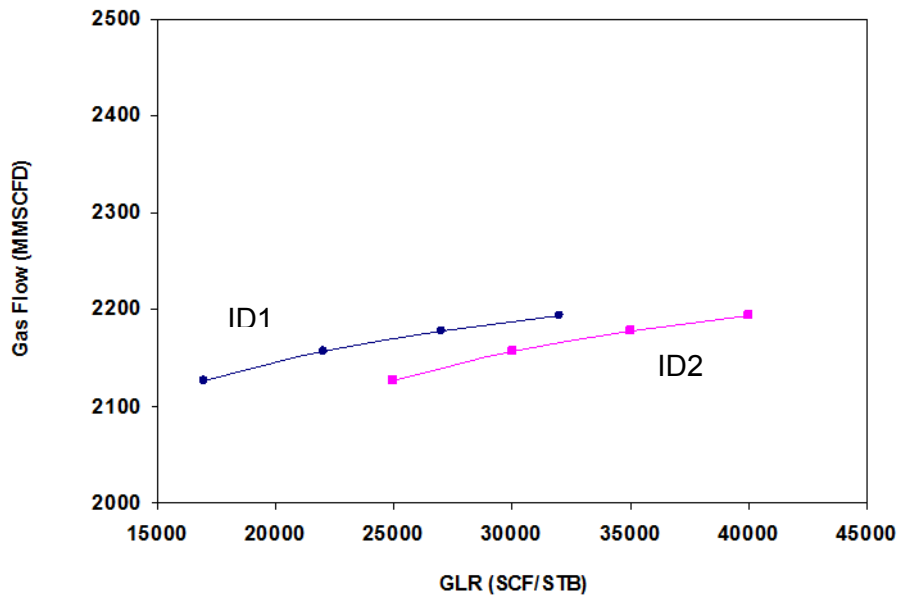

Figure 2-11: Simulated total rich gas flow rate for different GLR's

3 Well flow modelling

3.1 Introduction

In this chapter, wells are going to be simulated using Pipesim software. Since a variety of models can be utilized to simulate a typical well, firstly with the regard to the measured data of wells (PSP) a proper model was chosen, then with the aid of chosen model and output data from choke calculations discussed in the last chapter, the wells were simulated and bottom hole pressure was determined. Moreover, pressure-temperature profiles as well as condensate accumulation amount are more outputs of this simulation. Ultimately, a sensitivity analysis was performed for the parameters undergoing uncertainty.

3.2 Introducing PSP Tested Wells

Production Services Platform (PSP) is a kind of production logging tools which provides three-phase flow profiles and production monitoring or diagnostic information. It consists of a number of different tools such as Platform Basic Measurement Sonde (PBMS), casing collar locator (CCL), Flow-Caliper Imaging Sonde (PFCS), Gradiomanometer* Sonde (PGMS), PS Platform Inline Spinner (PILS), Gas Holdup Optical Sensor Tool (GHOST) and several other tools which have the capability to measure pressure and temperature gradient and other parameters, both in real-time and memory modes.

PSP test data of four wells of ID1 platform are available to simulate the wells. Each test is conducted at three different gas flow rates. The data of wells and flow rates is presented in the following table.

Table 3-1: PSP tested wells with the flow rates

Well number	**Well type**	**Flow rates**		
		(MMSCFD)		
ID1-01	deviated	31.6	43.5	63
ID1-06	deviated	30	50.5	88
ID1-07	deviated	29	57	72
ID1-13	vertical	33	57	82

As shown in the table among four PSP tested wells the well ID1-13 is vertical while the three others are deviated.

3.3 Model selection for simulation

3.3.1 Available Models

A variety of models can be used to simulate a well. For instance for gas-condensate reservoirs Duns and Ros, Gray, Ansari, Aziz, and Fogorasi and Govier are usually utilized. In this study, 11 models were applied for initial simulation and among those the best approach will be chosen. Applied models are brought in the following table.

Table 3-2: Applied model for well simulation

Number	Model	abbreviation
1	Ansari	ANSARI
2	Beggs and Bril (Original)	BBO
3	Duns and Ros	DR
4	Govier, Aziz and Fogarasi	GA
5	Gray (Original)	GRAYO
6	Gray (Modified)	GRAYM
7	Hagedorn and Brown	HBR
8	Mukherjee and Brill	MB
9	No slip Assumption	NOSLIP
10	Orkiszewski	ORK
11	TUFFP Unified 2-Phase	ZHANG

3.3.2 Model Selection Method

As mentioned in the last section, PSP tested wells data will be used to select the most proper model amongst all available models. In other words, this data are the basic criteria for comparison, and the model which has the closest estimate to these test values will be the best model chosen. The flowchart below describes the model selection process.

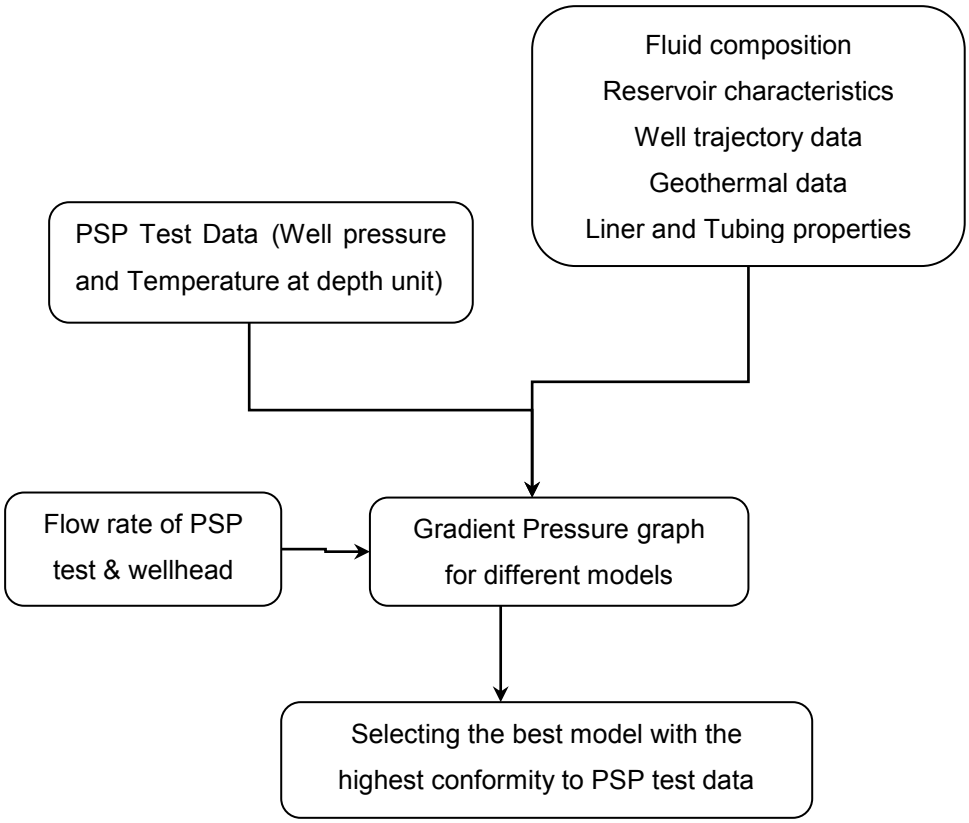

Figure 3-1: Model selection process for well simulation

3.4 Input data to Pipesim software

3.4.1 Reservoir fluid composition

The following will present the components of used fluid as well as properties and binary interaction coefficients of existing cuts in the fluid. It is noteworthy that the Peng- Robinson tri-parametric equation is concerned with calculating fluid properties.

Table 3-3: Reservoir fluid composition and its properties

Component	Mole Fraction	Boiling Point (˚F)	MW	SG	Tc (˚F)	Pc (psi)
N2-C1	0.861	-246.43	16.622	0.316	-122.46	659.135
H2S	0.0024	-76.63	34.08	0.801	212.09	1296.183
CO2	0.0193	-109.21	44.01	0.818	87.89	1069.865
C2-C3	0.072	-82.06	33.864	0.398	124.016	682.978
i-C4 to C6	0.0228	77.64	67.303	0.616	349.873	515.487
C7 to C12	0.0199	316.28	127.066	0.774	600.024	446.411
C13+	0.0026	652.1	274.609	0.861	807.362	215.219

Table 3-4: Interaction coefficients of existed cuts in the reservoir fluid

Component	N2-C1	H2S	CO2	C2-C3	i-C4 to C6	C7 to C12
H2S	0					
CO2	0	0				
C2-C3	0.00414	0	0			
i-C4 to C6	0.01874	0	0	0.00537		
C7 to C12	0.04162	0	0	0.02012	0.00481	
C13+	0.08657	0	0	0.05524	0.02724	0.0094

3.4.2 Reservoir properties

The table beneath demonstrates Pipesim input reservoir properties data.

Table 3-5: Reservoir properties

Property	
Reservoir Pressure (Psi)	5290
Reservoir Temperature (˚F)	215
Drainage Radius (m)	1000
Reservoir Thickness (m)	276.2
Skin	-2

It is noteworthy that wellbore diameter is considered equal to tubing pipe diameter (6.151) for simulation. In the following we will perform sensitivity analysis test for this variable.

Permeability is also another input parameter for well simulation. Below, the equation is defined to calculate the permeability for the reservoir with different layers [28].

$$k = \frac{\sum_{i=1}^{n} h_i k_i}{\sum_{i=1}^{n} h_i} \qquad (3-5)$$

In this equation, hi and ki are the thickness and permeability of each layer respectively. Based on the extracted data of different layers of the reservoir and equation 3-5 values of reservoir rock permeability is calculated 8.42 md.

3.4.3 Wells' deviation (trajectory) data

Wells' deviation data consists of measures depth (MD) and true vertical depth (TVD) provided from drilling reports.

3.4.4 Geothermal data

Here we use temperature values measured in PSP tests as input data.

3.4.5 Tubing and Liner specifications

As mentioned before, the wells are built cased hole with tubing and liner. Since there exist some corrosive components like H2S in the fluid constitution it is impossible to complete the well without tubing. Specifications of tubing used in ID1-01 wells are demonstrated in the following table as instances. It should be added that the great value of tubing diameter is due to production of high flow rate. In this table, bottom MD indicates final depth of production string.

Table 3-6: Tubing and Liner specifications for ID1-01

	Bottom MD	**ID**	**Thickness**	**Roughness**
	(m)	(inches)	(inches)	(inches)
Tubing	3114	6.151	0.707	0.0018
Liner 1	3881	6.151	0.707	0.0018
Liner 2	4456	6.059	0.783	0.0018

3.4.6 PSP test data of ID1-01

Temperature and pressure data obtained by running PSP log in terms of elevation should be used as input to the simulator. This PSP data with the aid of pressure gradient graph is a base for choosing the best correlation. Well head data and elevation data for the highest flow rate in PSP tests of ID1-01 wells are shown in the following table.

Table 3-7: PSP test data of ID1-01

Gas flow rate	**condensate flow rate**	**Wellhead pressure**	**GOR**
(MMSCFD)	(STBD)	(psi)	(SCF/STB)
31.6	1735	3635	18213.3
43.5	2984	3612	14577.7
63	4655	3538	13533.8

Table 3-8: Some pressure & temperature well data versus depth obtained from PSP Test of 63 MMSCFD

MD (m)	**P (psi)**	**T (˚C)**
3787.7496	4450.9819	101.879
3792.1692	4450.9814	101.8767
3796.7412	4451.1567	101.8758
3802.8372	4452.439	101.8937
3804.3612	4452.7969	101.8985
3808.9332	4453.9155	101.9137
3813.5052	4454.8652	101.9262

3.5 Well simulation results for choosing a proper model

In the following, we'll present obtained results from ID1-01 well simulation made by Pipesim software in 3 different flow rates. For aforesaid well, pressure is profiled in terms of elevation for 11 relevant models.

Also by pressure-elevation data of PSP test (mentioned as Measured Data) which are plotted in the same diagram, the models' match degree can be observed. Afterward, mean absolute error and percent error for entire models are tabulated for a more precise comparison. Simulation results for ID1-06, ID1-07 and ID1-13 are represented in Appendix C.

3.5.1 Well simulation results for ID1-01

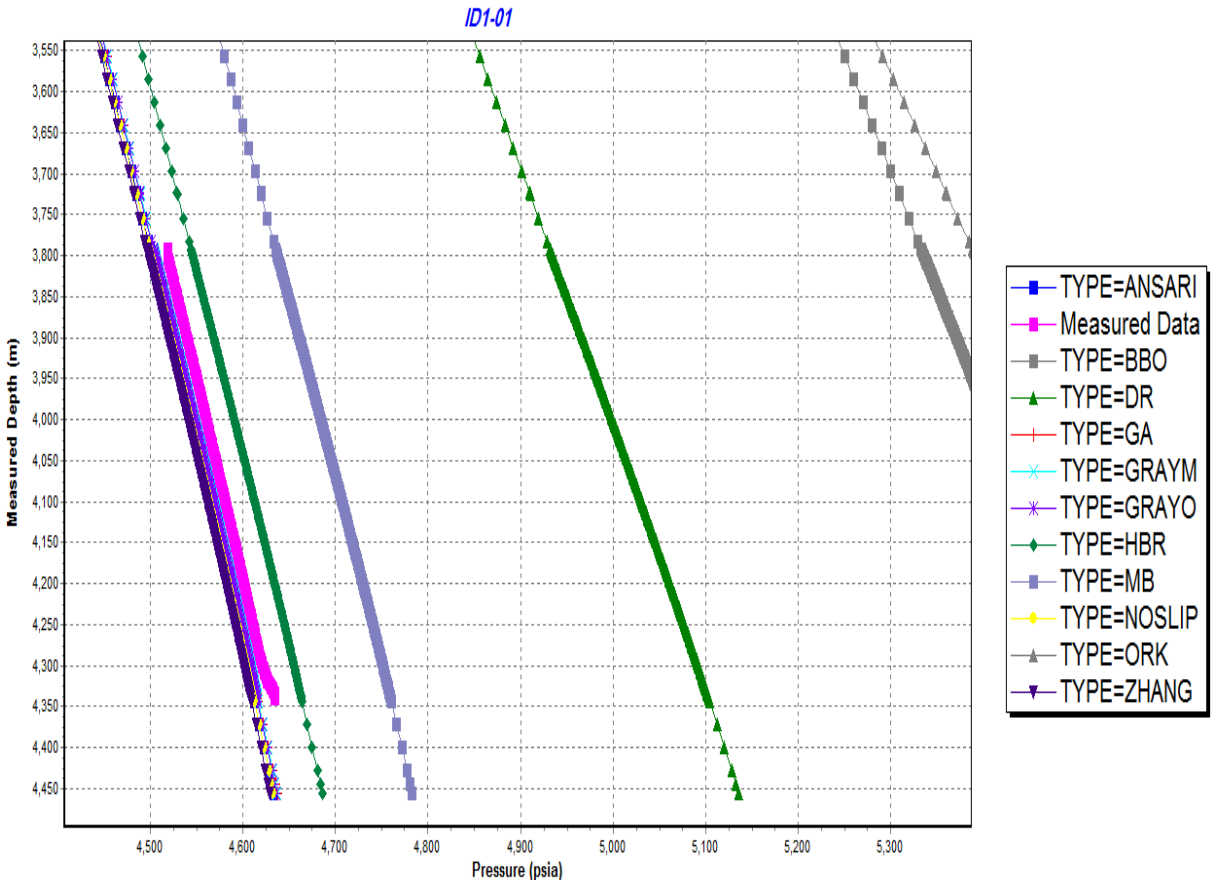

Figure 3-2: Pressure versus measured depth for ID1-01 with 31.6 MMSCFD Gas rates

Table 3-9: Model's Absolute error & Percent error for ID1-01 with 31.6 MMSCFD gas rate

Model	Absolute Error (Psi)	Percent Error
Gray (Modified)	13	0.3
Govier, Aziz and Fogarasi	13	0.3
Gray (Original)	14	0.3
Ansari	17	0.4
No slip Assumption	17	0.4
Zhang	20	0.5
Hagedorn and Brown	31	0.7
Mukherjee and Brill	125	2.7
Duns and Ros	446	9.8
Beggs and Bril (Original)	853	18.7
Orkiszewski	928	20.3

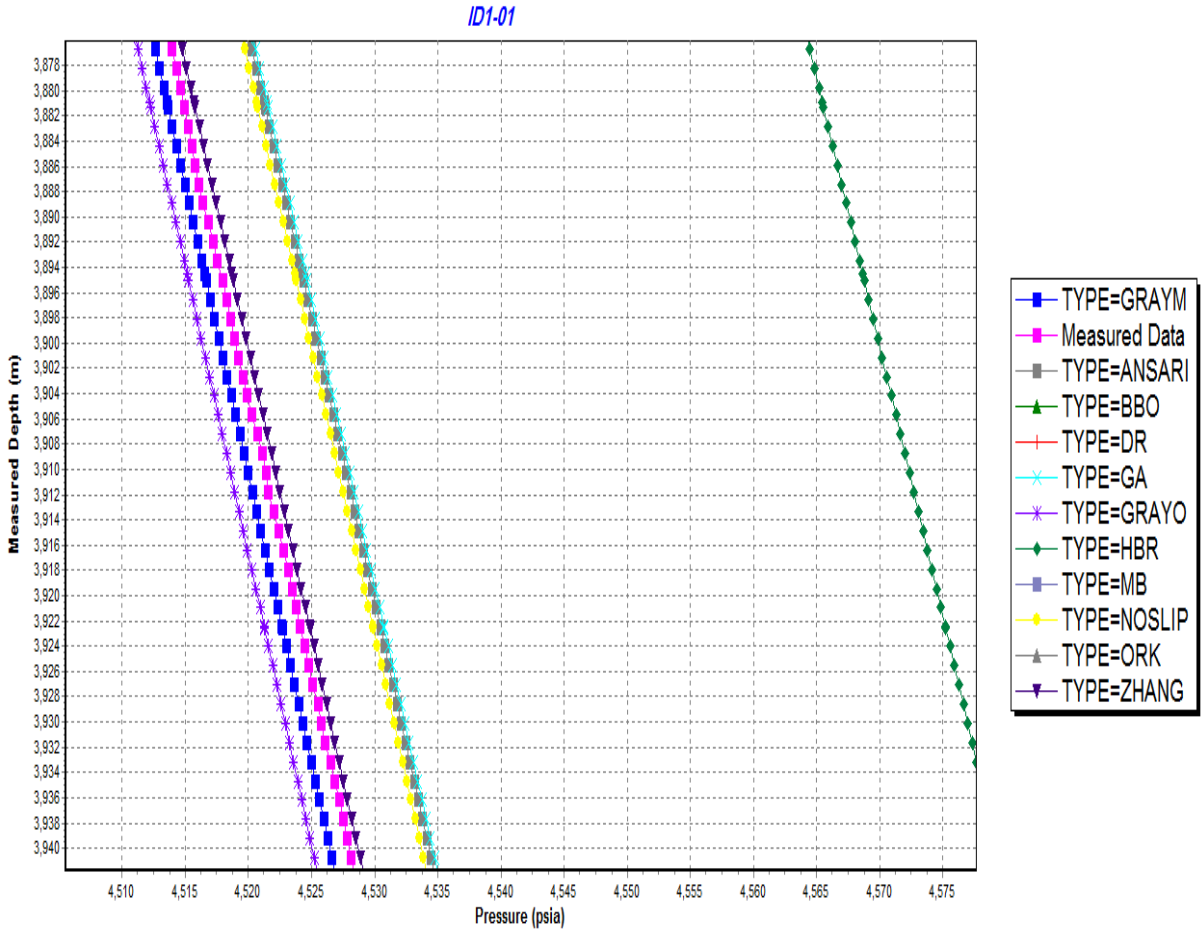

Figure 3-3: Pressure versus measured depth for ID1-01 with 43.5 MMSCFD Gas rates

Table 3-10: Model's Absolute error & Percent error for ID1-01 with 43.5 MMSCFD gas rate

Model	Absolute Error (Psi)	Percent Error
Zhang	1	0
Gray (Modified)	2	0
Gray (Original)	3	0.1
No slip Assumption	7	0.1
Ansari	7	0.2
Govier, Aziz and Fogarasi	7	0.2
Hagedorn and Brown	54	1.2
Mukherjee and Brill	125	2.8
Duns and Ros	322	7.1
Beggs and Bril (Original)	831	18.2
Orkiszewski	925	20.3

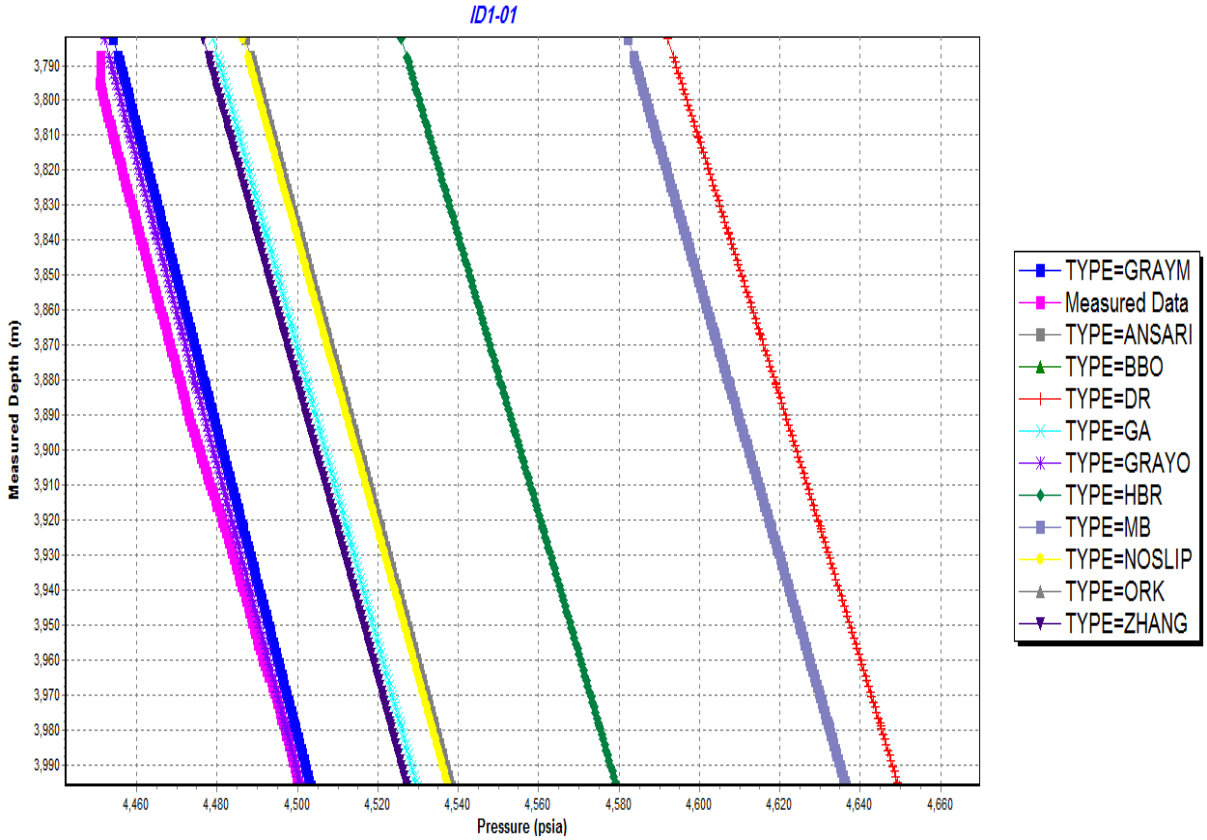

Figure 3-4: Pressure versus measured depth for ID1-01 with 63 MMSCFD Gas rates

Table 3-11: Model's Absolute error & Percent error for ID1-01 with 63 MMSCFD gas rate

Model	Absolute Error (Psi)	Percent Error
Gray (Original)	3	0.1
Gray (Modified)	5	0.1
Zhang	28	0.6
Govier, Aziz and Fogarasi	30	0.7
No slip Assumption	38	0.9
Ansari	39	0.9
Hagedorn and Brown	81	1.8
Mukherjee and Brill	139	3.1
Duns and Ros	153	3.4
Orkiszewski	797	17.6
Beggs and Bril (Original)	805	17.8

Table 3-12: Model's mean absolute error and mean percent error for ID1-01 including all gas rates

Model	Mean Absolute Error (Psi)	Mean percent Error
Gray (Modified)	6	0.1
Gray (Original)	6	0.1
Zhang	16	0.4
Govier, Aziz and Fogarasi	17	0.4
No slip Assumption	21	0.5
Ansari	21	0.5
Hagedorn and Brown	55	1.2
Mukherjee and Brill	130	2.9
Duns and Ros	307	6.7
Beggs and Bril (Original)	829	18.2
Orkiszewski	883	19.4

3.5.2 A chosen proper model

As simulation results show, the Gray Modified model has the least errors among the three deviated wells ID1-01, ID1-06, ID1-07 and for well ID1-13 which is absolutely vertical, Ansari model presents the best match. Thus, these two models are selected for simulating wells. A summary of model selection results are shown in the table beneath.

Table 3-13: Mean absolute error and mean percent error in chosen model for ID1

Well	Chosen Model	Mean absolute error (psi)	Mean percent error
ID1-01	Gray (Modified)	6	0.1
ID1-06	Gray (Modified)	10	0.2
ID1-07	Gray (Modified)	17	0.4
ID1-13	Ansari	13	0.3

It should be noted that in addition to Gray Modified and Gray Original models, Aziz and Fogarasi, Govier, Zhang, No slip Assumption, Ansari models show high accuracy and errors less than 1%. For simulated vertical wells, the so-called models, in addition to Hagedorn and Brown model show less-than 1% errors.

3.5.3 Temperature, Pressure, Liquid Hold-Up Profile, and Well Flow Regime

Temperature, pressure and liquid hold-up profile in terms of elevation with a PSP test (gas flow rate equal to 31.6 MMSCFD) for well ID1-01 are shown in the following table. According to these diagrams, fluid temperature varies from 178 to 215 ˚F inside the well, and there is an average increase of 0.8 with an increase of 100m in depth. Fluid pressure also varies from 3600 psi to 4600 psi. It can be said that a 22 psi increase is observed in every 100m of increase in depth. The amount of liquid hold-up is also calculated ranging from 0.009 to 0.026.

As we descend in depth, the liquid hold-up amount will decrease. The well flow regime is slug in this test. Profiles of other tests for PSP tested wells are brought in the appendix D.

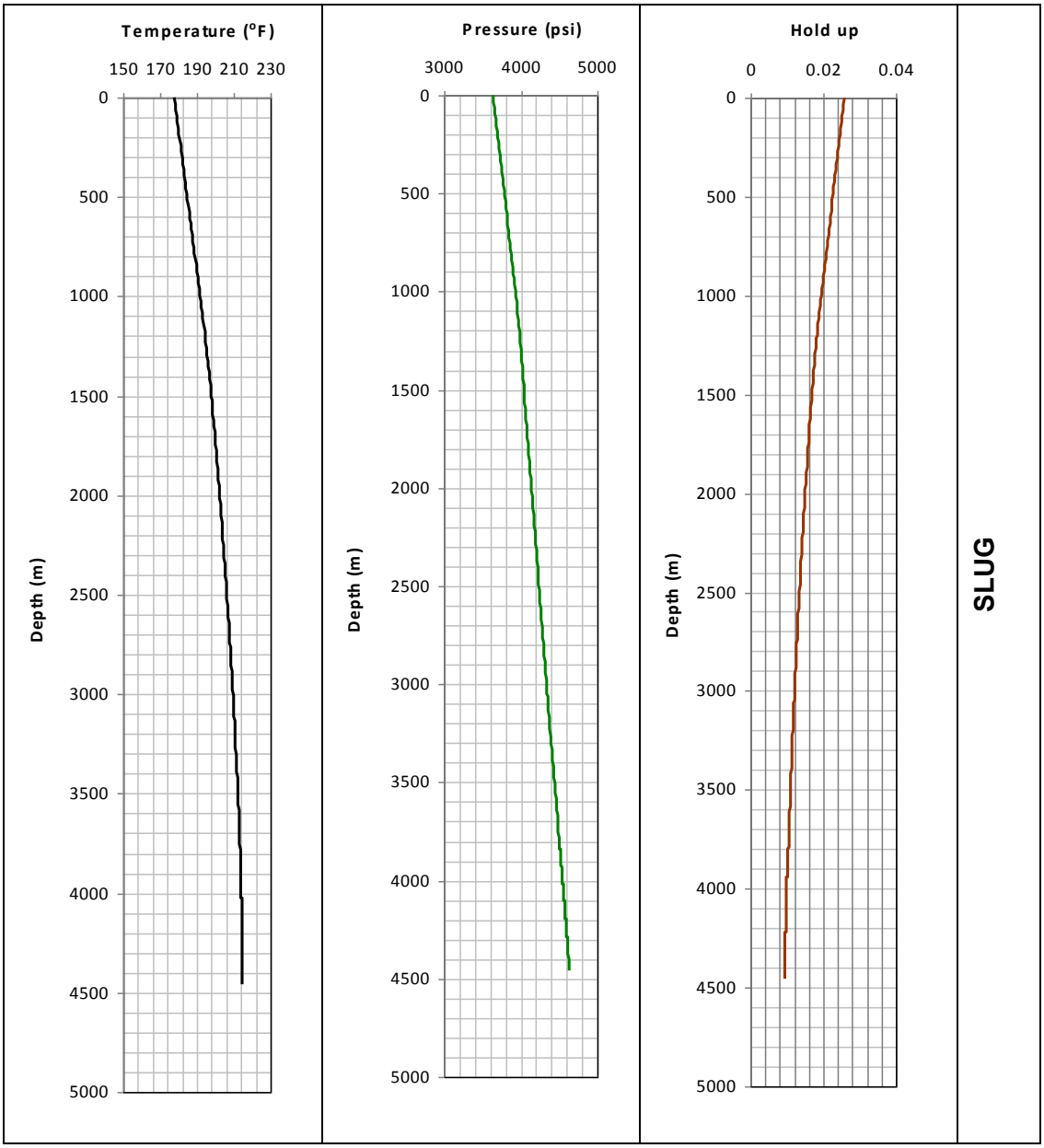

Figure 3-5: Temperature, Pressure, Liquid Hold-Up Profile, and Well Flow Regime for ID1-01 with 31.6 MMSCFD gas rate

3.5.4 Simulating bottom-hole pressure for wells

Choosing the best model among all the existing models, now we try to calculate bottom-hole pressure for PSP tested wells. To reach this goal we should specify gas-production flow rate for each well. Since there is no independent flow meter device for each well, measured gas flow rate which was obtained in choke simulations are utilized. Calculation sequences of bottom-hole pressure are as follows:

1) For a certain well (e.g. well ID1-01) we pick up a date (e.g. Nov 3 2010) among dates in which choke calculations is done.

2) Results of choke calculations executed by Pipesim simulator in chapter 3, obtained in the specified date will be used as input data for simulation. Table below illustrates choke calculation results used for bottom hole pressure simulation as an instance.

Table 3-14: An instance of choke calculation results used for bottom hole pressure simulation

Date	Well	Well head pressure	Gas flow rate
		(barg)	(MMSCFD)
03/11/2010	ID1-01	3122.9	103.21

3) Bottom-hole pressure will be calculated using the selected model and the data of previous stage.

4) These stages will be repeated for a well in several dates.

5) All of the stages above will be repeated for the entire wells.

A flowchart for these stages is represented in the following figure.

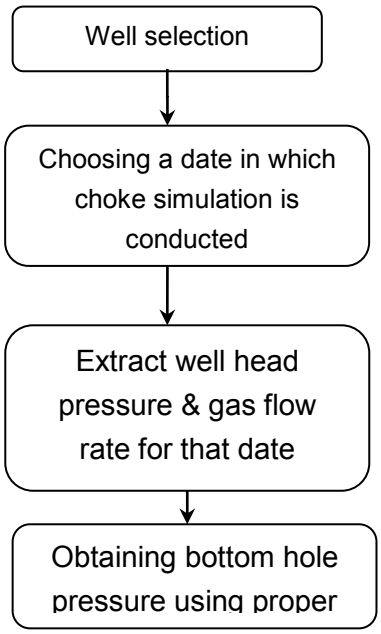

Figure 3-6: Flow chart for bottom hole calculation

Examples of Bottom-hole pressure calculations are shown in the table beneath.

Table 3-15: Bottom hole pressure results for ID1-01

Date	Wellhead pressure (Psi)	Gas flow rate (MMSCFD)	Bottom hole Pressure (psi)	Date	Wellhead pressure (Psi)	Gas flow rate (MMSCFD)	Bottom hole Pressure (psi)
30/10/2005	3403	117.2	4746	02/02/2008	3114	142.4	4632
14/11/2005	3385	116.7	4723	17/3/2008	3104	141.7	4616
05/12/2005	3381	116.5	4718	24/6/2008	3095	141.4	4604
14/1/2006	3805	44.9	4856	08/07/2008	3399	93.5	4588
26/2/2006	3380	116.5	4716	19/8/2008	3082	140.8	4584
18/3/2006	3364	116	4695	04/09/2008	3319	99.8	4536
03/04/2006	3370	116.2	4702	08/12/2008	3088	141.1	4593
31/5/2006	3390	116.8	4729	06/01/2009	3075	140.2	4572
14/6/2006	3361	115.9	4691	17/2/2009	3396	73.7	4482
16/7/2006	3327	114.9	4647	11/03/2009	3058	139.4	4546
02/08/2006	3332	115	4652	03/04/2009	3068	137.9	4544
03/09/2006	3348	115.4	4673	24/6/2009	3075	138.1	4553
19/10/2006	3383	116.6	4719	08/07/2009	3077	134.8	4527
24/11/2006	3316	114.5	4631	01/09/2009	3063	135.6	4520
20/12/2006	3319	114.6	4635	28/10/2009	3068	120.6	4402
09/01/2007	3323	114.8	4641	29/11/2009	3063	115.8	4361
27/2/2007	3323	114.8	4641	01/12/2009	3058	115.5	4352
04/03/2007	3319	114.6	4635	06/01/2010	3075	112.4	4349
19/4/2007	3309	114.3	4621	02/03/2010	3052	116.8	4356
05/05/2007	3544	65.5	4618	29/4/2010	3078	107.5	4317
19/6/2007	3296	113.9	4604	24/5/2010	3061	112.6	4334
01/07/2007	3284	113.4	4588	20/6/2010	3079	107.5	4319
27/8/2007	3298	113.9	4608	10/07/2010	3072	107.3	4309
01/09/2007	3294	113.8	4602	15/8/2010	3091	107.9	4335
06/10/2007	3136	143.2	4661	20/9/2010	3062	107.2	4298
06/12/2007	3216	117.4	4541	28/10/2010	3130	103.5	4348
06/01/2008	3116	142.2	4632	03/11/2010	3123	103.2	4338

A diagram of Bottom-hole pressure is provided in terms of the relevant dates to observe the trend of Bottom-hole pressure change in time lapse which is represented in the following figure.

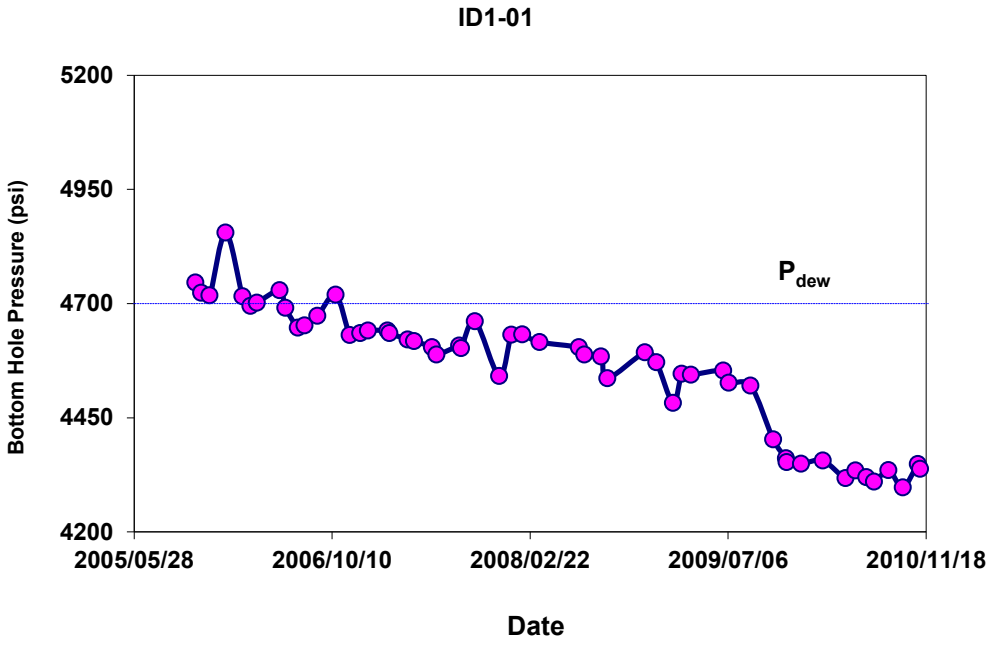

Figure 3-7: Decreasing bottom hole pressure during the years for ID1-01

Dew point pressure line is demonstrated in this figure to determine if the reservoir fluid is uniphasic (gas) or diphasic (gas-liquid) in the wellbore. Based on the studies about PVT data the pressure 4700 psi is considered as the dew point of reservoir fluid. In the following, Bottom-hole pressure profile in terms of time for PSP tested wells is presented. Dew point pressure line (P=Pdew) is also drawn in each diagram. Spots above and under this line are uniphasic and diphasic respectively.

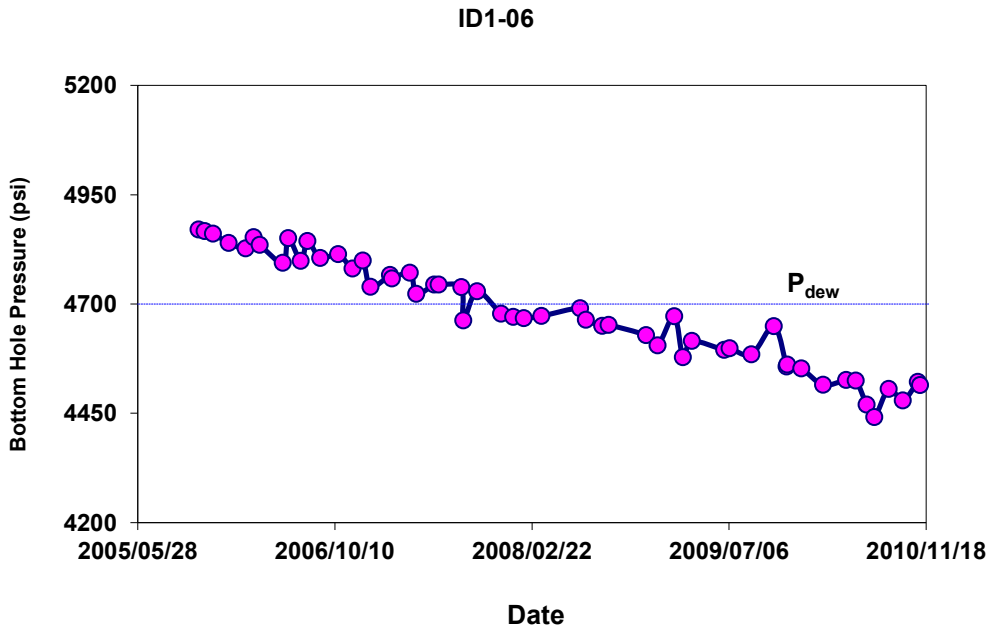

Figure 3-8: Decreasing bottom hole pressure during the years for ID1-06

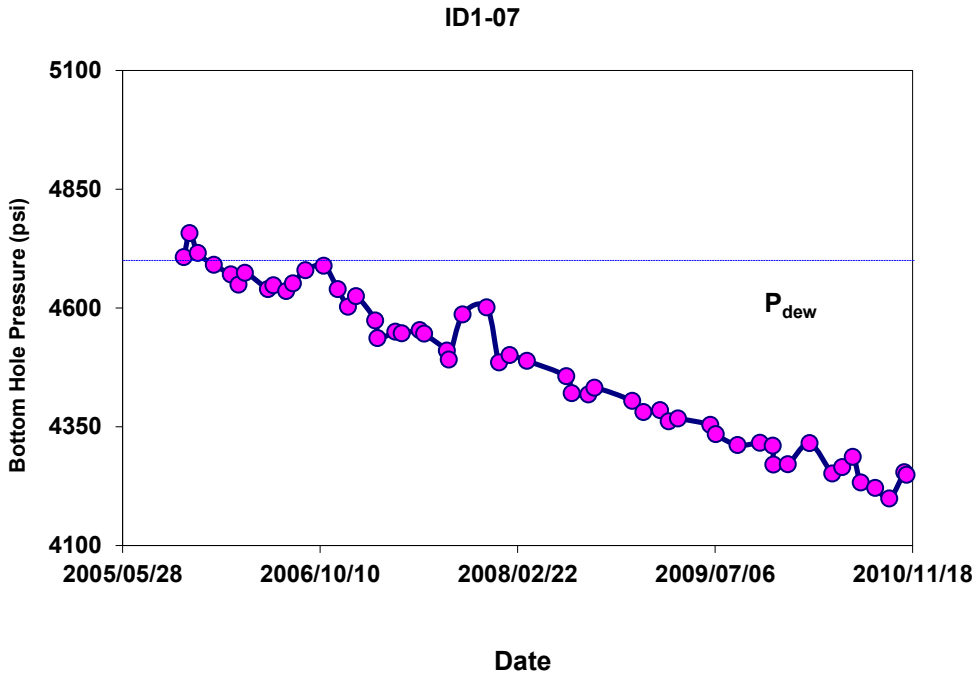

Figure 3-9: Decreasing bottom hole pressure during the years for ID1-07

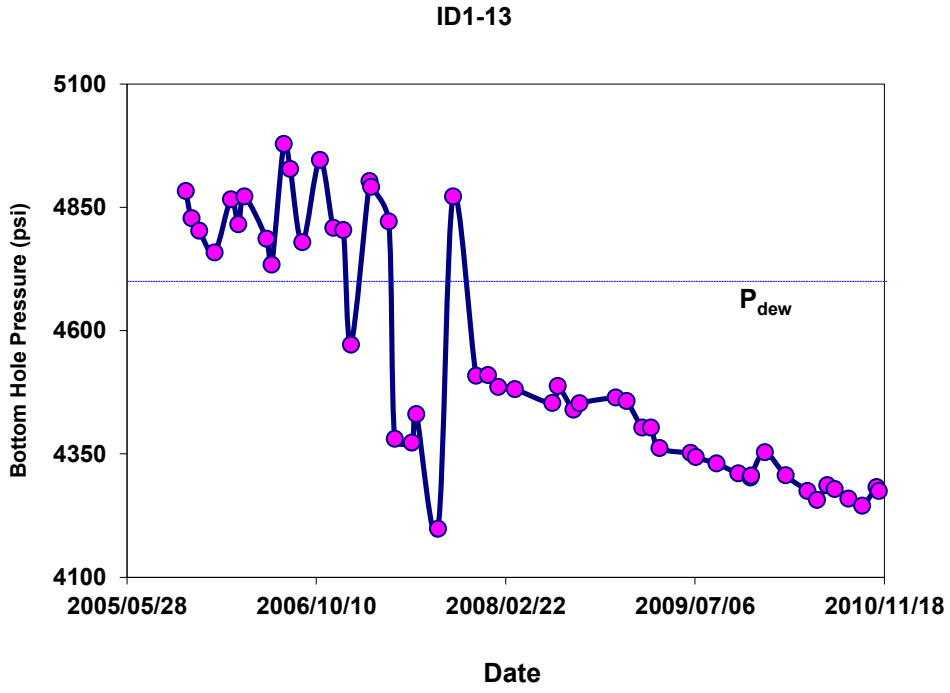

Figure 3-10: Decreasing bottom hole pressure during the years for ID1-13

As shown in the diagram, reservoir fluid used to be uniphasic at the beginning of production (year 2005) and it gradually turned into diphasic. The produced gas flow rate from each well has a direct relation with pressure difference in the bottom and the head of well. It means that with increase in pressure drop, production flow rate will increase as it is shown in following figure for wells ID1-01, ID1-06, ID1-07, and ID1-13.

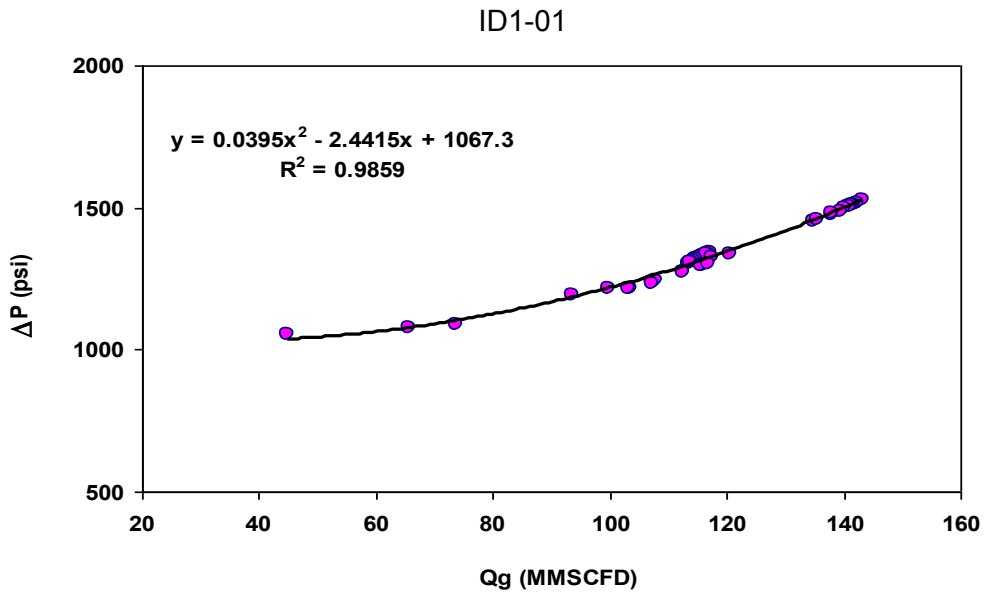

Figure 3-11: Pressure difference in the bottom and the head of well versus gas flow rate for ID1-01

The relation shown in the figure is produced from regression of a second-degree polynomial matched on the spots with a proper precision. Using this relation, one can calculate pressure difference in the bottom and the head of well for a certain flow rate. The diagram is provided for three other wells in the following.

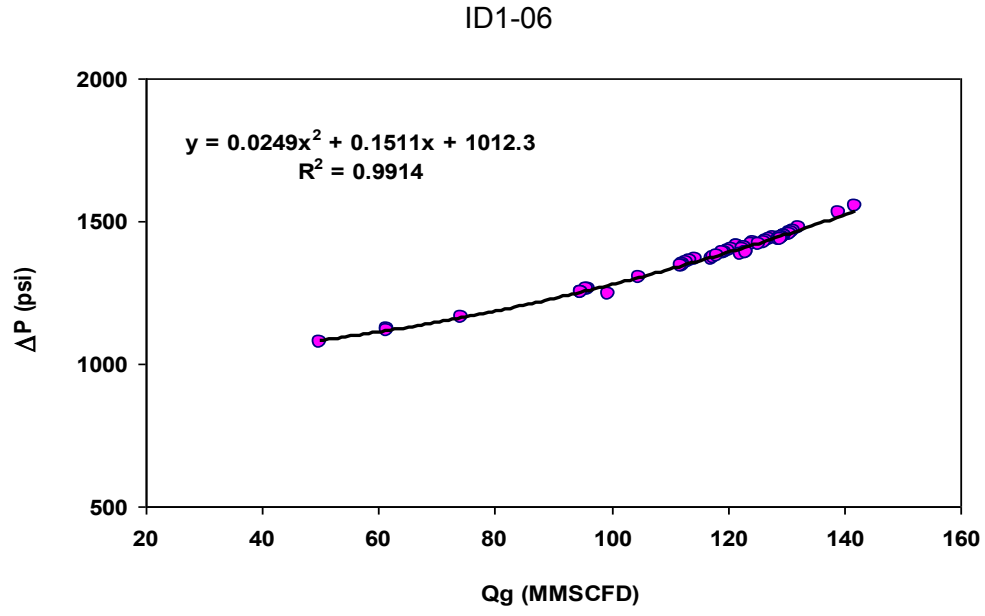

Figure 3-12: Pressure difference in the bottom and the head of well versus gas flow rate for ID1-06

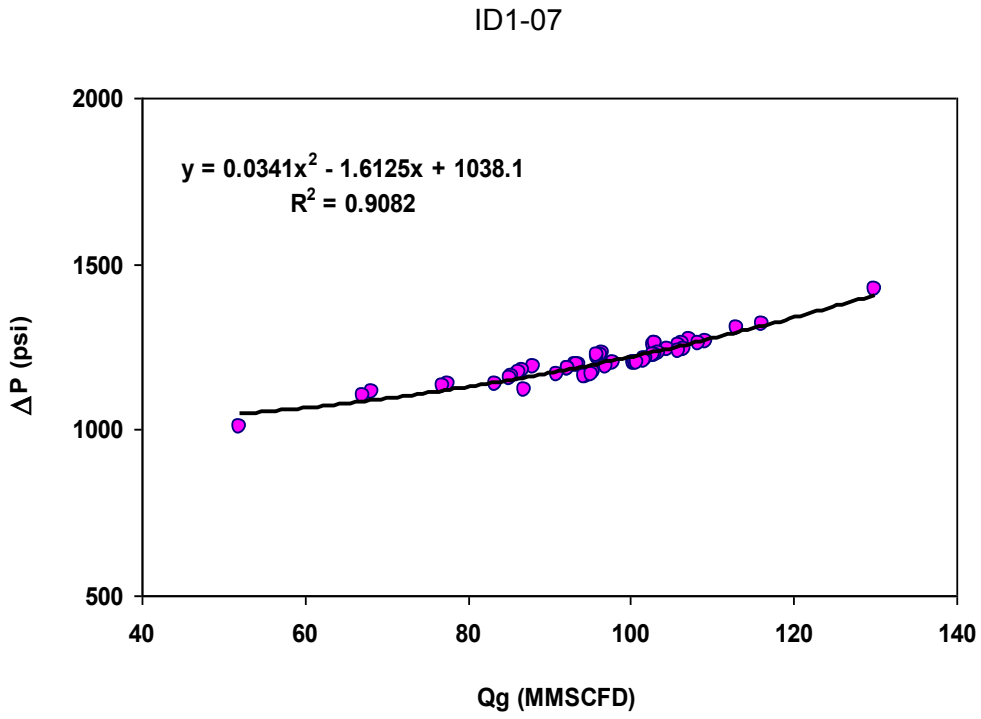

Figure 3-13: Pressure difference in the bottom and the head of well versus gas flow rate for ID1-07

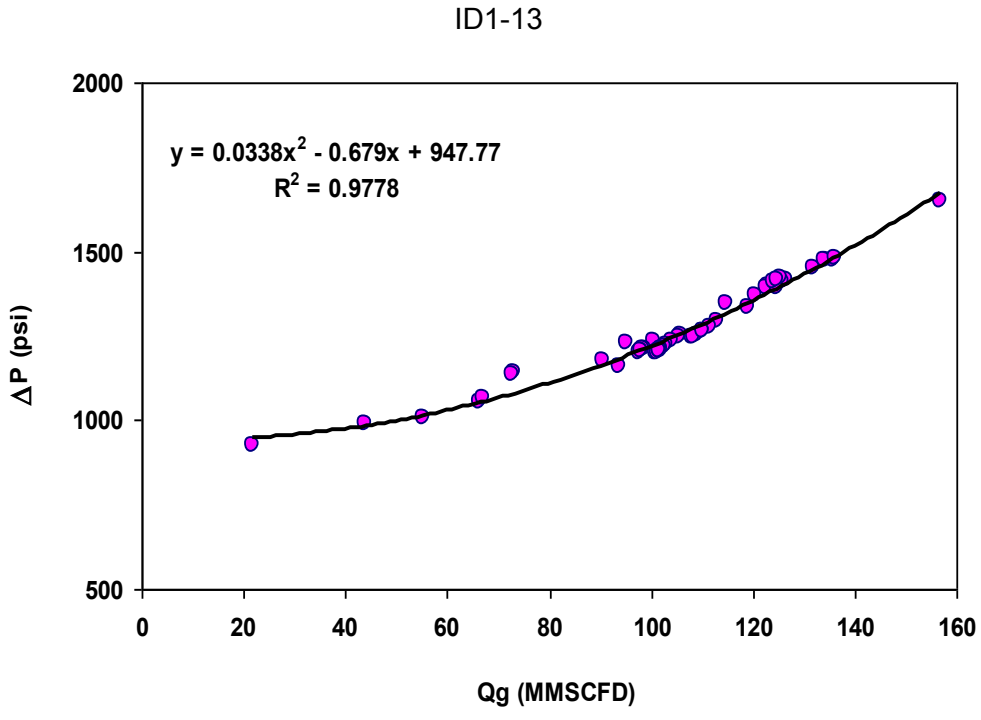

Figure 3-14: Pressure difference in the bottom and the head of well versus gas flow rate for ID1-13

Also it can be shown that the ratio of gas flow rate to pressure difference in well bottom and head (indicated as Qg/ΔP) in terms of gas flow rate on a diagram determines the relation using a second-degree regression. This diagram is shown for wells in figures 3-15 to 3-18.

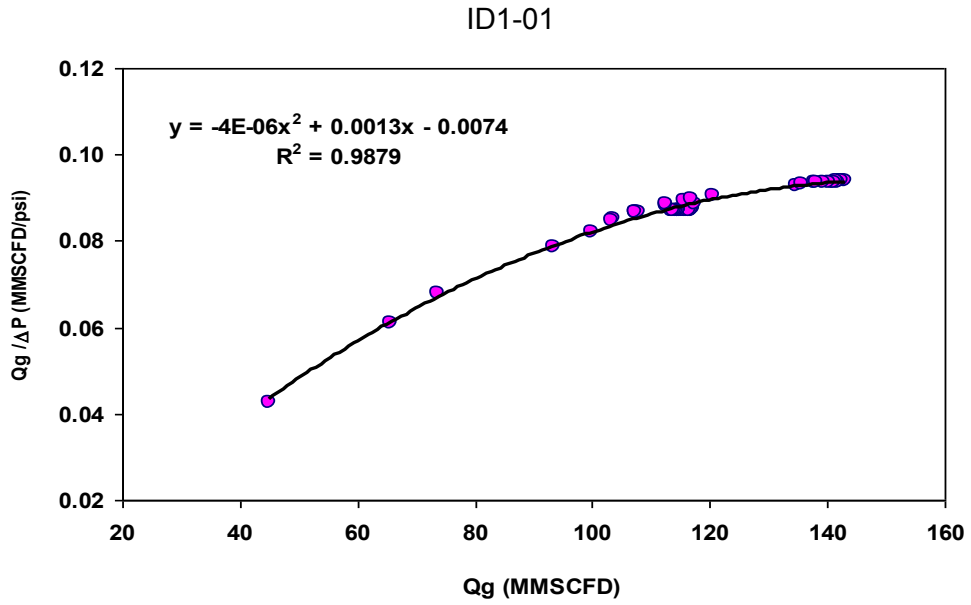

Figure 3-15: Ratio of gas flow rate to pressure difference in well bottom and head in terms of gas flow rate for ID1-01

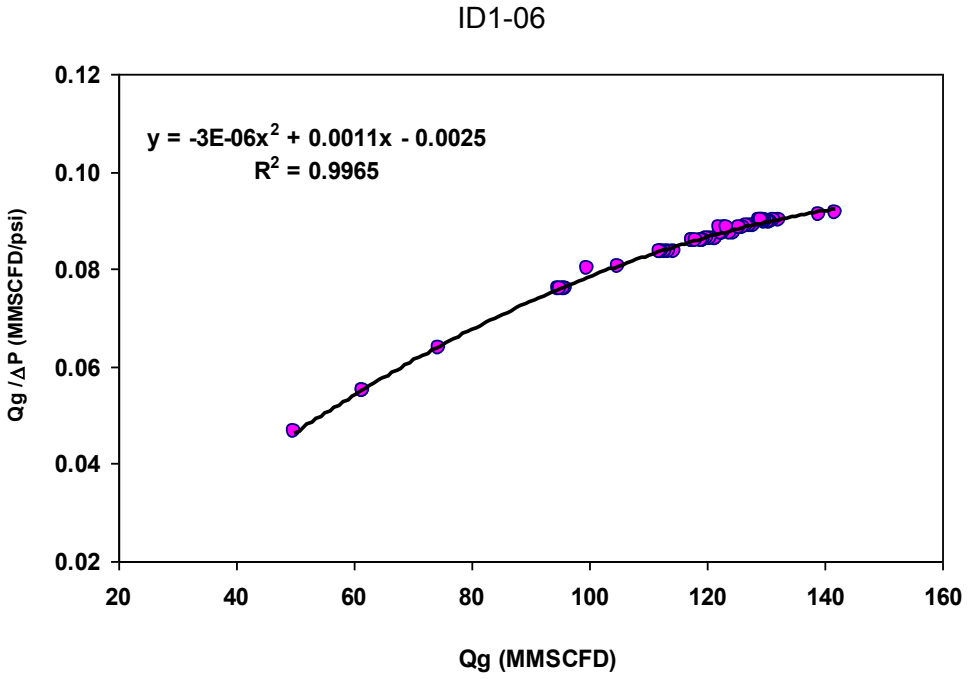

Figure 3-16: Ratio of gas flow rate to pressure difference in well bottom and head in terms of gas flow rate for ID1-06

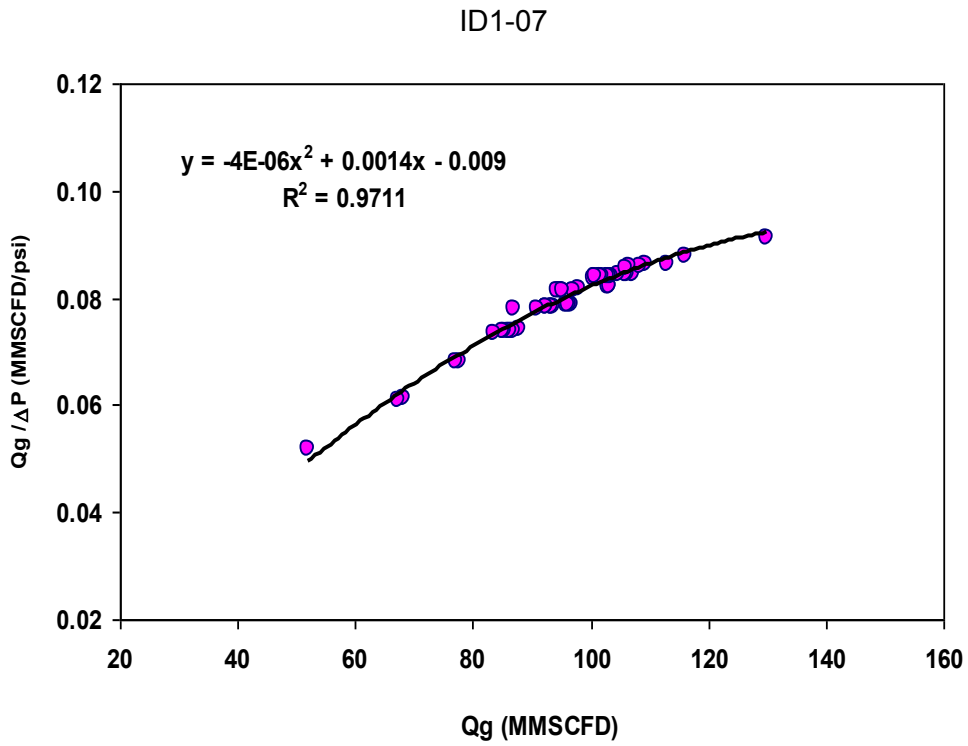

Figure 3-17: Ratio of gas flow rate to pressure difference in well bottom and head in terms of gas flow rate for ID1-07

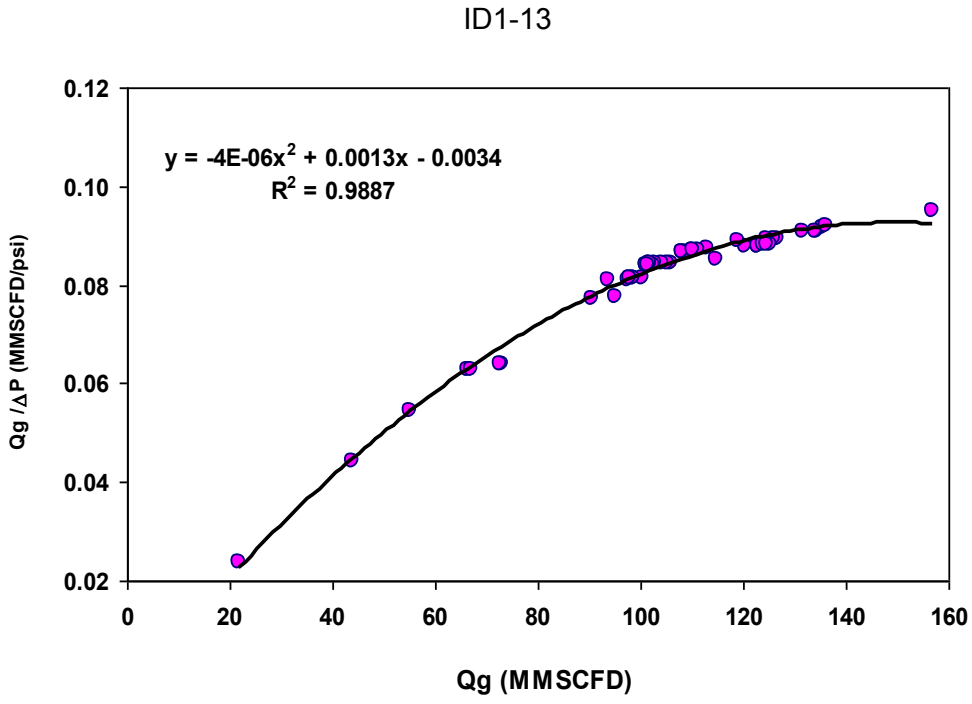

Figure 3-18: Ratio of gas flow rate to pressure difference in well bottom and head in terms of gas flow rate for ID1-13

The above figures indicate that pressure variations of well bottom and head are not steadily relative to flow rate and increase gradually in a non-linear manner. In other words, more intensity in pressure difference is necessary for gas production at higher flow rates.

For instance in case of well ID1-01, if gas production flow rate is 60 MMSCFD, in lieu of flow rate increase of 10 MMSCFD, pressure will decrease 27 psi; but in a 120 MMSCFD of flow rate, a 10 MMSCFD increase in flow rate necessitates a 74 psi of pressure difference.

3.6 Sensitivity analysis of different variables on bottom hole pressure calculations

Since there is a possibility that in simulations some values of input data to software are not of a proper accuracy and certainty, it is necessary to test the influence of these variables on bottom-hole pressure results, or in other words, a sensitivity analysis need to be carried out.

In order to execute a sensitivity analysis we consider simulation of well ID1-01 bottom-hole pressure as a criterion to make a comparison on variations. After simulation it was learnt that most parameters including reservoir rock permeability, reservoir fluid composition, gas-oil ratio (GOR), geothermal data, Skin factor, wellbore diameter, pipe roughness, drainage radius, and reservoir temperature don't have significant impact on the results. Thus they're not framed in this report while simulation results of effective parameters are demonstrated in the following figures.

3.6.1 Sensitivity Analysis of black oil Model

A compositional model is utilized in this study in which hydrocarbons and other fluid's constitutional components and their mole-fractions are input to the simulator to introduce the reservoir's fluid. It is also possible to use Black Oil model as an alternative. In Black Oil model GOR, gas density and API of condensates are input to the software. Reservoir fluid properties are calculated with the aid of Pipesim software and Peng-Robinson tri-parametric equation. The so-called properties are brought in table 3-16.

Table 3-16: Reservoir fluid properties used in black oil model simulation

Property	
Gas condensate ratio	33098.1 SCF/STB
Gas density	0.69
API	48.6

Bottom-hole pressure simulation results of well ID1-01 executed by Black Oil model are shown in figure 3-19.

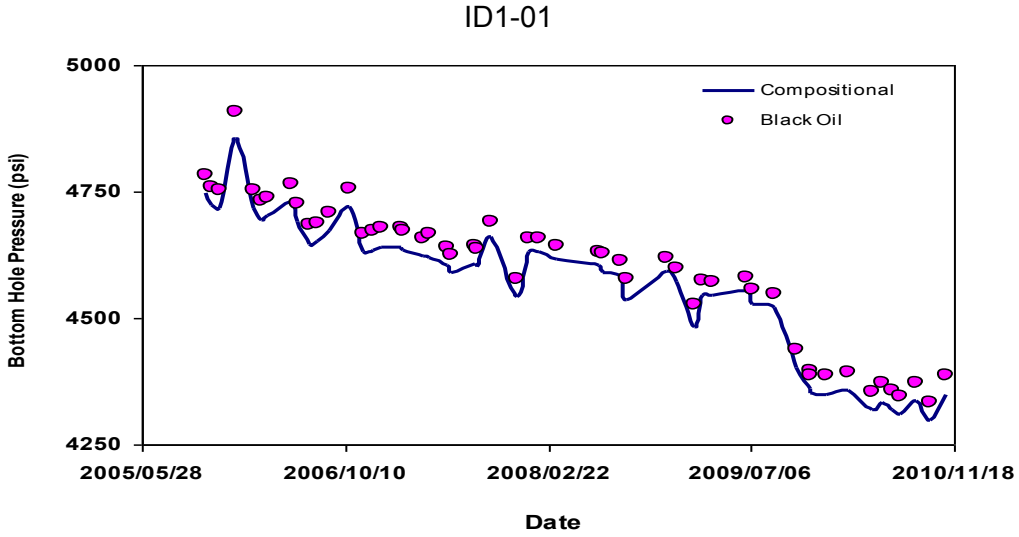

Figure 3-19: Sensitivity Analysis of black oil Model on bottom hole pressure for ID1-01

As demonstrated in the figure, using black oil model which causes bottom-hole pressure shows a slightly higher value compared to the compositional method. There is no substantial difference in this case and the two methods show a 35 psi difference in results which is less than 1%.

3.6.2 Sensitivity analysis on tubing diameter

Here we're going to study impacts of variations in tubing diameter on bottom-hole pressure. To reach this goal, we altered tubing diameter (with initial value of 6.151") 5% wider at the first time and 5% narrower at another time and executed a simulation for each new diameter. Results are demonstrated in figure 3-20.

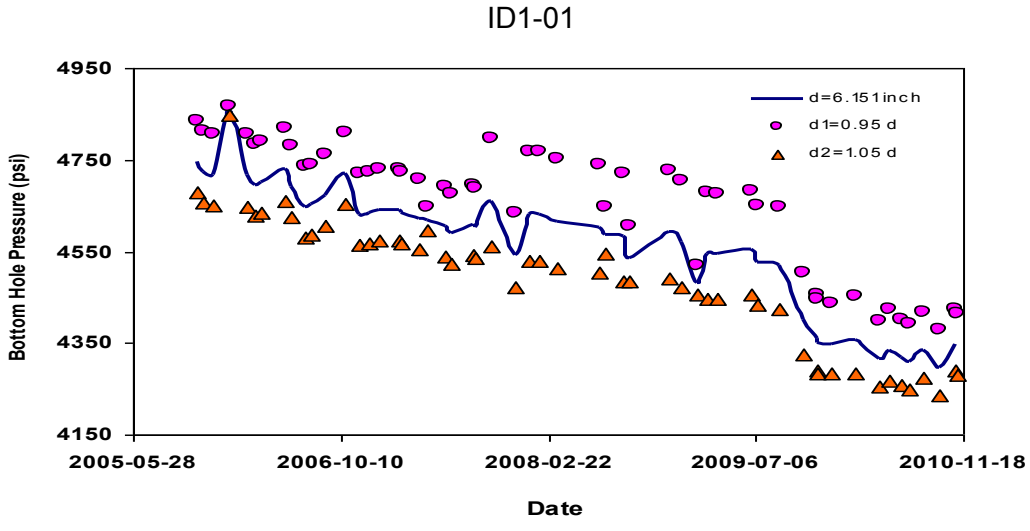

Figure 3-20: Sensitivity Analysis of tubing diameter on bottom hole pressure for ID1-01

As expected, decrease in tubing diameter causes increase in well bottom and head pressure difference. And for a constant well head pressure, bottom-hole pressure will increase. In this case, a 5% decrease in tubing diameter results in a 95-psi increase in bottom-hole pressure on average. And a 5% increase in tubing diameter causes an average decrease of 71 psi in bottom-hole pressure. These values make 2.1% and 1.6% difference with the initial diameter case (6.151") respectively.

We can demonstrate tubing diameter sensitivity analysis on diagram BHP-Qg. To do this, for different flow rates in a constant tubing diameter and constant wellhead pressure (3200 psi) we calculate bottom-hole pressure and then repeat this calculation for the other two altered diameters. Results are indicated in the following figure.

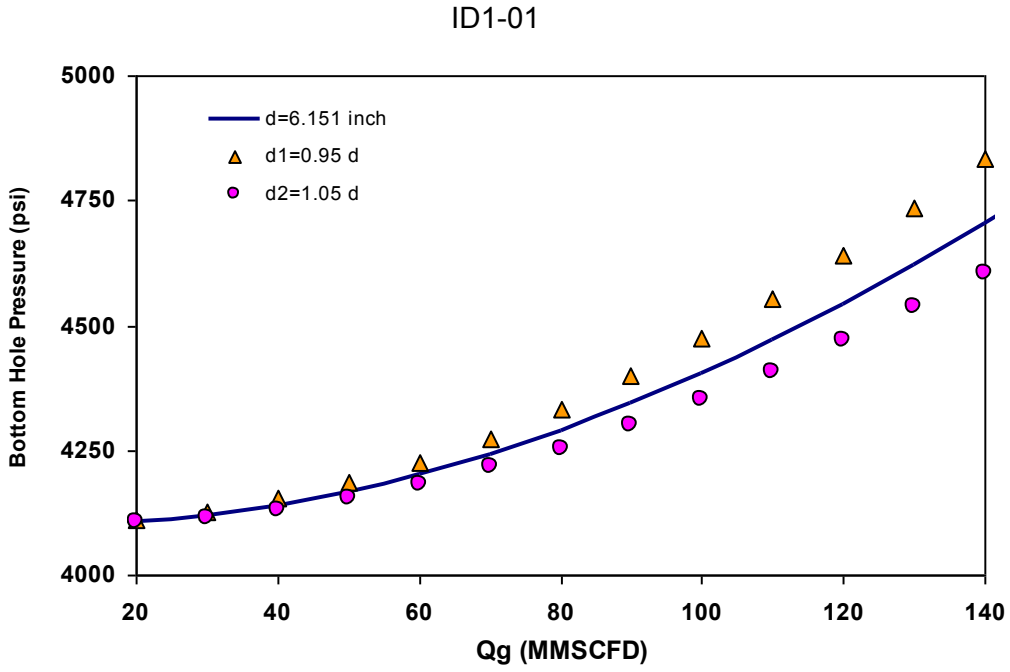

Figure 3-21: Sensitivity Analysis of tubing diameter on bottom hole pressure for ID1-01 in BHP-Qg diagram

In this case, a 5% decrease in diameter causes a 70-psi increase in bottom-hole pressure on average. And a 5% increase in diameter causes an average decrease of 52 psi in bottom-hole pressure. These conditions are 1.5% and 1.1% varying from the initial diameter case (6.151") respectively.

3.6.3 Produced Gas Flow Rate Sensitivity Analysis

Two conditions are examined to study the impact of gas flow rate on bottom-hole pressure. In the first condition, the produced gas flow rate had a 10% decrease and in the second condition a 10% increase in each day. The results are illustrated as below.

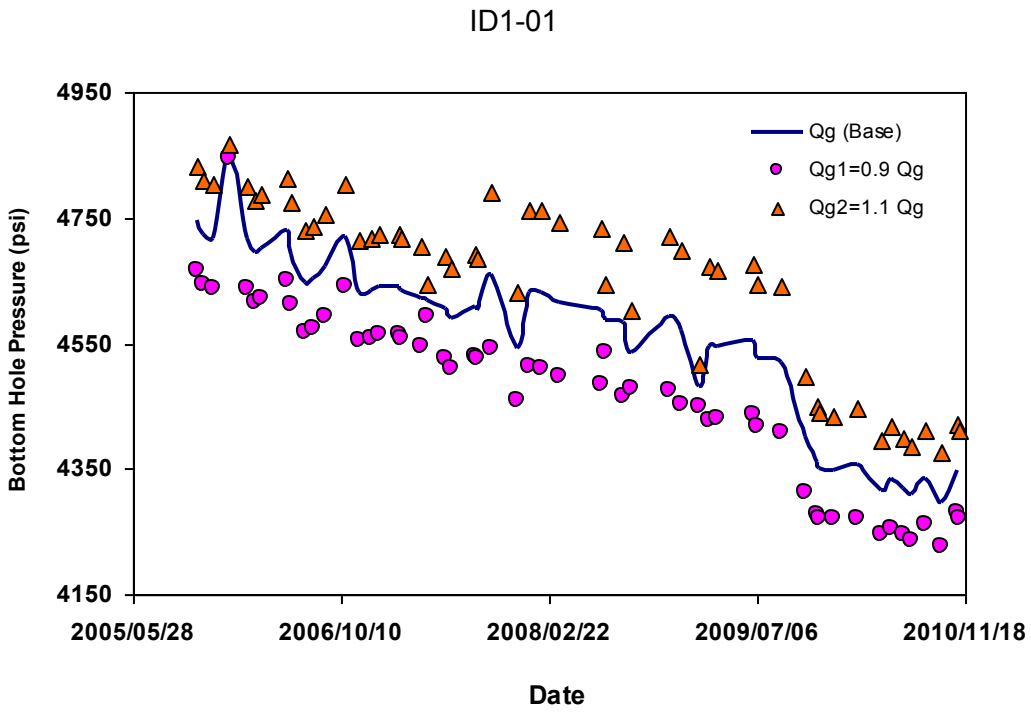

Figure 3-22: Produced Gas Flow Rate Sensitivity Analysis on bottom hole pressure for ID1-01

As expected, with the flow rate decreasing, the bottom-hole pressure decreases. Therefore, less pressure difference is required to produce less flow rate and thus, with the well head pressure being assumed constant, the bottom hole pressure will decrease. Also on aforesaid ground, as gas flow rate increases bottom-hole pressure increases. According to the diagram, a 10% decrease in flow rate will cause an average 83-psi decrease in bottom-hole pressure and with a 10% increase in flow rate an average increase of 90 psi in bottom-hole pressure is observed. These conditions are 1.8% and 2.0% varying from the initial diameter case (6.151") respectively.

3.6.4 Wellhead Pressure Sensitivity Analysis

To study the impacts of wellhead pressure variations on bottom-hole pressure calculations 3 values were considered for wellhead pressure as 3100psi, 3300psi, 3300psi, then we calculated bottom-hole pressure for different flow rates in a constant wellhead pressure and

finally calculations are done for other wellhead pressures. Results are shown in the figure below.

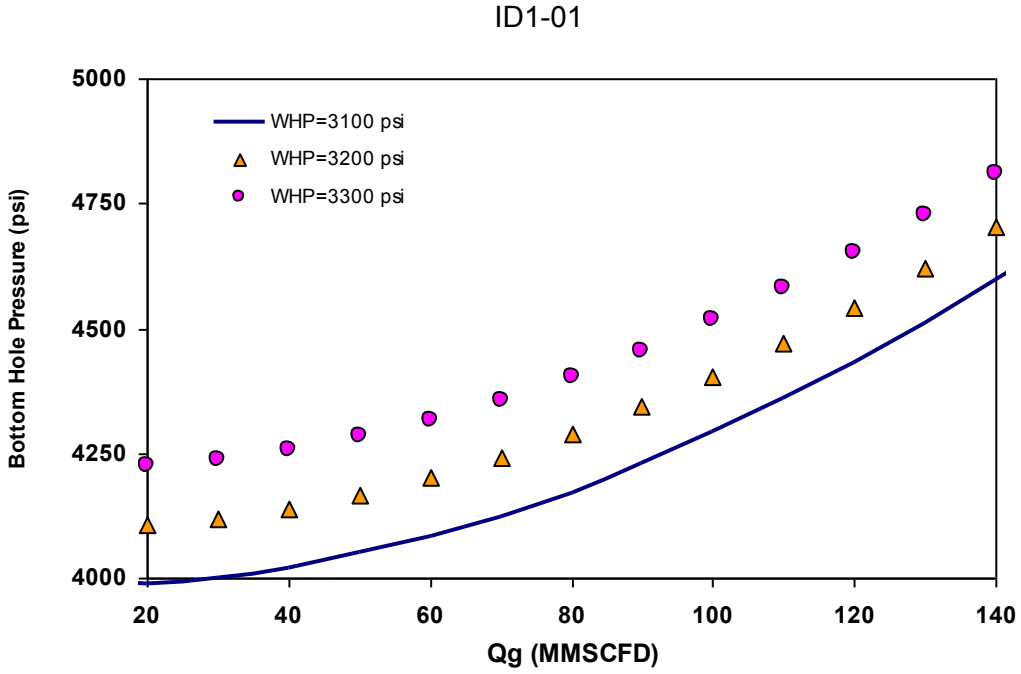

Figure 3-23: Wellhead Pressure Sensitivity Analysis on bottom hole pressure for ID1-01

As demonstrated in the figure, with a 100psi increase in wellhead pressure, bottom-hole pressure increases up to almost the same value (123 psi).

3.7 Impact of Wellhead Pressure and Production Rate in Liquid Accumulation

In gas condensate reservoirs, due to pressure drop, condensates accumulate near the wellbore and causes gas production decreased. In this section, we will study the impact of wellhead pressure and production rate on liquid hold-up. For this, the well ID1-01 is chosen with the production rate of 31.6 MMSCFD. Liquid hold-up is calculated for different values of wellhead pressure in terms of elevation. The figure below shows the results. According to the diagram it is observed that liquid hold-up decreases as wellhead pressure increases.

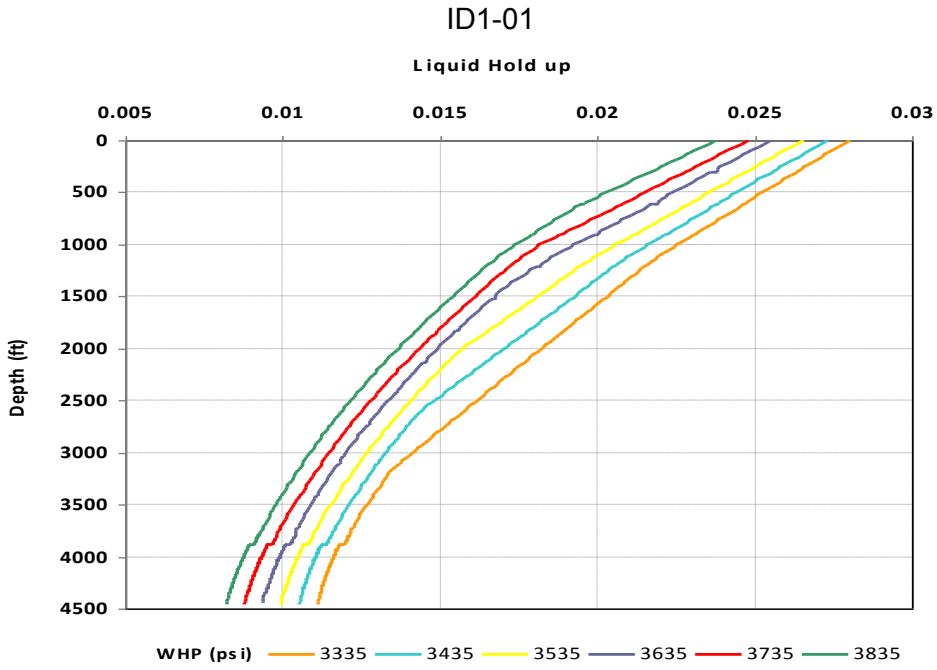

Figure 3-24: Impact of Wellhead Pressure on Liquid holdup for ID1-01 with gas rate of 31.6MMSCFD

To study impact of production rate, well ID1-01 with a wellhead pressure of 3635 psi is considered and liquid hold-up is calculated in terms of elevation for different production rates. The figure below shows impact of production rate on liquid hold-up.

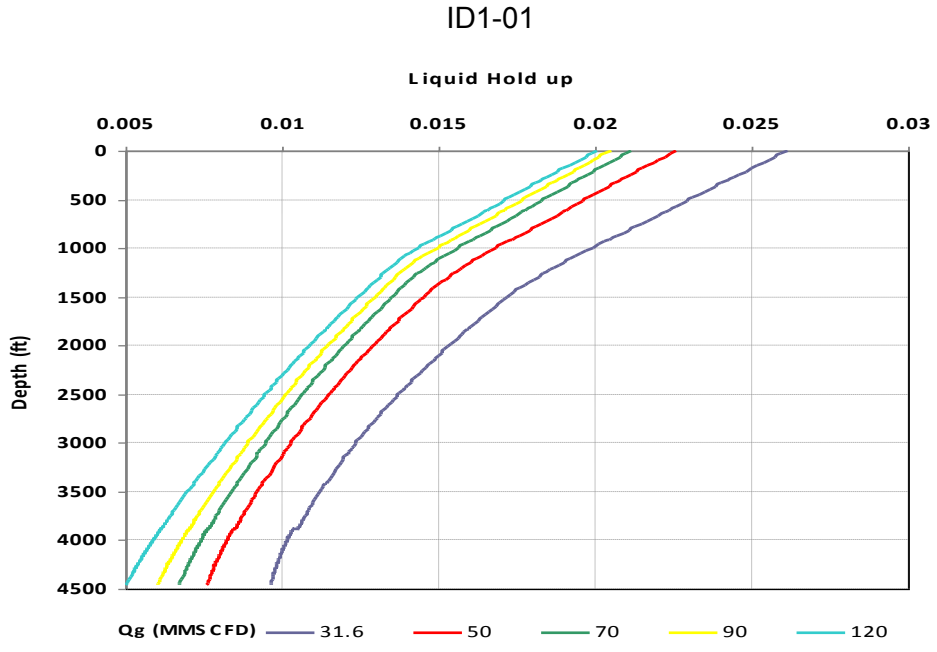

Figure 3-25: Impact of production rate on Liquid holdup for ID1-01 with wellhead pressure of 3635 psi

According to the figure, it can be seen that liquid hold-up decreases in well as production rate increases. Therefore, condensate accumulation can be prevented in well by increasing wellhead pressure.

4 Conclusion and Discussion

Based on the results of this study, the following conclusions have been drawn:

- Calculating gas and condensate flow rate for 20 wells of 2 platforms (ID1, ID2) is one of the main objectives of this study. Therefore, to obtain production contribution of each well, wellhead chokes of the wells are simulated individually by Pipesim software and then, based on test separator data a relation between bean size and choke opening percentage is derived.

- Constants of relation are determined for each well. Obtained corresponding coefficient of determinations demonstrates a good value of 0.93 to 0.99.

- This choke relation is subjected to a practical test when half of the production system is out of service. Studies show that the suggested model may be used successfully to calculate the gas and condensate flow rate of each platform separately. Consequently, this model will help to determine the optimum choke to obtain the optimum production.

- Sensitivity analysis of water cut and API for bean size is studied. It is illustrated that these parameters has no considerable effect on the choke simulation.

- The total enriched gas flow rate of ID1 and ID2 in different dates is calculated. Afterwards, total simulated enriched gas flow rate is compared with the reported enriched gas flow rate by the mean of percentage error. This statistical error demonstrates a value of 3.4 which is not considered as a great difference.

- As it is expected, the critical pressure ratio is often less than 0.55, which means that the flow is often critical.

- In order to determine the gas and condensate flow rates in simulation of choke, average value of GLR's was used. Using the average value of GLR's does not lead to a considerable error in the simulation results.

- To find out the best pressure drop correlation using Pipesim simulator, 11 different models is compared to the measured data of wells (PSP). As simulation results show, the Gray Modified model has the least errors among the deviated wells and for the vertical well, Ansari model presents the best match. Thus, these two models are selected for simulating wells in which pressure-temperature profiles, flow regimes, as well as liquid hold up are obtained for all 20 wells.

- It should be noted that in addition to Gray Modified and Gray Original models, Aziz and Fogarasi, Govier, Zhang, No slip Assumption, and Ansari models show high accuracy and errors less than 1%. For the simulated vertical wells, the so-called models in addition to Hagedorn and Brown model show less-than 1% errors.

- In this work, the impact of wellhead pressure and production rate on liquid hold up is studied. It is illustrated that liquid hold-up decreases as wellhead pressure increases. Also liquid hold up decreases in the wells when production rate increases. Thus, it is simply possible to prevent high condensate accumulation in wells by increasing wellhead pressure.

- From 2005 to 2010, the bottom hole pressure for a certain wellhead is calculated using selected model and choke simulation results. Therefore, one can calculate the pressure difference in the bottom and the wellhead for a certain flow rate.

- The dew point is often above the bottom hole pressure which indicates the 2 phase flow in the well.

- Since there is a possibility that in simulations some values of input data to software are not of a proper accuracy and certainty, , a sensitivity analysis needs to be carried out. Therefore, well simulation is conducted for many parameters in which tubing diameter, Gas Flow Rate, and Wellhead Pressure indicate more impact on bottom hole pressure. After simulation it was learnt that most parameters including reservoir rock permeability, reservoir fluid composition, geothermal data, Skin factor, wellbore diameter, pipe roughness, drainage radius, and reservoir temperature don’t have significant impact on results.

5 Reference

1. Sarfraz, A.J., Djebbar Tiab, *Establishing Inflow Performance Relationship (IPR)for Gas Condensate Wells.* SPE 77503, 2002.

2. Craft, B.C.H., M.F. Revised by Terry, Ronald E, *Applied Petroleum Reservoir Engineering*. second ed. 1991.

3. Danesh, A., *PVT and Phase Behavior of Petroleum Reservoir Fluids*. second ed. 1998, Elsevier Science, Amsterdam, Netherlands

4. Sadeghi Boogar, G.A., S. , and Masihi M., *Investigation into the capability of a modern decline curve analysis for gas condensate reservoirs.* Scientia Iranica 2011.

5. Fan, L., *Understanding Gas Condensate Reservoirs*. 2006.

6. COSKUNER, G., Strocen Bogdan, T., *Production Optimization of Liquid Loading Gas Condensate Wells: A Case Study. Canadian Petroleum Technology.* Journal of Canadian Petroleum Technology, 2003.

7. Persad, S., *Evaluation of Multiphase-Flow Correlations for Gas Wells Located Off the Trinidad Southeast Coast.* SPE 93544 2005.

8. Pucknell, J.K., Manson, J.N.E. and Vervest, E.G., *An Evaluation of Recent "Mechanistic" Models of Multiphase Flow for Predicting Pressure Drops in Oil and Gas Wells.* SPE 26682 1993.

9. Brill, J.P., Mukherjee, H., *Multiphase Flow in wells.* SPE, 1999.

10. Time, R.W., *Two-Phase Flow in Pipelines*. 2009.

11. Brennen, C.E., *Fundamentals of Multiphase Flow. Cambridge University press*. 2005.

12. Fortunati, F., *Two phase Flow Through Wellhead Chokes.* SPE 3742, 1972.

13. Ellul, I.R., Saether, G. and Shippen, M.E. , *The Modeling of Multiphase Systems under Steady-State and Transient Conditions.* PSIG 0403 2004.

14. Yahaya, A.U., Gahtani, A.A., Fahd, K., *A comparative Study Between Empirical Correlation & Mechanistic Model of Vertical Multiphase Flow.* SPE 136931, 2010.

15. Brill, J.P., Mukherjee, H., *Multiphase Flow in Wells.* SPE 16242, 1987.

16. Ansari, A.M., Sylvester, N.D., Sarica, C., Shoham, O. and Brill, J.P., *A Comprehensive Mechanistic Model for Upward Two-Phase Flow in Wellbores.* SPE 20630, 1994.

17. Vatani, A.M., S., *Principle of Hydraulic Design of Two-Phase Flow Transmission Pipelines*. 3rd ed. 2009.

18. Shoham, O., *Mechanistic Modeling of Gas -liquid Two-Phase Flow In Pipes.* SPE books, 2005.

19. Hasan, A., R. and Kabir, C., S., *A Study of Multiphase Flow Behavior in Vertical Wells.* SPE Production Engineering, 1988.

20. Ozon, P.M., Ferschneider, G., Chwetzoff, A., *A New Multiple Flow Model Predicts Pressure and Temperature Profiles.* SPE 16535, 1987.

21. Chokshi, R.N., Schmidt, Zelimir, Doty, Dale R., *Experimental Study and the Development of a Mechanistic Model for Two-Phase Flow Through Vertical Tubing.* SPE 35676, 1996.

22. Kaya, A.S., Sarica,C., Brill,J. P., *Comprehensive Mechanistic Modeling of Two-Phase Flow in Deviated Wells.* SPE 56522, 1999.

23. Felizola, H., Shoham, O., *A Unified Model for Slug Flow in Upward Inclined Pipes.* ASME J. Energy Resources Technology, 1995.

24. Petalas, N., Aziz, K., *Development and Testing of a New Mechanistic Model for Multiphase Flow in Pipes.* ASME, Fluid Eng, 1996.

25. Gomez, L.E., Shoham, O., Schmidt, Z., *Unified Mechanistic Model for Steady-State Two-Phase Flow in Wellbores and Pipelines.* SPE 56520, 1999.

26. Zhang, H., Wang,Q., Sarica,C., Brill, J., *Unified Model for Gas-Liquid Pipe Flow via Slug Dynamics.* Energy Resource Technolgy, 2003.

27. Khasanov, m.K., Krasnov, R., Pashali, V., Guk,V.A., *A Simple Mechanistic Model for Void-Fraction and Pressure-Gradient Prediction in Vertical and Inclined Gas/Liquid Flow.* SPE 108506, 2008.

28. Schlumberger, *Pipesim ver. 2008.1 User Manual.* 2008.

29. George, W., Govier, C., Maria Fogarasi, *Pressure Drop in Wells Producing Gas and Condensate.* canadian Petroleum Technology, 1974.

30. Peffer, J.W., Miller, M.A., Hill, A.D., *An Improved Method for calculation Bottomhole Pressures in Flow Wells With Liquid Present.* SPE, 1988.

31. Kabir, C.S., Hasan, A.R., *Simplified Wellbore-Flow Modeling in Gas/Condensate Systems.* SPE Production & Operations, 2006.

32. Bizanti, M., Alrumah, M., *New Choke Correlations for Sabryiah field, Kuwait.* SPE 105103, 2007.

33. Guo, B., Al-Bemani, A.S., Ghalambor, A., *Aplicability of Sachdeva's choke flow model in southwest Louisiana gas condensate wells.* SPE 75507, 2002.

34. Nasriani, H.R., Kalantariasl, A., *Two-phase flow choke performance in high rate gas condensate wells.* SPE Paper 145576, 2011.

35. Masoud Ahmadi Nia, A.A., Hamid Reza Nasriani, *An Improvement on Gilbert Type Choke Performance Relationship for Iranian Gas Condensate Reservoirs.* IChEC, 2011.

36. Guo, B., Lyons, W.C., Ghalambor, *Petroleum Production Engineering Elsevier Science &Technology*. 2007.

37. Tangeren, R.E., Dodge, C.H., Seifert, H.S., *Compressibility effects of two-phase flow.* App. Phys. 20, 637– 645., 1949.

38. Ashford, F.E., *An evaluation of critical multiphase flow performance through wellhead chokes.* J. Pet. Tech.,850–863., 1974.

39. Ros, N.C.J., *An analysis of critical simultaneous gas–liquid flow through a restriction and its application to flow metering.* Appl. Sci. Res. 2, 374, 1960.

40. Gould, T.L., *Discussion of paper: an evaluation of critical multiphase flow performance through wellhead chokes, by Ashford.* P.E. J. Pet. Tech. 843, 1976.

41. Ashford, P.E., Pierce, P.E., *Determining multiphase pressure drop and flow capabilities in down hole safety valves.* J. Pet.Tech. 27, 1145–1152, 1975.

42. Pilehvari, A.A., *Experimental study of subcritical two-phase flow through wellhead chokes.* 1980.

43. Sachdeva, R., Schmidt, Z., Brill, J.P., Blais, R.M., *Two-Phase Flow Through Chokes.* SPE 15657, 1986.

44. Perkins, T.K., *Critical and subcritical flow of multiphase mixtures through chokes.* SPEDC 271, 1993.

45. Baxendell, P.B., *Bean performance-lake wells.* 1957.

46. Gilbert, W.E., *Flowing and Gas Lift Performance.* American Petroleum Institute, 1954.

47. Poettmann, F., and Beck, R., *New Charts Developed to Predict Gas-Liquid Flow Through Chokes.* World Oil, 1963.

48. Osman, M.E., Dokla,M.E, *Gas condensate flow through chokes.* SPE Paper 20988, 1990.

49. Al-Attar, H., *Performance of Wellhead chokes during subcritical flow of gas condensate.* Journal of Petroleum Science and Engineering, 2009.

50. Khan, A.U.H., W. Bartley, *Case studies in public budgeting and financial management*. 2003.

6 Appendices

Appendix A

Table 6-1: Simulated Bean size using test separator data points for ID1

Date	Well	choke opening	Wellhead P.	Wellhead T.	Downstream P.	GLR	Simulated bean size
		%	barg	°C	barg	SCF/STB	inch
02/09/2008	ID1-01	36	212.8	83.1	120	22010	1.67
03/09/2008	ID1-01	22	222.9	83.6	120	20391	1.49
04/09/2008	ID1-01	21	228.1	83.6	120	21079	1.38
06/01/2011	ID1-01	21	214.8	83.2	120.3	21368	1.44
06/01/2011	ID1-01	15	231.3	79.3	120.1	16096	0.86
06/01/2011	ID1-01	20	220.6	82.8	120.2	18152	1.32
06/01/2011	ID1-01	24	209.7	83	120.3	21301	1.55
06/01/2011	ID1-01	25	207.1	83	120.4	26271	1.59
20/09/2008	ID1-02	23	211.8	71	122	21503	1.56
21/09/2008	ID1-02	21	218.6	71.5	122	18150	1.47
22/09/2008	ID1-02	19	226.6	81.5	122	19700	1.32
29/10/2010	ID1-02	20	211.5	81.3	126	20334	1.46
29/10/2010	ID1-02	16	225.8	79.7	126	18112	1.07
29/10/2010	ID1-02	19	217	81.1	126	19464	1.34
29/10/2010	ID1-02	22	206.1	81.2	120.1	23022	1.55
29/10/2010	ID1-02	24	201.3	81	120.2	21272	1.63
10/10/2008	ID1-03	36	211.3	81.4	122	22746	1.7
11/10/2008	ID1-03	26	214.8	81.5	122	20896	1.64
12/10/2008	ID1-03	21	228.3	81.8	121.9	19459	1.4
29/10/2010	ID1-03	24	210.3	81.2	120.2	21590	1.55
29/10/2010	ID1-03	18	229.8	79.7	119.9	17122	1.09
29/10/2010	ID1-03	21	219.7	81.2	120.1	19821	1.37
29/10/2010	ID1-03	23	214.2	81.3	131.5	20915	1.53
29/10/2010	ID1-03	25	208.2	81.2	106.7	21558	1.58
15/10/2008	ID1-04	37	210.9	83.2	122	21696	1.68
16/10/2008	ID1-04	26	216.1	83.5	122	21553	1.58
17/10/2008	ID1-04	22	219.6	83.7	122	21536	1.51
03/12/2010	ID1-04	21	211.4	83.2	120.3	21019	1.47
03/12/2010	ID1-04	16	224.4	82.4	119.9	17214	1.1
03/12/2010	ID1-04	19	217.3	83.3	120.2	20756	1.33
03/12/2010	ID1-04	24	207	83.2	120.3	23787	1.57
03/12/2010	ID1-04	28	205.9	83.1	120.2	24020	1.58
18/10/2008	ID1-06	27	217.8	80.9	122	21881	1.66
19/10/2008	ID1-06	24	222.6	81.2	122	20420	1.59
20/10/2008	ID1-06	21	230.8	81.4	122	19165	1.44
06/12/2010	ID1-06	20	226.1	81	120.1	28896	1.28
06/12/2010	ID1-06	17	234	79.5	120.2	13701	1.06

06/12/2010	ID1-06	21	222.1	81	120.4	22816	1.39
06/12/2010	ID1-06	24	216	81	120.4	25071	1.53
06/12/2010	ID1-06	25	212.2	80.8	120.3	21615	1.61
29/10/2008	ID1-07	36	209.8	83.7	122.1	22077	1.68
30/10/2008	ID1-07	24	216.6	84	122	20241	1.56
31/10/2008	ID1-07	19	221.4	82.7	120.1	15151	1.19
06/01/2011	ID1-07	17	226.3	81.2	120.2	15209	1.02
06/01/2011	ID1-07	19	222.2	82.6	120.2	17032	1.17
06/01/2011	ID1-07	21	216.6	83.4	120.3	21077	1.33
06/01/2011	ID1-07	22	212.3	83.5	120.4	19258	1.45
06/01/2011	ID1-09	40	211.7	82.7	122.1	21126	1.68
16/11/2008	ID1-09	30	214	82.8	122	19640	1.6
17/11/2008	ID1-09	25	224.7	83.1	121.9	17270	1.43
18/11/2008	ID1-09	20	230.4	81.4	120.1	18459	1.01
09/01/2011	ID1-09	23	221	83	120.4	20724	1.33
09/01/2011	ID1-09	28	210.2	83	120.3	21149	1.56
09/01/2011	ID1-09	35	205.1	82.6	120.5	26298	1.64
09/01/2011	ID1-10	35	209	81.9	122.1	21311	1.64
09/01/2011	ID1-10	24	213.1	82.2	122	20907	1.56
25/11/2008	ID1-10	21	221.1	82.3	122	19501	1.4
26/11/2008	ID1-10	21	212.3	81.9	120.3	20313	1.4
27/11/2008	ID1-10	16	227.3	79.6	120.1	16599	0.97
14/12/2010	ID1-10	20	216.1	81.8	120.1	22085	1.31
14/12/2010	ID1-10	23	206.7	82	120.3	21871	1.52
14/12/2010	ID1-10	26	201.9	81.8	120.4	23670	1.61
14/12/2010	ID1-12	24	209.9	81.2	122.1	19629	1.6
14/12/2010	ID1-12	21	217.5	81.4	121.9	18123	1.47
02/12/2008	ID1-12	21	210.8	81.2	120.3	21284	1.43
03/12/2008	ID1-12	18	220.8	80.8	120.3	18281	1.21
16/12/2010	ID1-12	21	211.6	81.3	106.8	17919	1.42
16/12/2010	ID1-12	22	207.3	81.3	120.3	21495	1.5
16/12/2010	ID1-12	25	199.1	81	120.5	24421	1.63
16/12/2010	ID1-13	34	209.2	83.2	122	22526	1.71
16/12/2010	ID1-13	22	215.9	83.3	122	21802	1.56
26/10/2008	ID1-13	19	224.7	83.3	122	20384	1.35
27/10/2008	ID1-13	20	213.8	82.9	120.4	21893	1.4
28/10/2008	ID1-13	16	225.9	81.1	120.1	17491	1.02
26/12/2010	ID1-13	20	214.6	83.2	120.2	20662	1.39
26/12/2010	ID1-13	22	208.7	83.2	120.4	21176	1.53
26/12/2010	ID1-13	24	203.7	83	120.4	23993	1.63

Simulated Bean size using test separator data points for ID2							
Date	**Well**	**choke opening**	**Wellhead P.**	**Wellhead T.**	**Downstream P.**	**GLR**	**Simulated bean size**
		%	barg	°C	barg	SCF/STB	inch
06/08/2008	ID2-01	25	210.7	82.8	122	23649	1.64
05/08/2008	ID2-01	20	223.6	83.3	122	24342	1.35
08/08/2008	ID2-01	19	226.1	83.3	122	23496	1.3
29/10/2010	ID2-01	21	211	82.9	118.7	49187	1.41
29/10/2010	ID2-01	23	206.7	82.8	119.9	38990	1.52
11/07/2008	ID2-02	19	229.7	81.8	121.9	21696	1.21
07/07/2008	ID2-02	22	218.2	82.1	122	23859	1.44
09/07/2008	ID2-02	23	214.9	82	122.1	21946	1.51
10/07/2008	ID2-02	25	209	81.8	121.2	21499	1.6
23/07/2009	ID2-02	15	236.5	78.6	119.9	57178	0.8
24/07/2009	ID2-02	19	226.2	81.6	120	40753	1.18
25/07/2009	ID2-02	24	209.3	81.9	120.1	49703	1.49
27/07/2008	ID2-03	24	213.2	82.2	120	21202	1.55
26/07/2008	ID2-03	22	219.4	82.3	120	20858	1.45
28/07/2008	ID2-03	21	223.8	82.3	120	27178	1.35
29/07/2008	ID2-03	19	232.3	81.7	120	20721	1.22
28/07/2009	ID2-03	16	237	79.8	119.7	45373	0.93
29/07/2009	ID2-03	20	224.1	82	120	41147	1.26
30/07/2009	ID2-03	24	210	82.1	120.1	49606	1.49
04/11/2010	ID2-03	21	214.6	81.8	119.8	44989	1.35
04/11/2010	ID2-03	21	215.6	82.1	120	46264	1.35
04/11/2010	ID2-03	25	202.6	81.8	120	31037	1.57
02/06/2008	ID2-04	20	212.3	80.8	121.9	23400	1.31
03/06/2008	ID2-04	18	216.8	80.7	122	24374	1.23
03/08/2009	ID2-04	16	225.2	78.9	122.7	48360	0.97
04/08/2009	ID2-04	17	220.5	80.1	122.8	54908	1.06
11/11/2010	ID2-04	18	209	80.4	119.8	22991	1.22
11/11/2010	ID2-04	17	214.6	80.2	119.8	29324	1.09
11/11/2010	ID2-04	19	203.4	80.6	120.1	28763	1.32
16/10/2008	ID2-06	21	231	83.5	122	22066	1.36
18/10/2008	ID2-06	25	218.4	83.3	122.1	21398	1.59
17/10/2008	ID2-06	24	218.3	83.4	122.1	28729	1.57
15/10/2008	ID2-06	36	211.3	83	122.1	22645	1.7
28/07/2009	ID2-06	15	242.1	80.2	122.6	37055	0.84
29/07/2009	ID2-06	19	231	83.3	122.8	43044	1.23
14/11/2010	ID2-06	23	211.3	83.2	120.2	21153	1.57
14/11/2010	ID2-06	16	234.7	81.6	119.8	28759	1
14/11/2010	ID2-06	21	219.7	83.4	120	21791	1.42
14/11/2010	ID2-06	22	215	83.4	120.1	21372	1.51
14/11/2010	ID2-06	24	210	83.2	120.1	20490	1.61
04/08/2008	ID2-07	19	231.2	81.5	125	24979	1.24
03/08/2008	ID2-07	22	221.3	81.8	125	23018	1.47

29/07/2008	ID2-07	24	215.9	81.7	123	22817	1.57
05/08/2009	ID2-07	17	231.5	80.1	122.8	61442	0.98
06/08/2009	ID2-07	21	219.9	81.9	123	48502	1.35
07/08/2009	ID2-07	24	210.9	81.6	123	53395	1.53
15/11/2010	ID2-07	22	210.3	81.5	120	39998	1.46
15/11/2010	ID2-07	15	230	78.5	130	26337	0.87
15/11/2010	ID2-07	19	221	81.2	119.9	36701	1.23
15/11/2010	ID2-07	21	214.8	81.6	120	30361	1.4
15/11/2010	ID2-07	24	206.3	81.4	120.1	26692	1.58
23/07/2008	ID2-09	19	234.2	83.1	122.1	21351	1.24
22/07/2008	ID2-09	22	222.6	83.3	122.1	22047	1.45
20/07/2008	ID2-09	24	216.3	83.1	122	19702	1.57
21/07/2008	ID2-09	26	213.4	82.9	122	21233	1.62
21/07/2008	ID2-09	27	213	83	122	21066	1.63
08/08/2009	ID2-09	19	229.6	82.9	122.9	44282	1.18
09/08/2009	ID2-09	21	221.9	83.2	122.9	43981	1.34
18/11/2010	ID2-09	23	210.6	82.9	120.1	25578	1.51
18/11/2010	ID2-09	21	218.3	83.1	120	24470	1.38
18/11/2010	ID2-09	22	214.5	83	120.2	23915	1.45
18/11/2010	ID2-09	24	208.1	82.8	120	24042	1.57
11/08/2009	ID2-10	22	219.8	81.5	123	47136	1.31
12/08/2009	ID2-10	25	210.3	81.4	123	50763	1.5
20/11/2010	ID2-10	24	209.1	81.3	120	31287	1.47
20/11/2010	ID2-10	18	228.2	79.8	119.7	35441	1.01
20/11/2010	ID2-10	23	213.5	81.4	120	30422	1.4
20/11/2010	ID2-10	25	207.2	81.3	120.1	28403	1.52
20/11/2010	ID2-10	26	203.5	81.1	120.2	28910	1.59
22/08/2008	ID2-12	25	212.4	81.2	125.1	23012	1.45
20/08/2008	ID2-12	24	216.9	81.4	125.2	21809	1.4
23/08/2008	ID2-12	23	219.8	81.3	125	28808	1.33
24/08/2008	ID2-12	21	230.5	81.4	124.9	22784	1.2
12/08/2009	ID2-12	20	229.5	81	122.8	47498	1.1
13/08/2009	ID2-12	22	221.5	81.4	122.9	44105	1.23
14/08/2009	ID2-12	25	209.4	81.3	123	44829	1.4
22/11/2010	ID2-12	27	205.8	80.9	119.9	30501	1.42
22/11/2010	ID2-12	29	199.1	80.5	119.9	30214	1.51
23/06/2008	ID2-14	34	209.8	84.6	122.1	21285	1.63
24/06/2008	ID2-14	29	216.1	84.8	122.1	20567	1.53
25/06/2008	ID2-14	25	227.8	84.7	122	17738	1.34
24/11/2010	ID2-14	27	212.4	84.5	119.9	25797	1.43
24/11/2010	ID2-14	25	218	84.6	120.1	27707	1.32
24/11/2010	ID2-14	28	210.8	84.6	119.9	26286	1.46
24/11/2010	ID2-14	40	202.5	84.3	120.1	25513	1.63

Appendix B

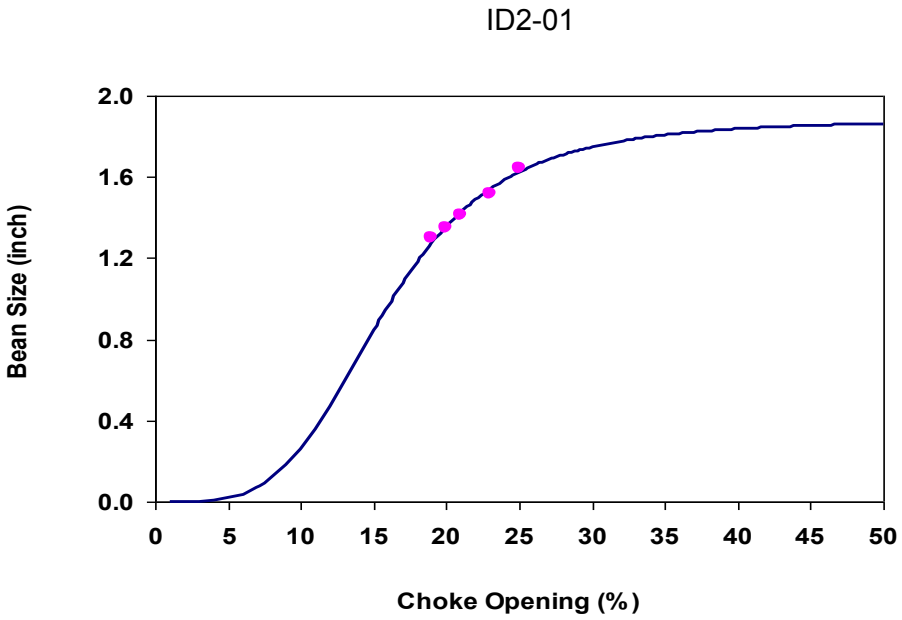

Figure 6-1: Regression analysis results ID2-01 well

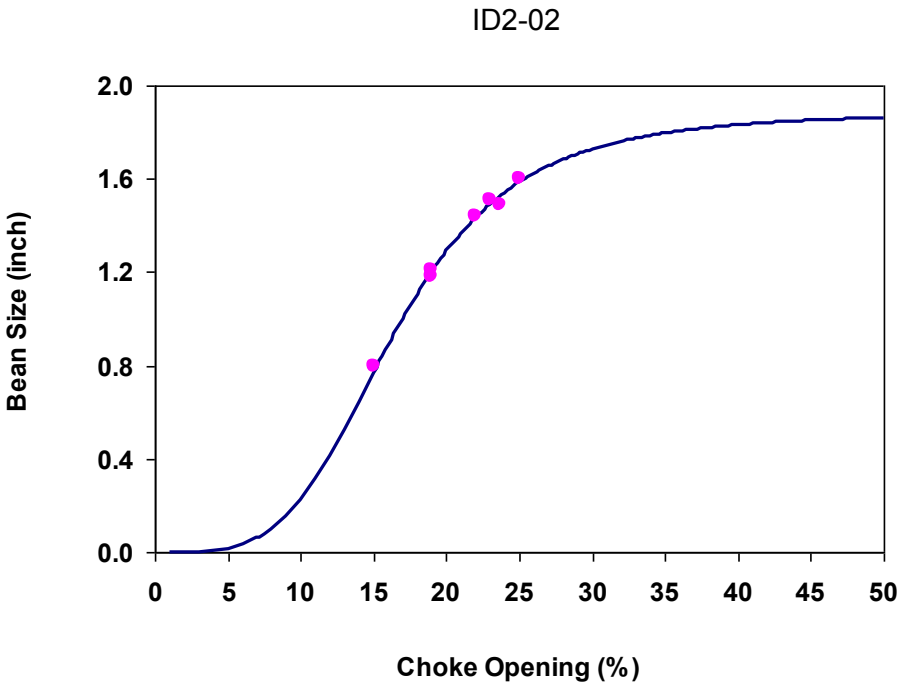

Figure 6-2: Regression analysis results ID2-02 well

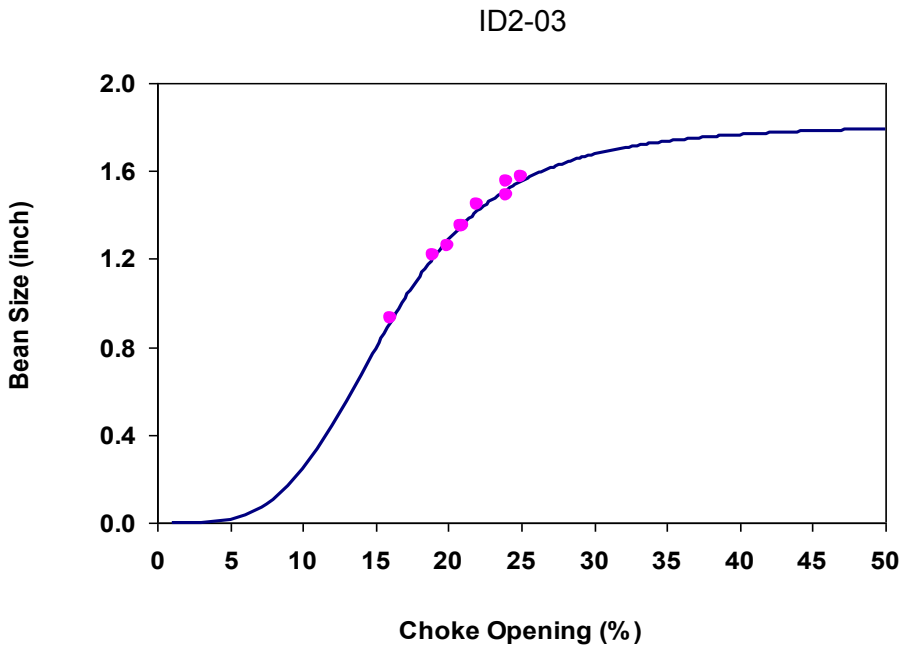

Figure 6-3: Regression analysis results ID2-03 well

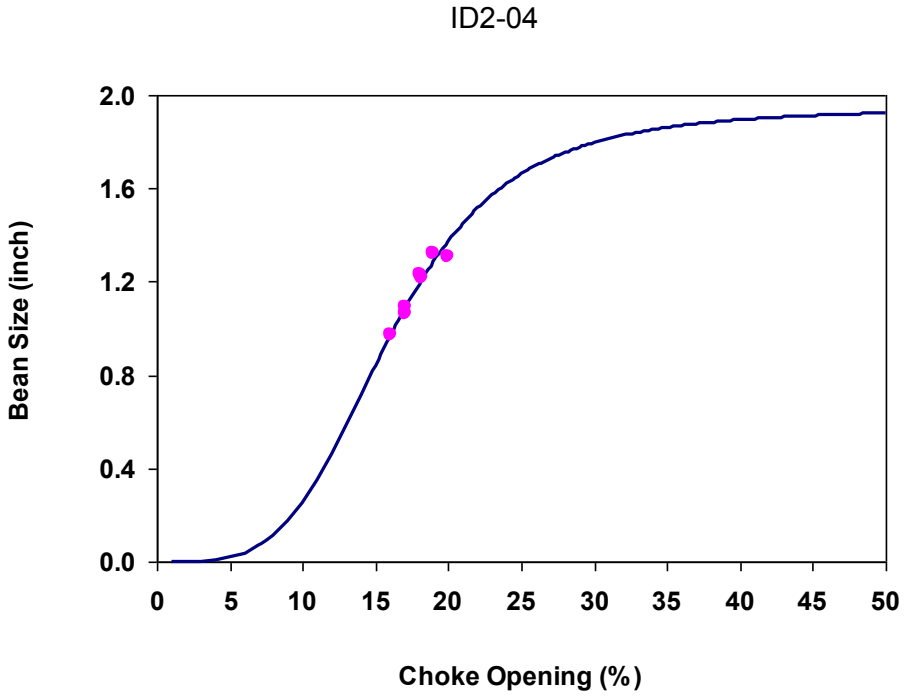

Figure 6-4: Regression analysis results ID2-04 well

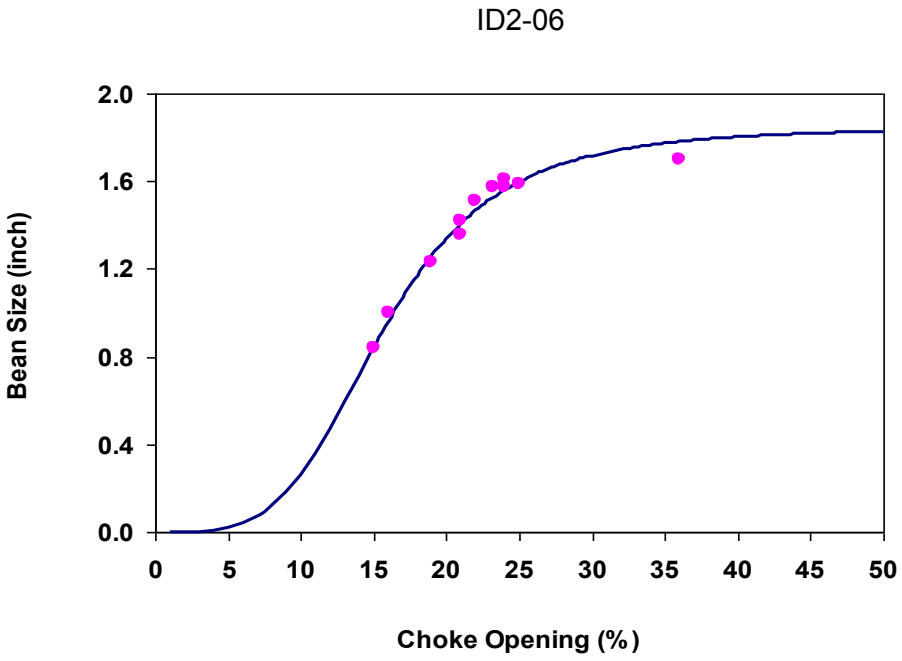

Figure 6-5: Regression analysis results ID2-06 well

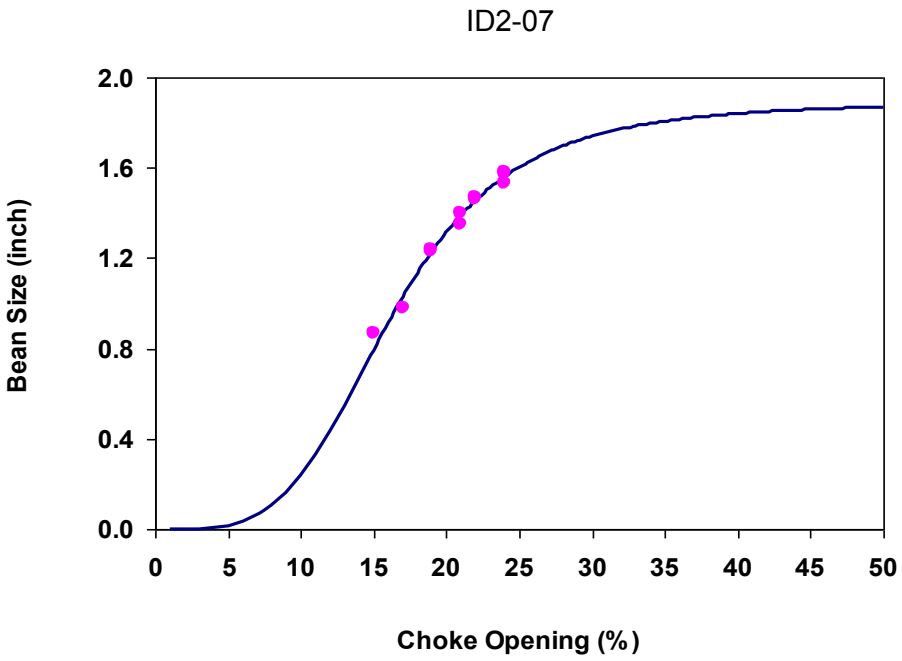

Figure 6-6: Regression analysis results ID2-07 well

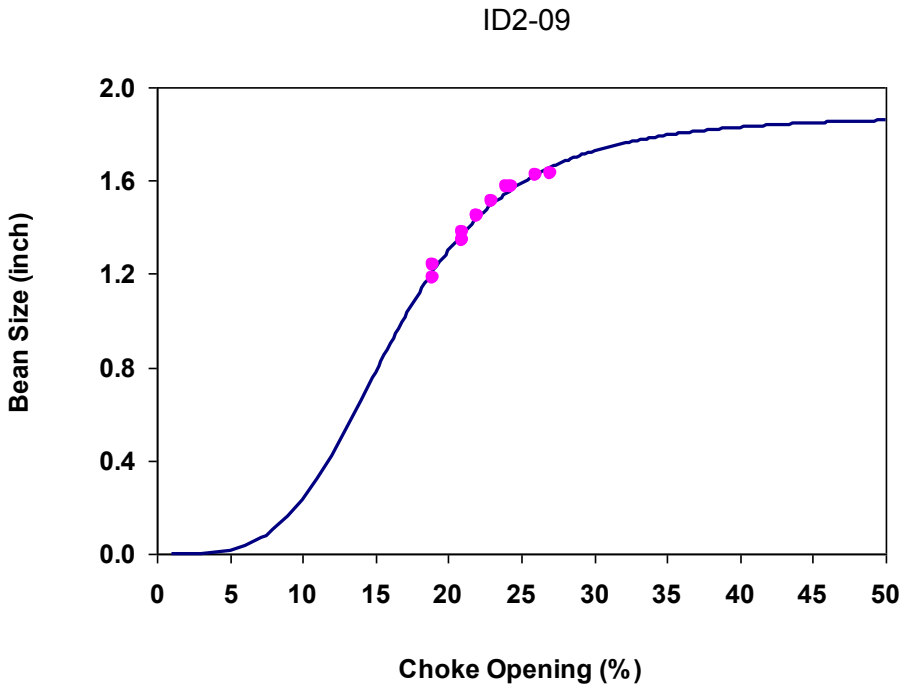

Figure 6-7: Regression analysis results ID2-09 well

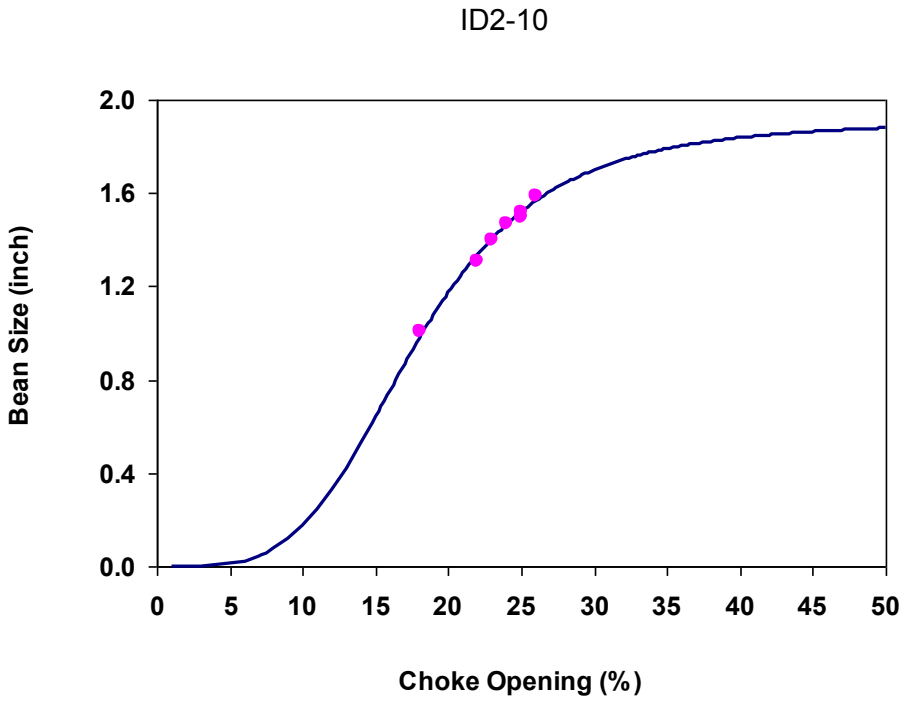

Figure 6-8: Regression analysis results ID2-10 well

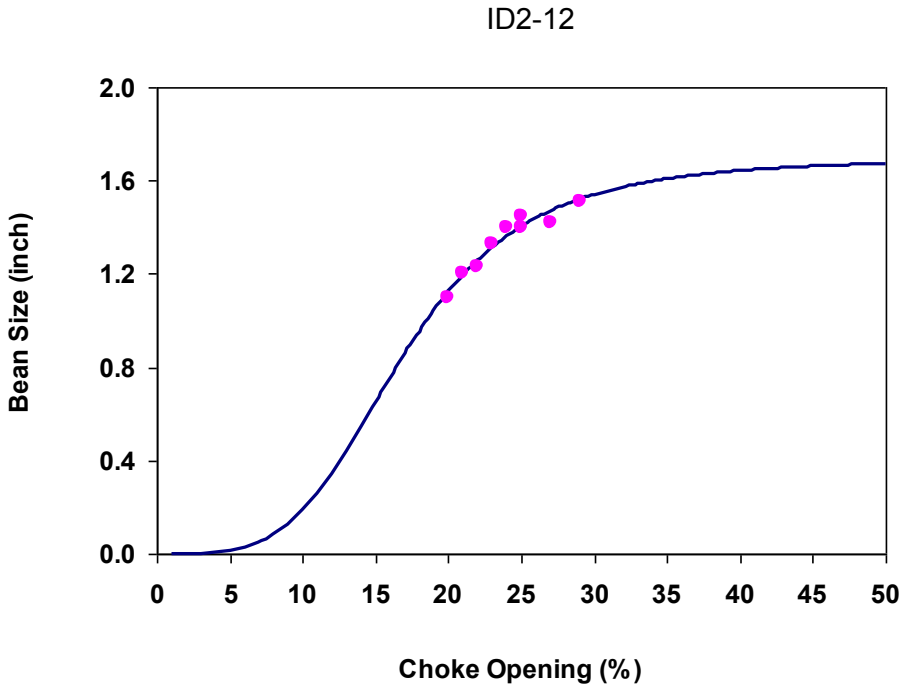

Figure 6-9: Regression analysis results ID2-12 well

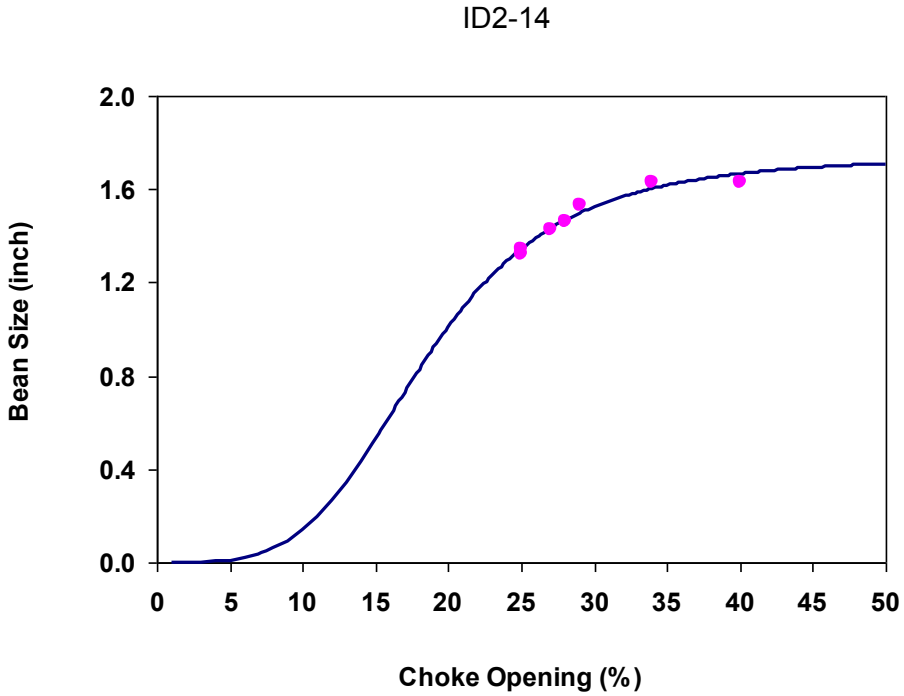

Figure 6-10: Regression analysis results ID2-14 well

Appendix C

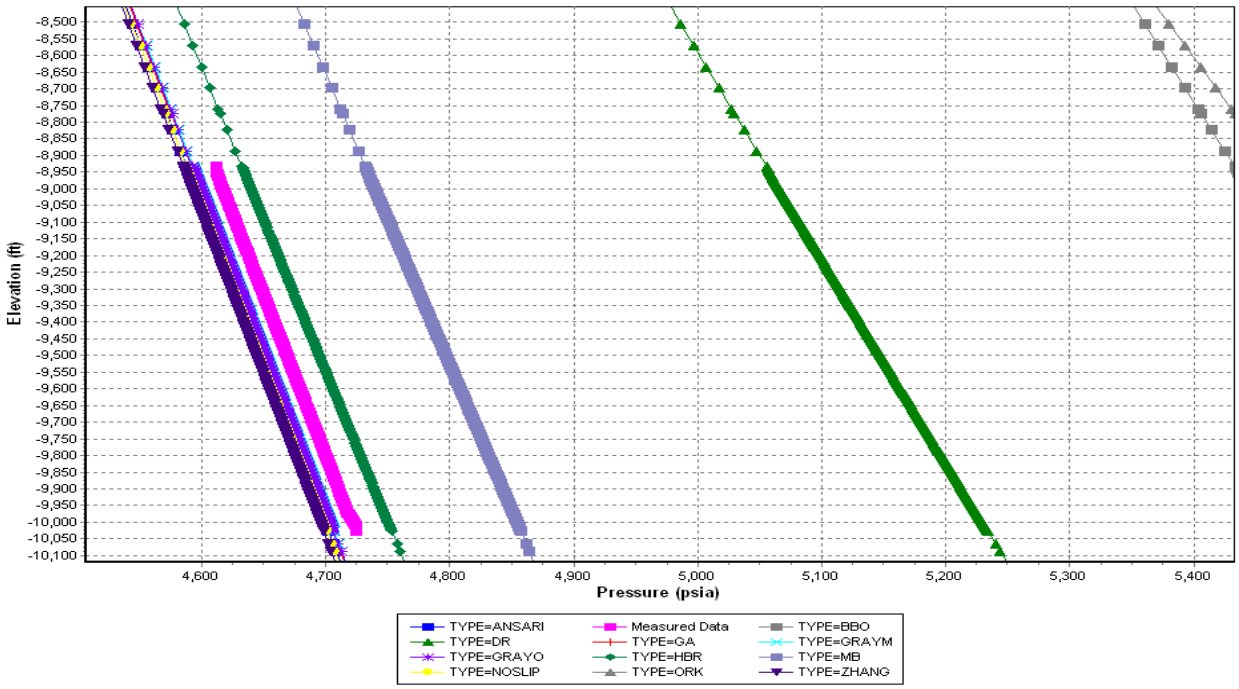

Figure 6-11: Pressure versus measured depth for ID1-06 with 30 MMSCFD Gas rates

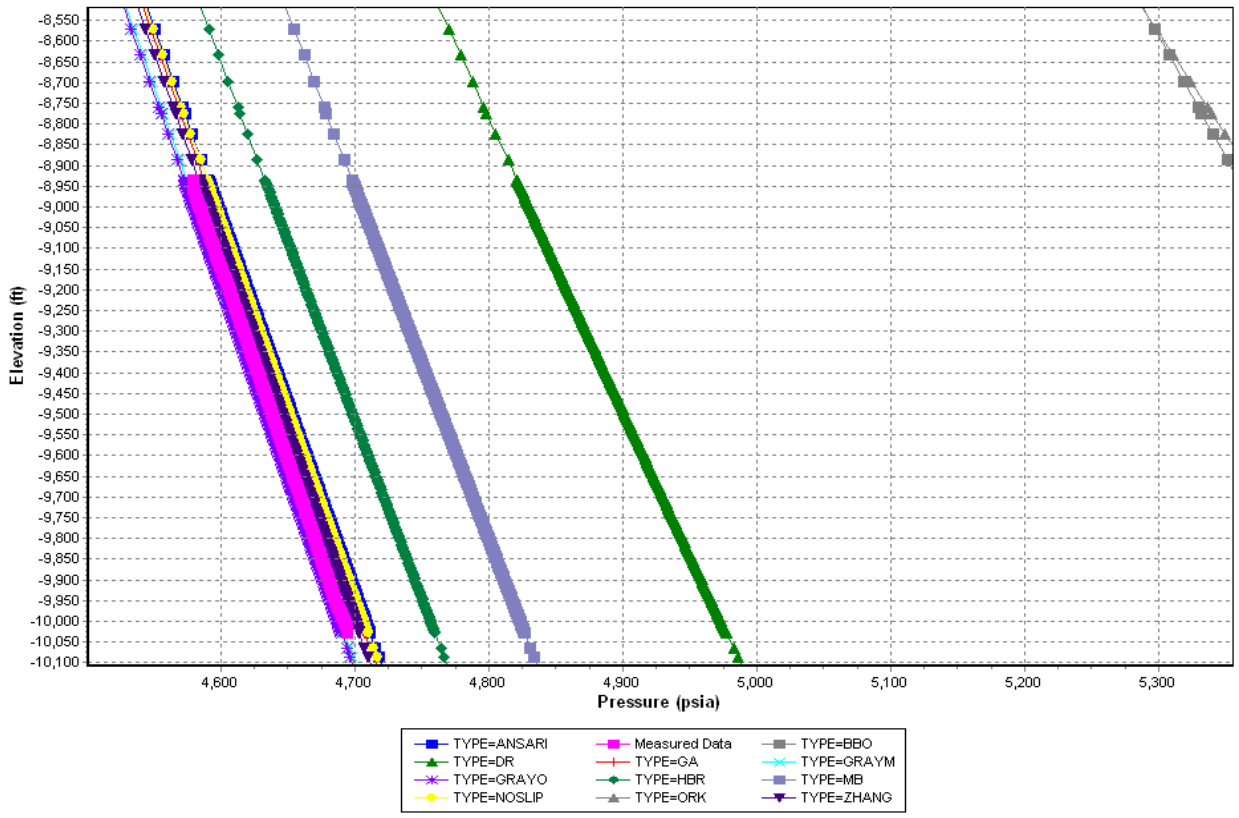

Figure 6-12: Pressure versus measured depth for ID1-06 with 50.5 MMSCFD Gas rates

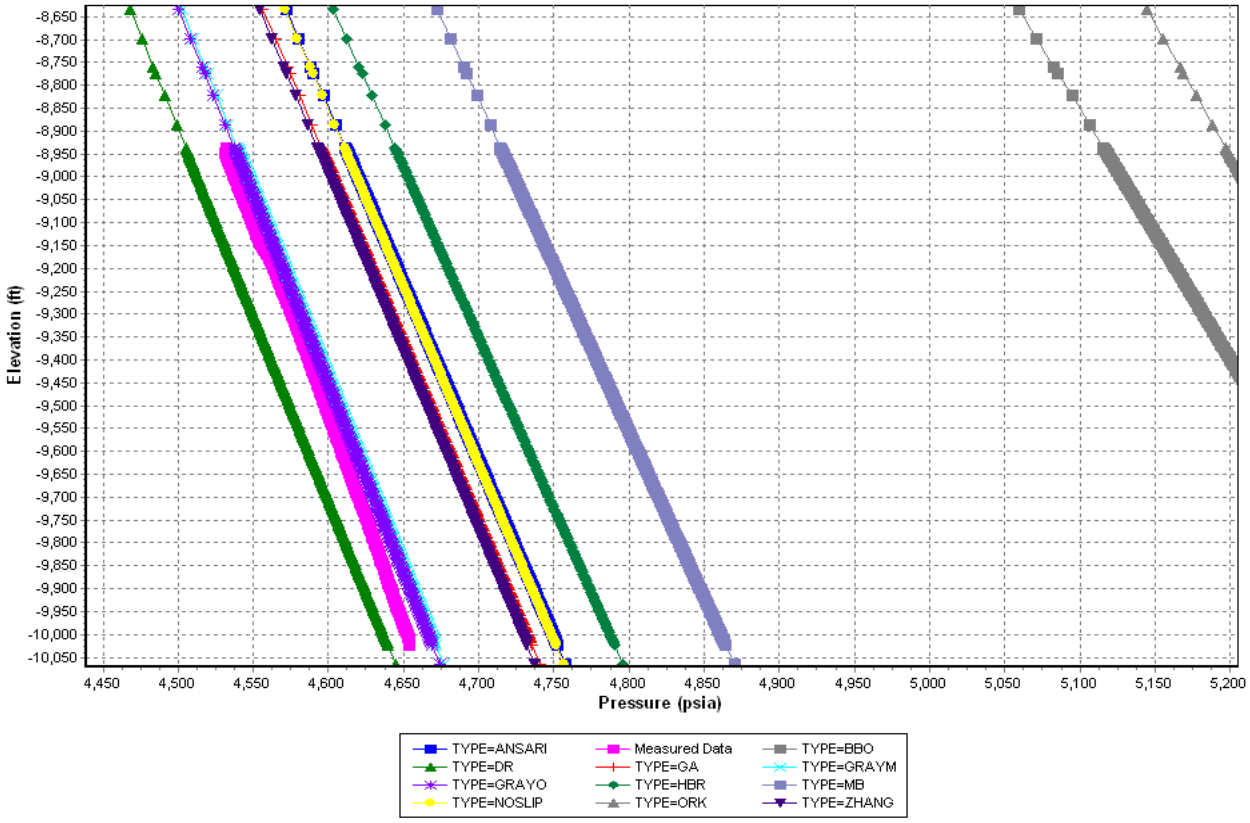

Figure 6-13: Pressure versus measured depth for ID1-06 with 88 MMSCFD Gas rates

Table 6-2: Model's mean absolute error and mean percent error for ID1-06 including all gas rates

Model	Mean Absolute Error (Psi)	Mean percent Error
Gray (Modified)	10	0.2
Gray (Original)	10	0.2
Govier, Aziz and Fogarasi	33	0.7
Zhang	34	0.7
No slip Assumption	41	0.9
Ansari	41	0.9
Hagedorn and Brown	70	1.5
Mukherjee and Brill	150	3.2
Duns and Ros	254	5.5
Beggs and Bril (Original)	764	16.5
Orkiszewski	816	17.6

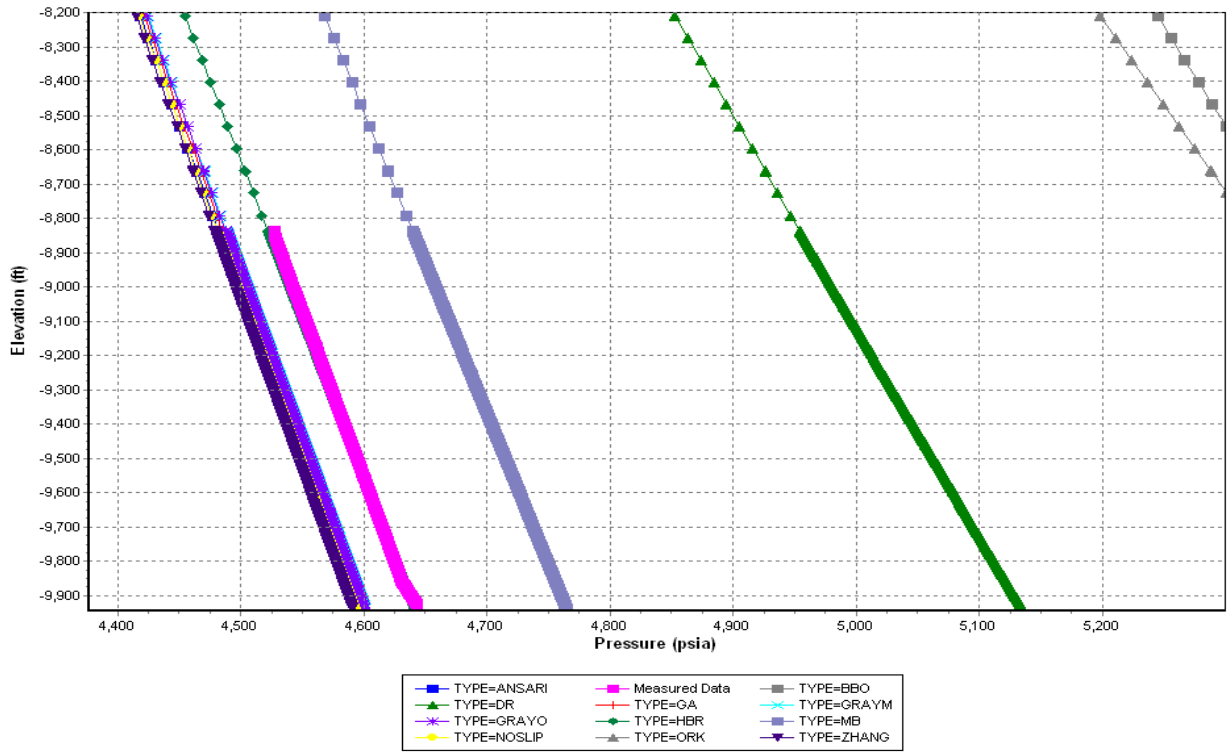

Figure 6-14: Pressure versus measured depth for ID1-07with 29 MMSCFD Gas rates

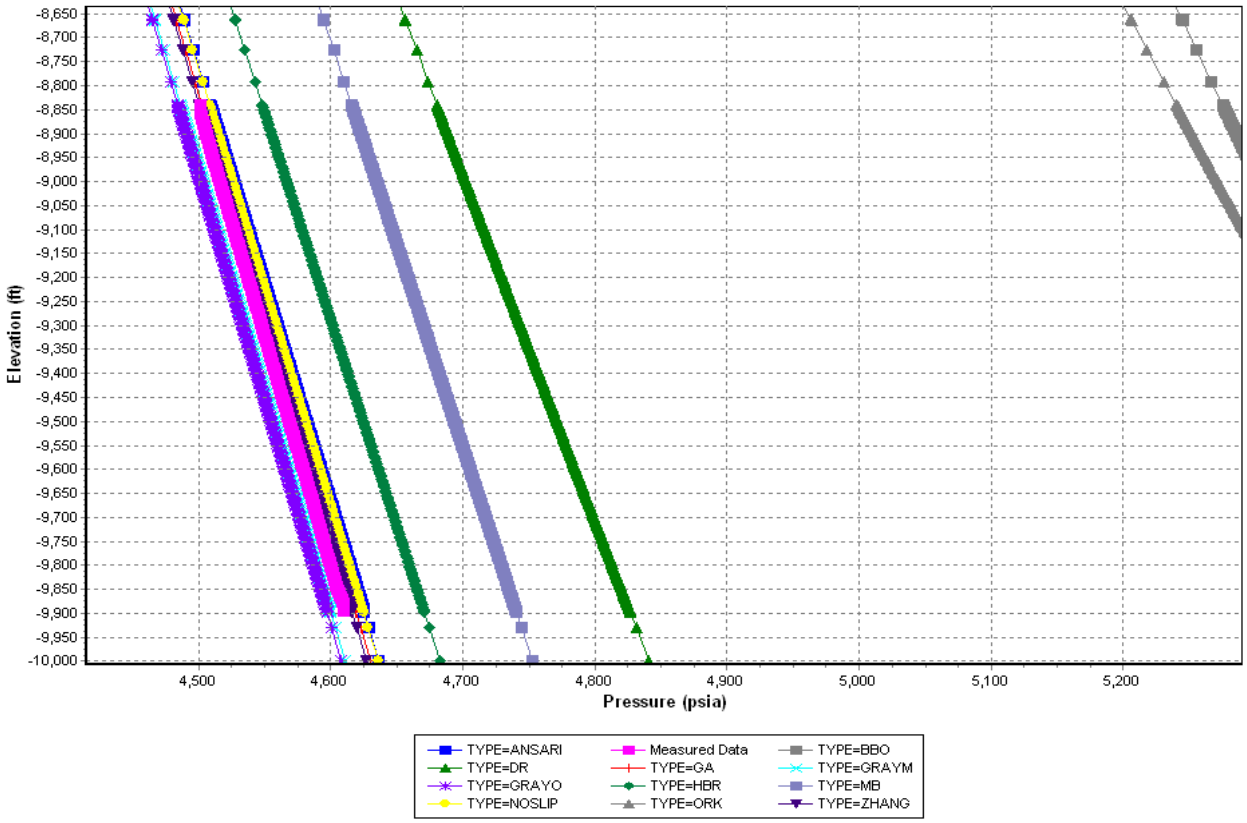

Figure 6-15: Pressure versus measured depth for ID1-07with 57 MMSCFD Gas rates

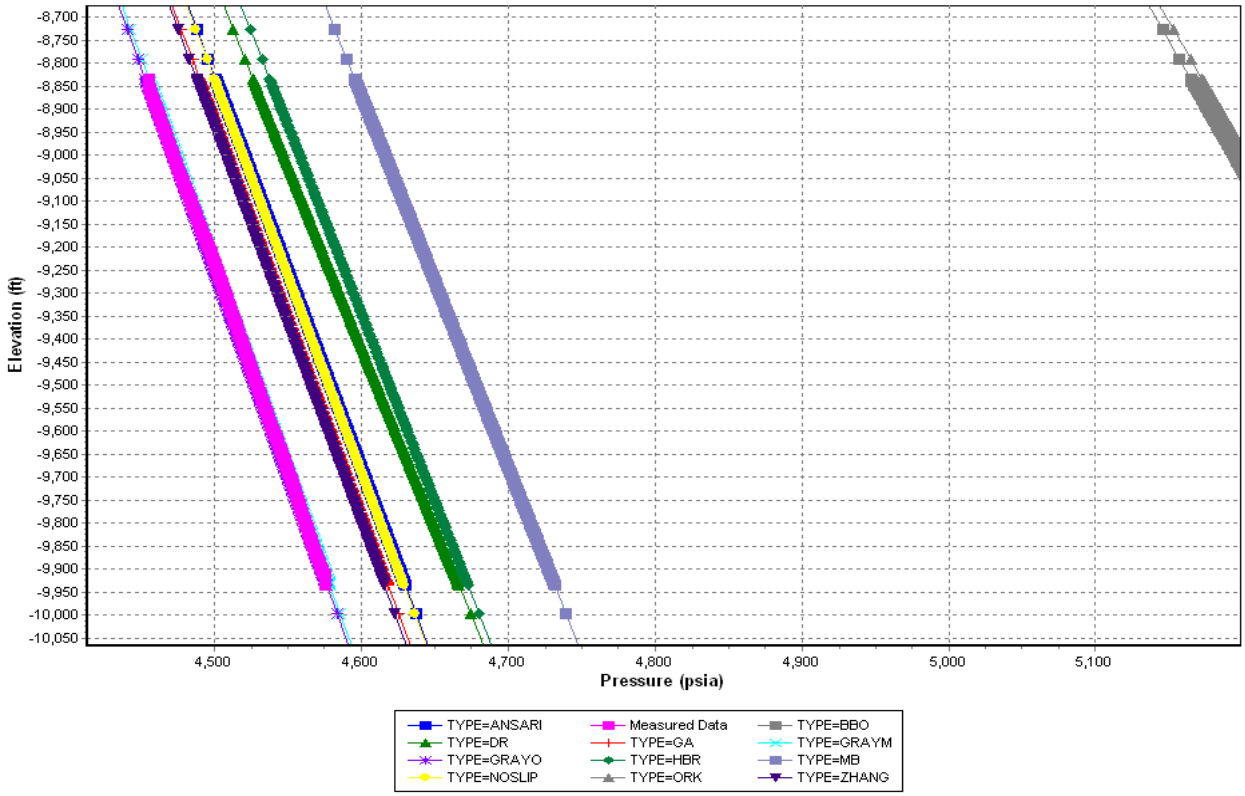

Figure 6-16: Pressure versus measured depth for ID1-07with 72 MMSCFD Gas rates

Table 6-3: Model's mean absolute error and mean percent error for ID1-07 including all gas rates

Model	Mean Absolute Error (Psi)	Mean percent Error
Gray (Modified)	17	0.4
Gray (Original)	18	0.4
Govier, Aziz and Fogarasi	30	0.7
Zhang	30	0.7
No slip Assumption	36	0.8
Ansari	37	0.8
Hagedorn and Brown	49	1.1
Mukherjee and Brill	131	2.9
Duns and Ros	245	5.4
Orkiszewski	797	17.5
Beggs and Bril (Original)	805	17.7

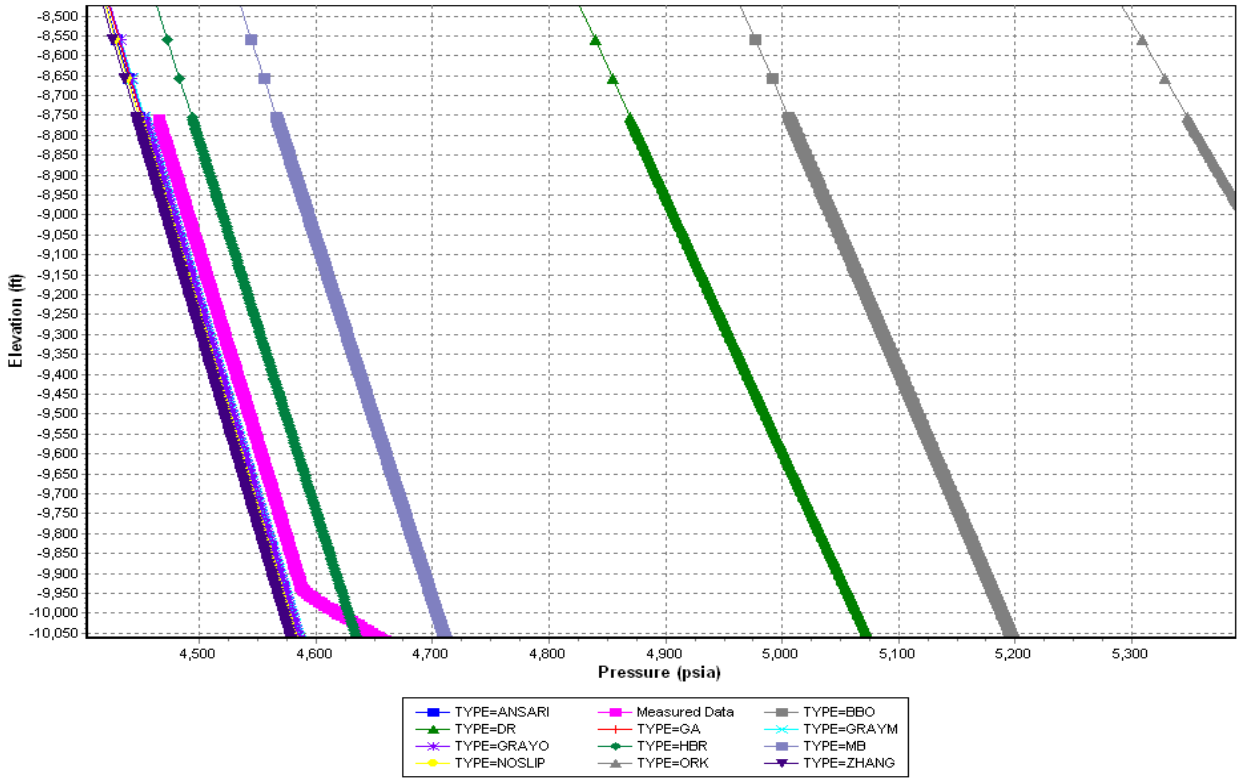

Figure 6-17: Pressure versus measured depth for ID1-13with 33 MMSCFD Gas rates

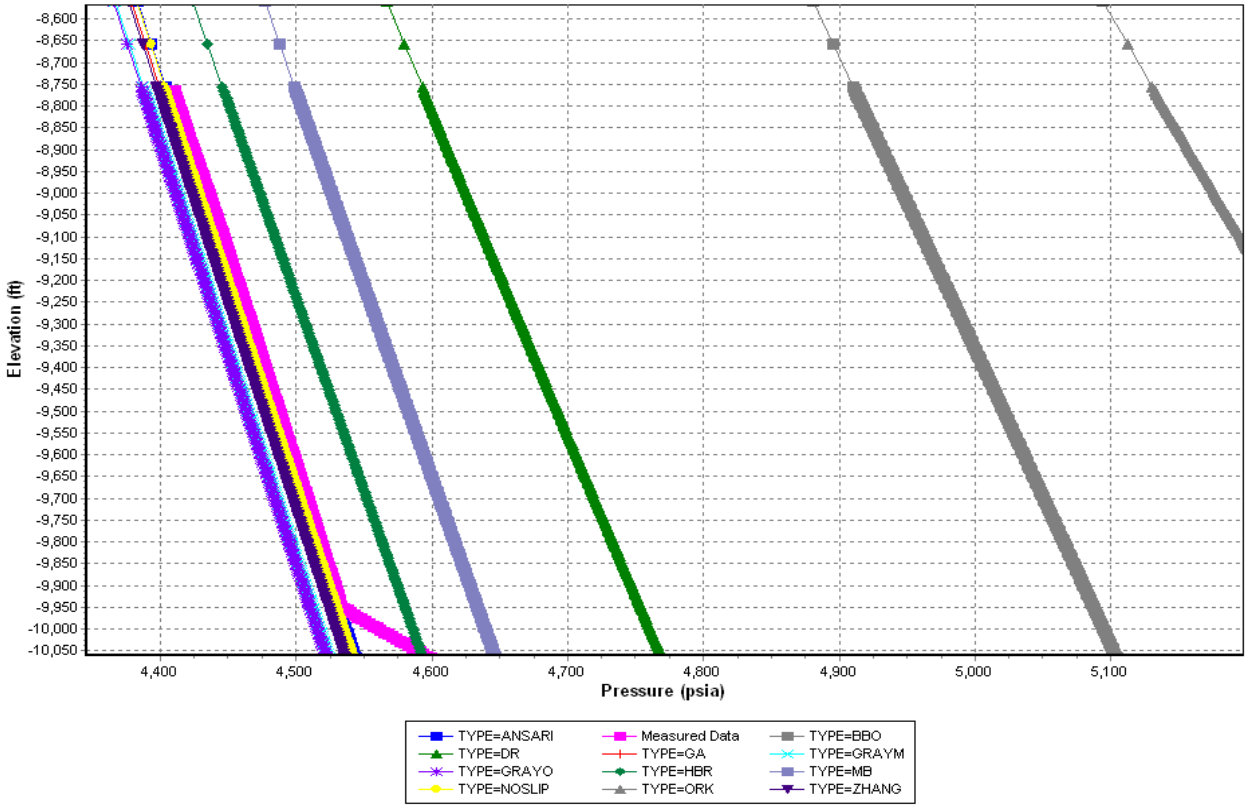

Figure 6-18: Pressure versus measured depth for ID1-13with 57 MMSCFD Gas rates

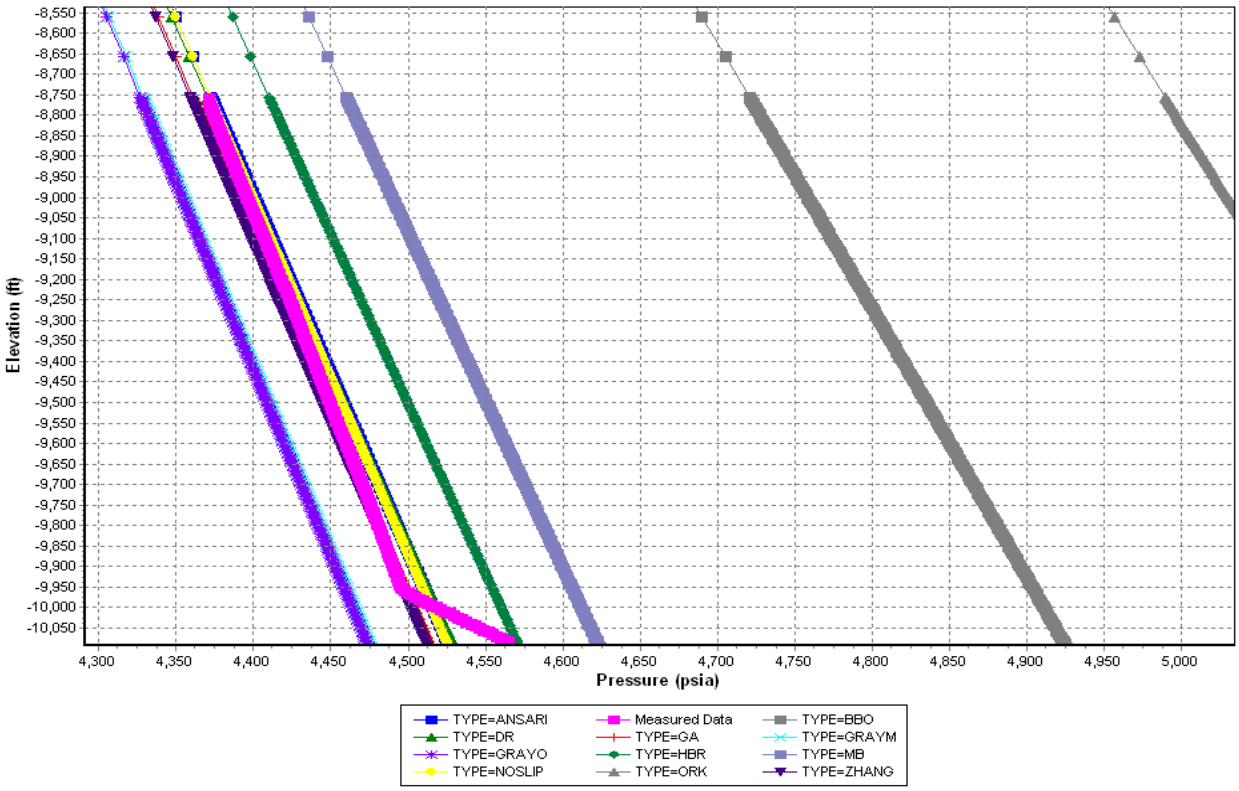

Figure 6-19: Pressure versus measured depth for ID1-13with 82 MMSCFD Gas rates

Table 6-4: Model's mean absolute error and mean percent error for ID1-13 including all gas rates

Model	Mean Absolute Error (Psi)	Mean percent Error
Ansari	13	0.3
No slip Assumption	13	0.3
Govier, Aziz and Fogarasi	13	0.3
Zhang	16	0.4
Gray (Modified)	29	0.6
Gray (Original)	30	0.7
Hagedorn and Brown	38	0.9
Mukherjee and Brill	97	2.2
Duns and Ros	215	4.8
Beggs and Bril (Original)	491	10.9
Orkiszewski	792	17.6

Appendix D

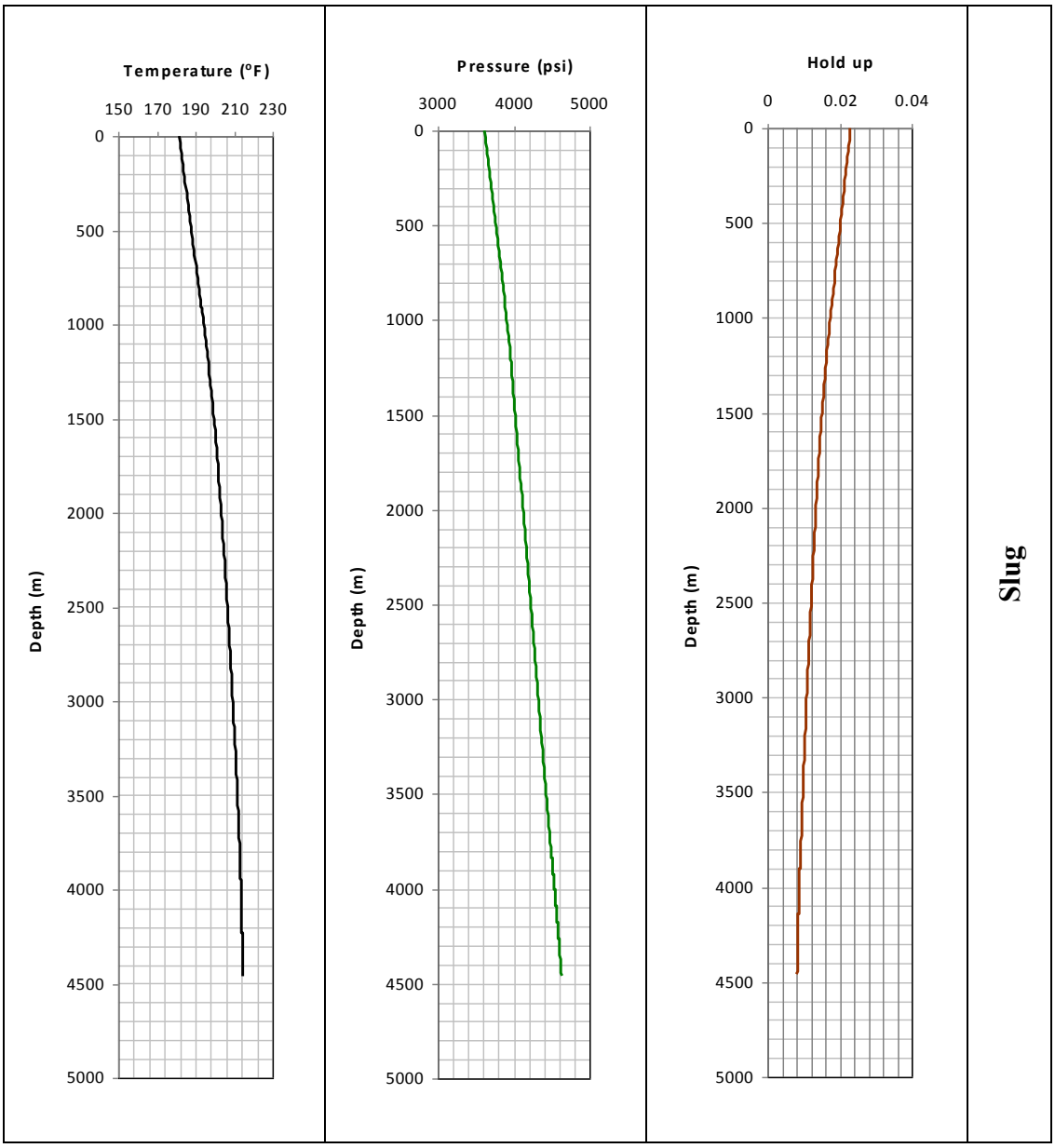

Figure 6-20: Temperature, Pressure, Liquid Hold-Up Profile, and Well Flow Regime for ID1-01 with 43.5 MMSCFD gas rate

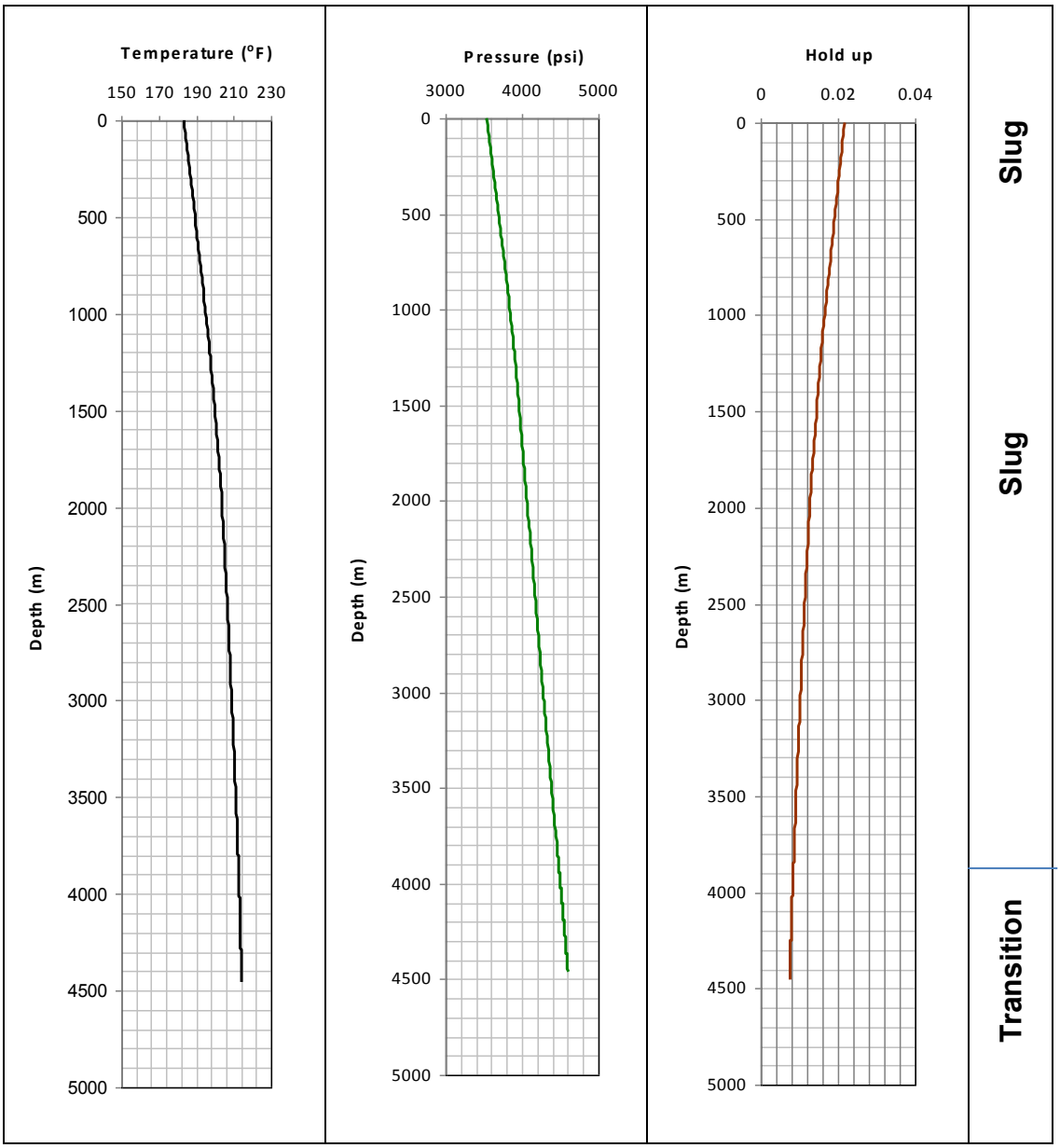

Figure 6-21: Temperature, Pressure, Liquid Hold-Up Profile, and Well Flow Regime for ID1-01 with 63 MMSCFD gas rate

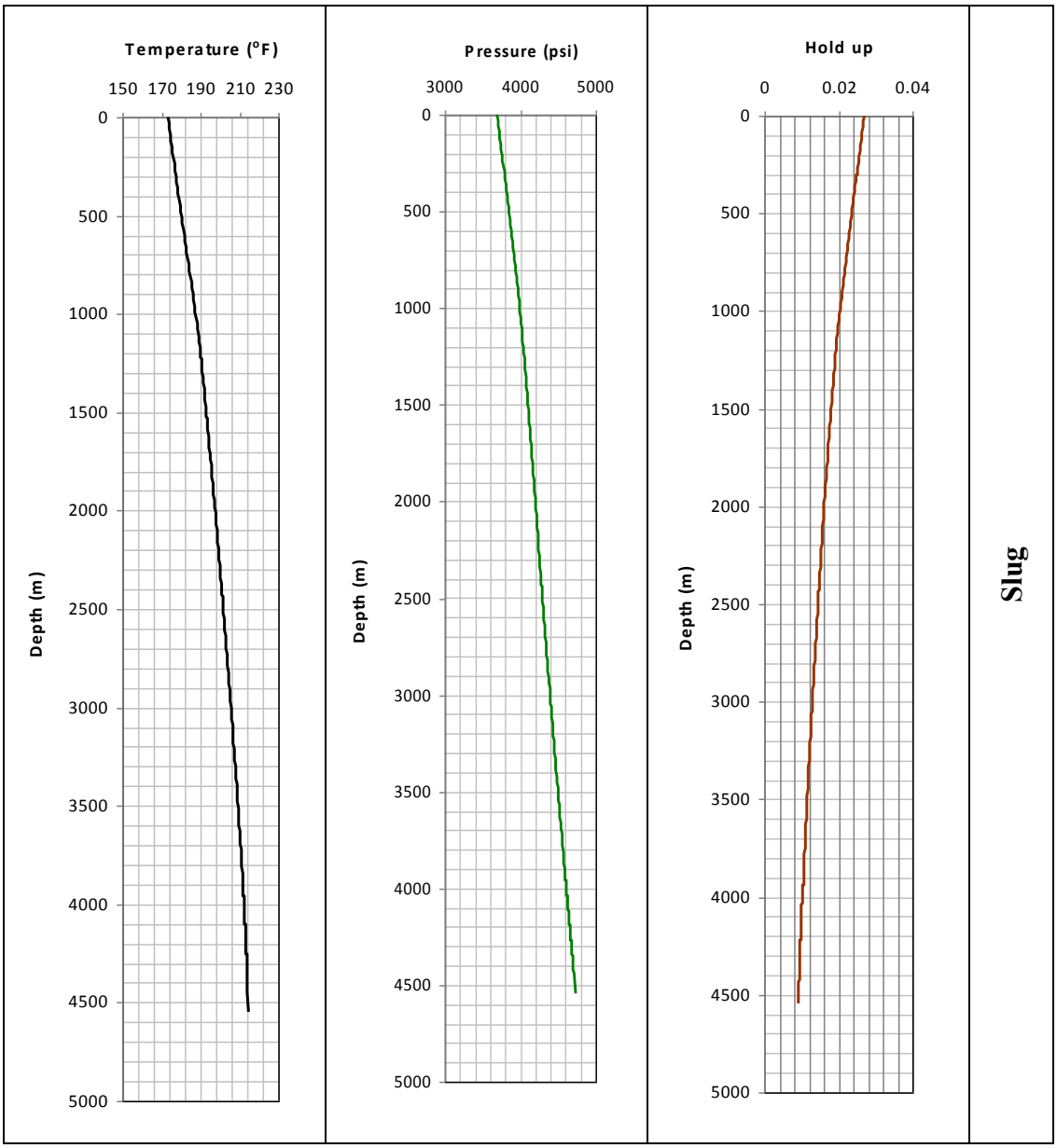

Figure 6-22: Temperature, Pressure, Liquid Hold-Up Profile, and Well Flow Regime for ID1-06 with 30 MMSCFD gas rate

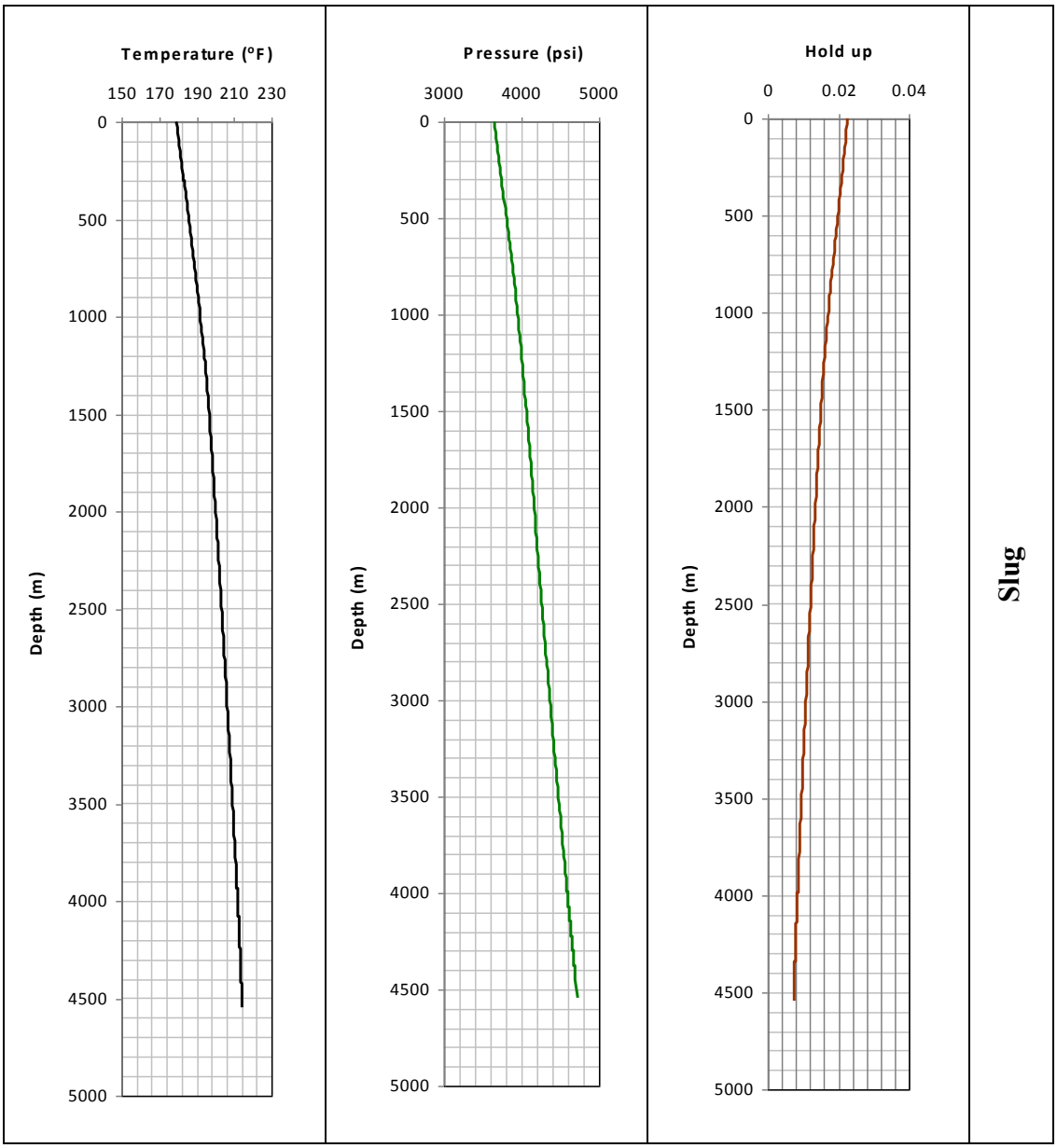

Figure 6-23: Temperature, Pressure, Liquid Hold-Up Profile, and Well Flow Regime for ID1-06 with 50.5 MMSCFD gas rate

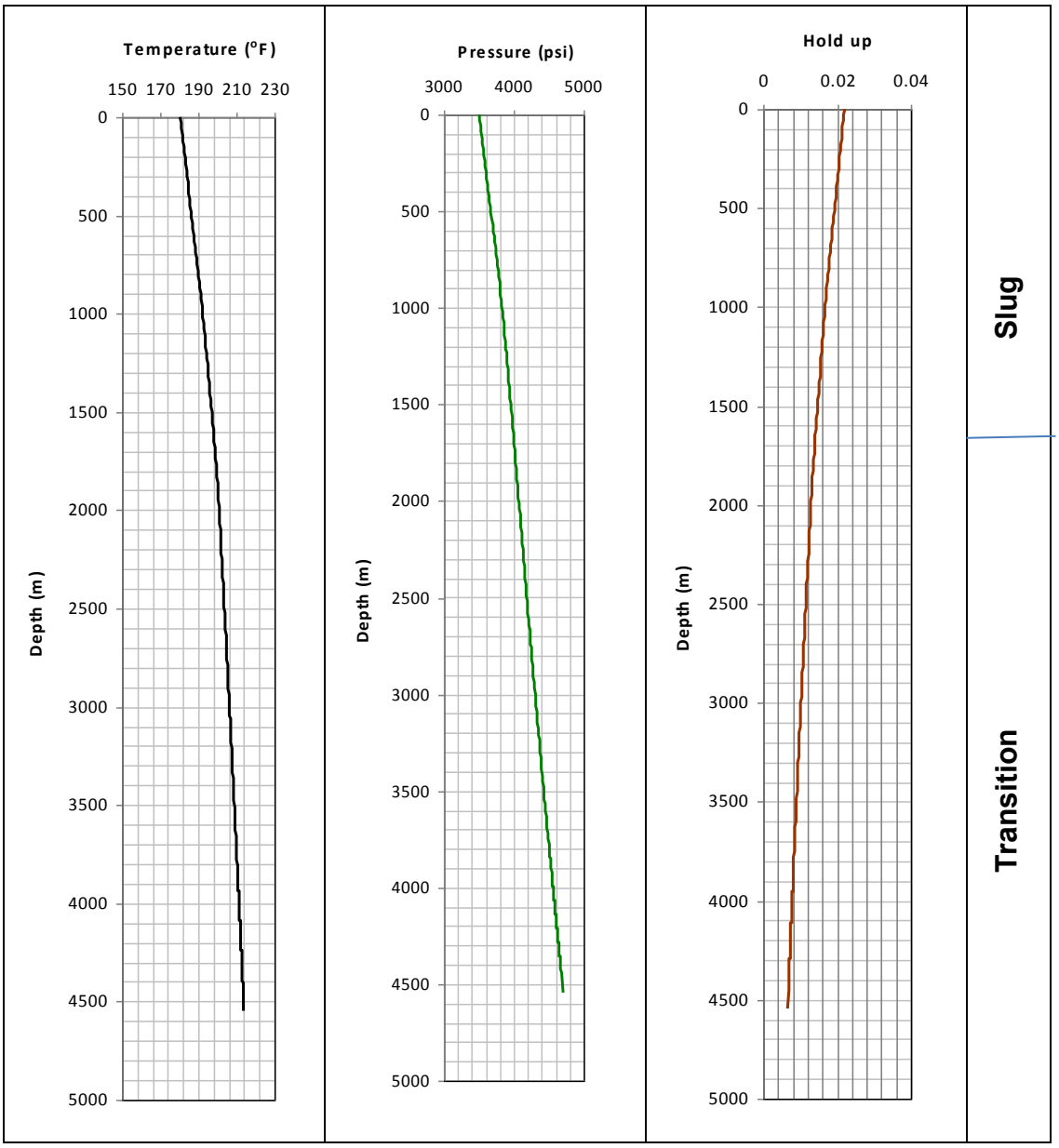

Figure 6-24: Temperature, Pressure, Liquid Hold-Up Profile, and Well Flow Regime for ID1-06 with 88 MMSCFD gas rate

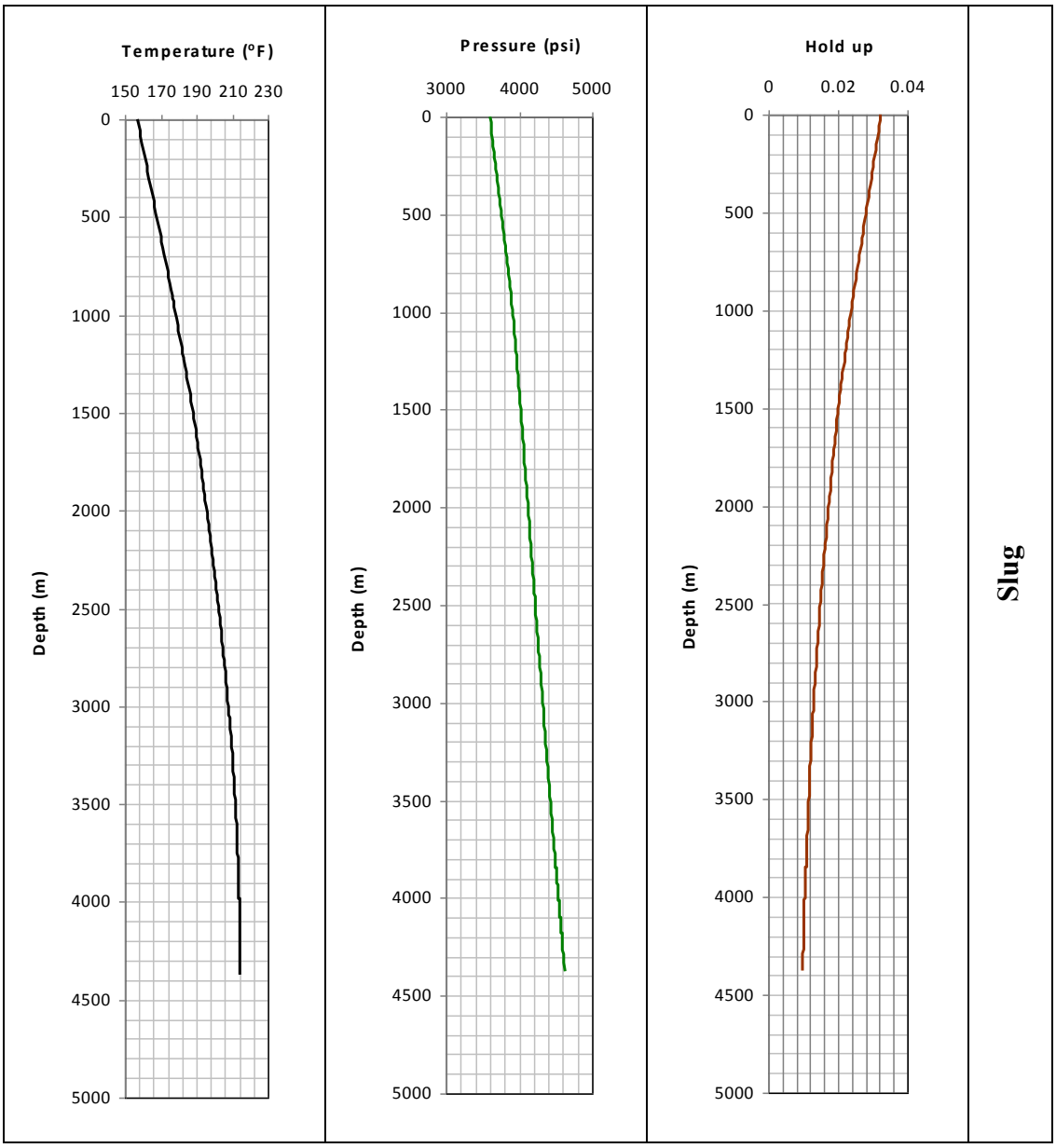

Figure 6-25: Temperature, Pressure, Liquid Hold-Up Profile, and Well Flow Regime for ID1-07 with 29 MMSCFD gas rate

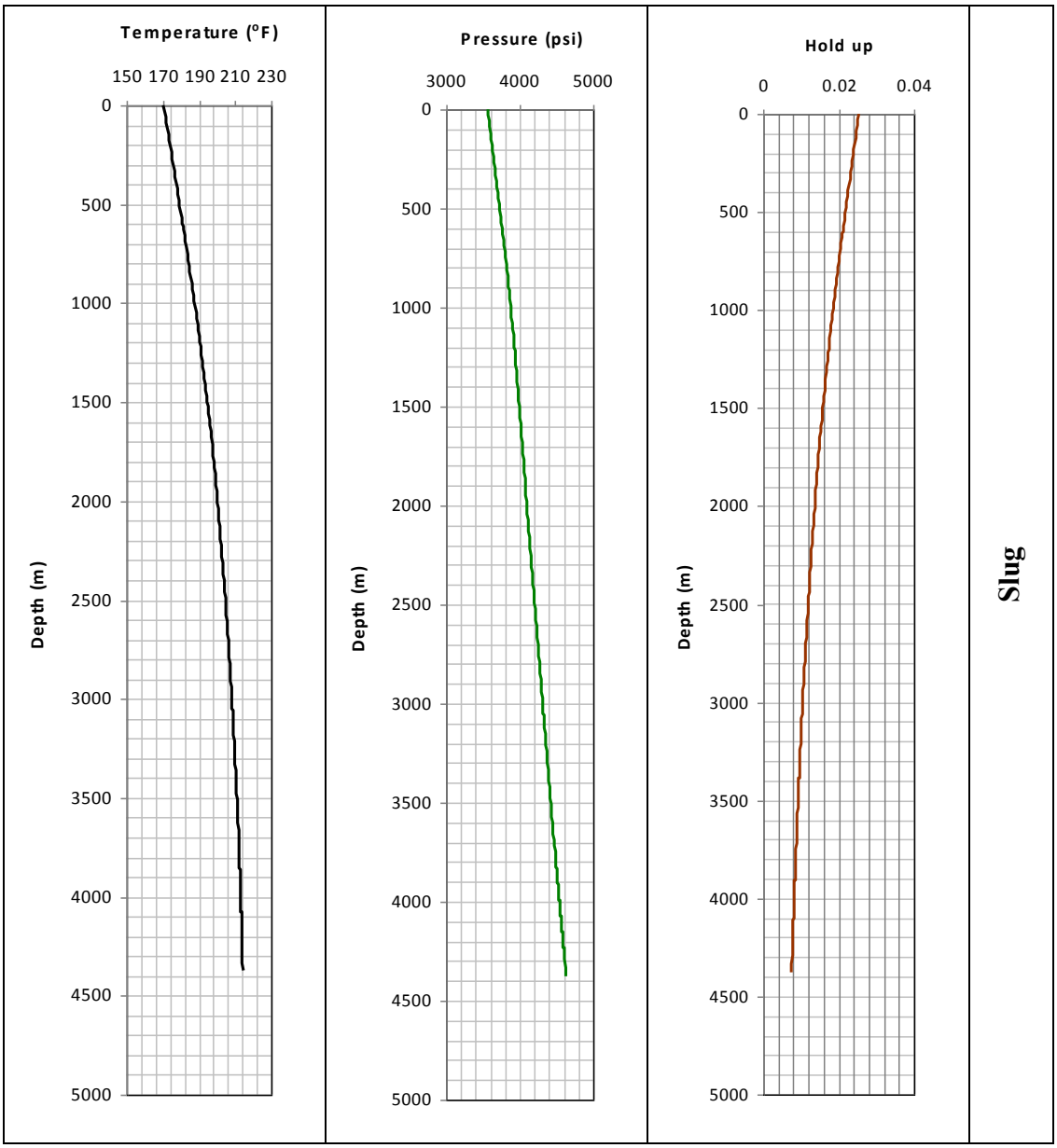

Figure 6-26: Temperature, Pressure, Liquid Hold-Up Profile, and Well Flow Regime for ID1-07 with 57 MMSCFD gas rate

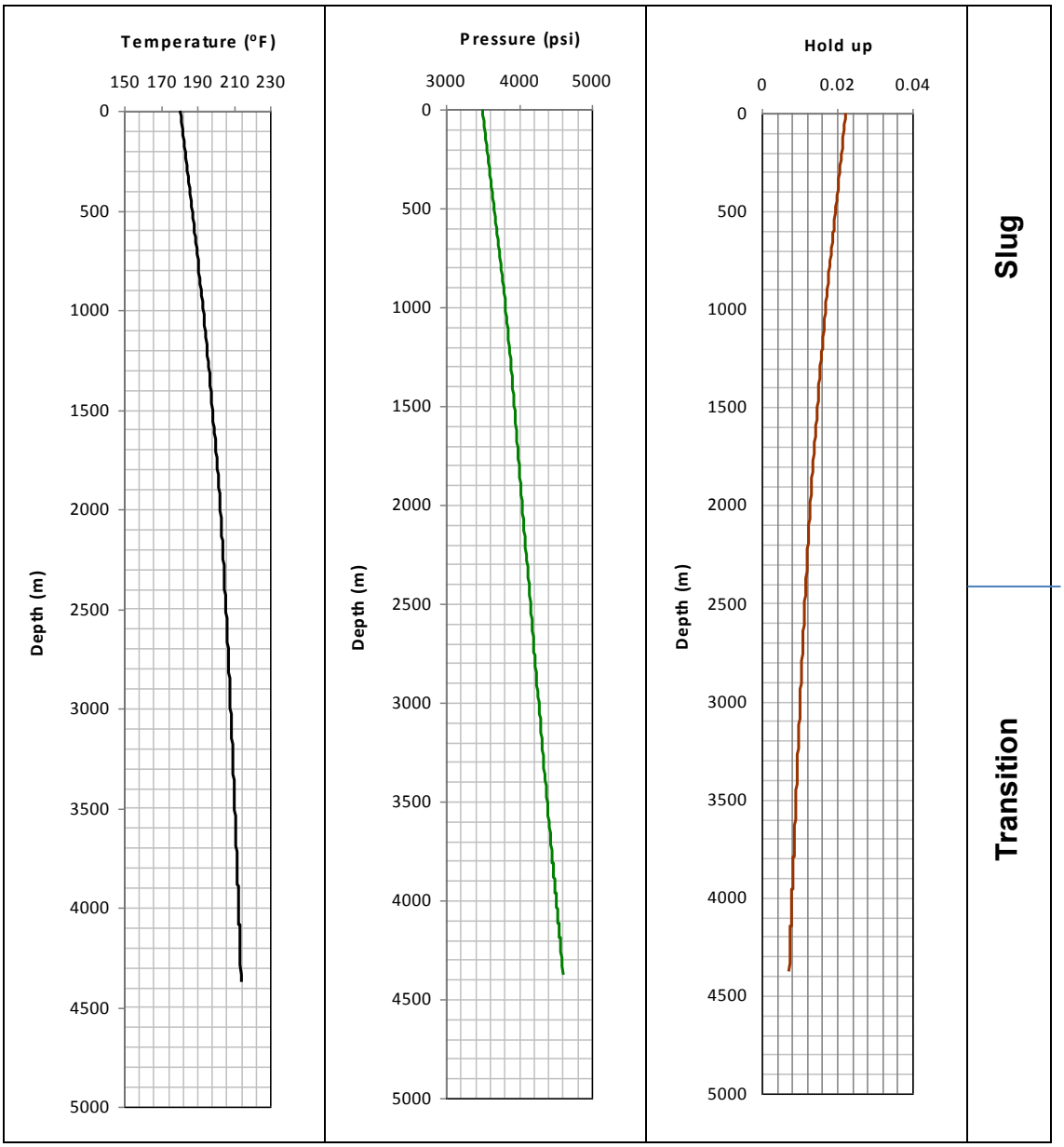

Figure 6-27: Temperature, Pressure, Liquid Hold-Up Profile, and Well Flow Regime for ID1-07 with 72 MMSCFD gas rate

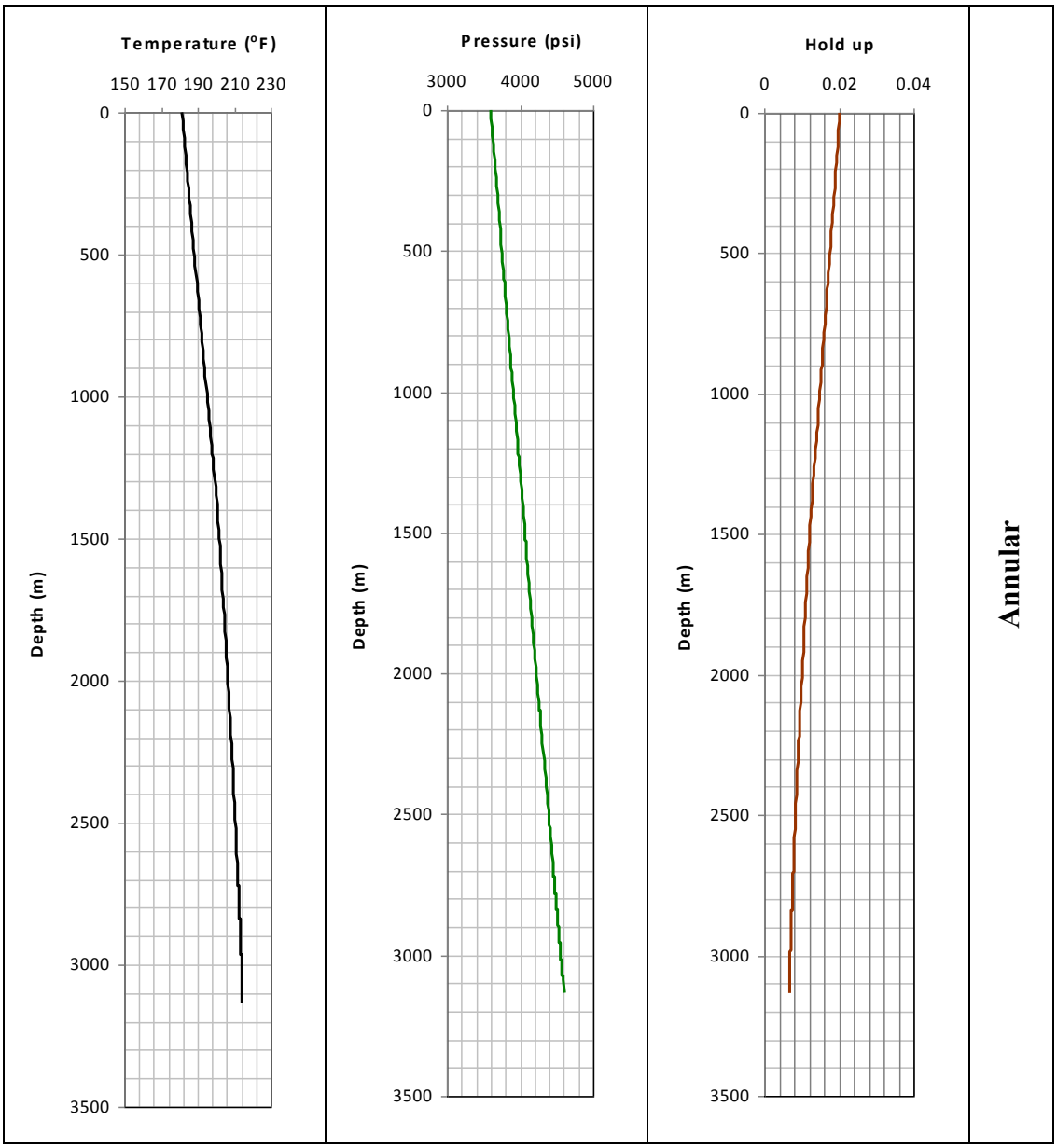

Figure 6-28: Temperature, Pressure, Liquid Hold-Up Profile, and Well Flow Regime for ID1-13 with 33 MMSCFD gas rate

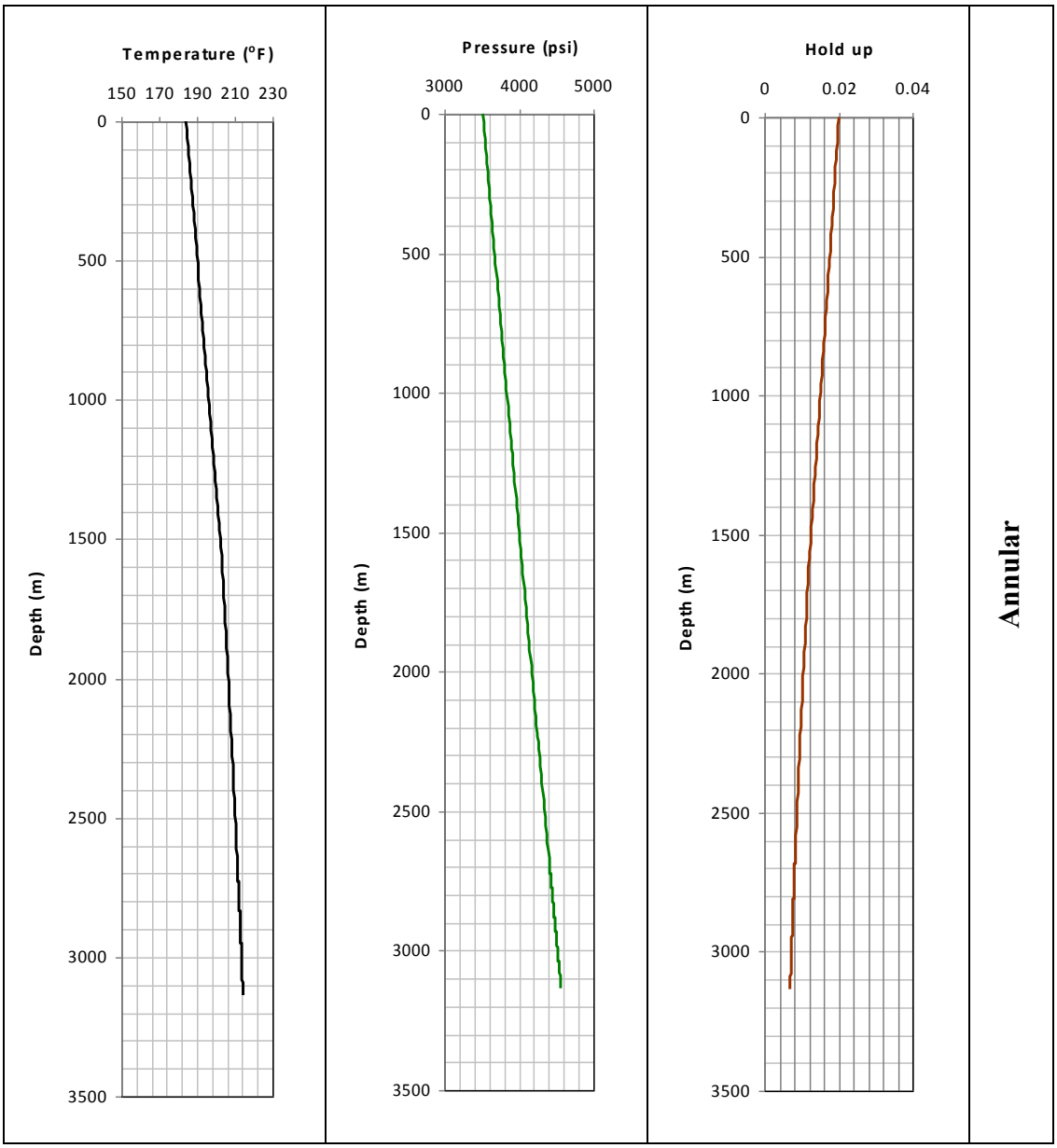

Figure 6-29 : Temperature, Pressure, Liquid Hold-Up Profile, and Well Flow Regime for ID1-13 with 57 MMSCFD gas rate

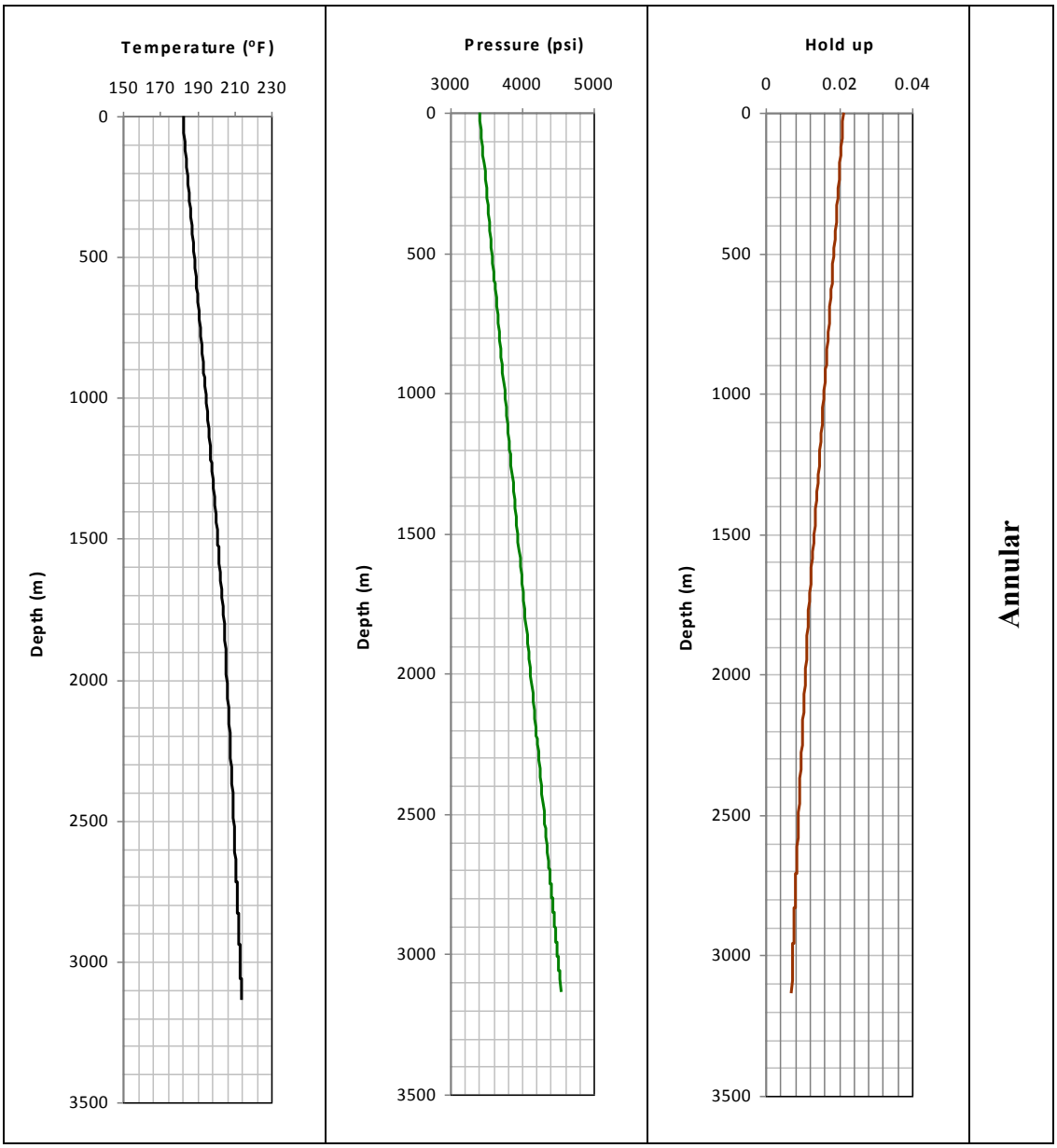

Figure 6-30: Temperature, Pressure, Liquid Hold-Up Profile, and Well Flow Regime for ID1-13 with 82 MMSCFD gas rate